



LUND UNIVERSITY

Novel diagnostics and treatment of acute lung injury and transplantation - Preclinical and clinical implementation

Stenlo, Martin

2021

Document Version:

Publisher's PDF, also known as Version of record

[Link to publication](#)

Citation for published version (APA):

Stenlo, M. (2021). *Novel diagnostics and treatment of acute lung injury and transplantation - Preclinical and clinical implementation*. Lund University, Faculty of Medicine.

Total number of authors:

1

General rights

Unless other specific re-use rights are stated the following general rights apply:

Copyright and moral rights for the publications made accessible in the public portal are retained by the authors and/or other copyright owners and it is a condition of accessing publications that users recognise and abide by the legal requirements associated with these rights.

- Users may download and print one copy of any publication from the public portal for the purpose of private study or research.
- You may not further distribute the material or use it for any profit-making activity or commercial gain
- You may freely distribute the URL identifying the publication in the public portal


Read more about Creative commons licenses: <https://creativecommons.org/licenses/>

Take down policy

If you believe that this document breaches copyright please contact us providing details, and we will remove access to the work immediately and investigate your claim.

LUND UNIVERSITY

PO Box 117
221 00 Lund
+46 46-222 00 00



Novel diagnostics and treatment of acute lung injury and transplantation

– Preclinical and clinical implementation

MARTIN STENLO

DEPARTMENT OF CLINICAL SCIENCES LUND | LUND UNIVERSITY



Novel diagnostics and treatment of acute lung injury and transplantation

– Preclinical and clinical implementation

Martin Stenlo, MD



LUND
UNIVERSITY

DOCTORAL DISSERTATION

by due permission of the Faculty of Medicine, Lund University, Sweden.
To be defended at Belfragesalen, BMC, Lund. Friday 12 November 2021 at 13:00.

Faculty opponent

Associate Professor Are Martin Holm (MD, PhD) Oslo University, Norway

Examining committee

Associate Professor Gaetano Perchiuzzi (MD, PhD) Uppsala University, Sweden

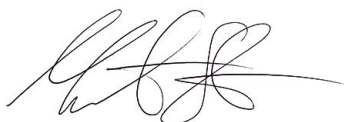
Professor Henrik Engblom (MD, PhD) Lund University, Sweden

Associate Professor Michael Perch (MD, PhD) Copenhagen University, Denmark

Organization LUND UNIVERSITY Faculty of Medicine Department of Clinical Sciences, Lund Anesthesia and Intensive Care Author Martin Stenlo, MD		Document name Lund University, Faculty of Medicine Doctoral Dissertation Series 2021:112	
		Date of issue 2021-11-12	
		Sponsoring organization	
Title and subtitle: Novel diagnostics and treatment of acute lung injury and transplantation – Preclinical and clinical implementation			
Abstract <p>Acute lung injury (ALI) and its most severe form, acute respiratory distress syndrome (ARDS) limit the utilization of donor lungs for transplantation but is also a common cause of death in the intensive care unit. There is a general lack of diagnostic tools by which to assess lung function in ARDS but, in addition, the treatments offered are limited.</p> <p>In the present thesis, the aim was to explore particles in exhaled air as a diagnostic tool for ALI, but also the use of cytokines as a treatment target for such injury. A porcine model was used where ALI and ARDS were induced, using either lipopolysaccharide (LPS), repeated lavage or gastric content aspiration. The lungs were evaluated <i>in vivo</i> during non-transplant and transplant conditions and with or without extra corporal membrane oxygenation (ECMO) support. The lungs were also evaluated by machine perfusion using <i>ex vivo</i> lung perfusion (EVLP).</p> <p>Measurements of exhaled breath particles (EBP), expressed as particle flow rate (PFR), from the airways preceded early signs of ARDS, not only in an LPS-induced ARDS porcine model but could also be used for monitoring lung injury during ECMO treatment both in pigs but also in patients with COVID-19-induced ARDS. Increased PFR also preceded clinical signs of ALI in the gastric aspiration model, whereas only a trend could be seen in the repeated lavage model. The LPS models showed a similar pattern of massive cytokine release as also seen in the COVID-19 patients. The cytokines were detected both in plasma and in bronchoalveolar lavage fluid (BALF). The cytokine release was not as prominent in the repeated lavage model and in the gastric aspiration model. In the collected samples of EBPs, specific proteins connected to lung injury were detected in all animal models. Given the role of cytokines in lung injury, cytokines are interesting targets for lung repair and regeneration.</p> <p>EVLP has lately gained acceptance as an evaluation platform for marginal lungs initially declined for transplantation. A new aspect is using the platform to repair or restore lung function of donor lungs with ALI that are declined both for EVLP and for transplantation. A cytokine filter was connected to the EVLP during perfusion of LPS-damaged donor lungs. The cytokine filter restored lung function after 4 hours of EVLP, shown by improved oxygenation and confirmation by histology. For optimal treatment, the restored lungs were transplanted into a healthy recipient and received another 12 hours of cytokine filtration post-transplantation. The lungs were evaluated regarding the development of primary graft dysfunction (PGD) where cytokines seem to be an important target given the outcome of significantly less PGD in the group receiving cytokine filtration.</p> <p>In conclusion, PFR may be used as a diagnostic tool in mechanical ventilation and to detect ALI, but also to monitor lung injury over time. Cytokines as a treatment target have their role in restoring lung function in damaged donor lungs.</p>			
Key words: Acute lung injury. Acute respiratory distress syndrome. Exhaled breath particles. Transplantation.			
Classification system and/or index terms (if any)			
Supplementary bibliographical information		Language: English and Swedish	
ISSN and key title 1652-8220 Lund University, Faculty of Medicine Doctoral Dissertation Series 2021:112		ISBN 978-91-8021-119-2	
Recipient's notes		Number of pages: 119	
		Price	
		Security classification	

I, the undersigned, being the copyright owner of the abstract of the above-mentioned dissertation, hereby grant to all reference sources permission to publish and disseminate the abstract of the above-mentioned dissertation.

Signature



Date 2021-09-27

Novel diagnostics and treatment of acute lung injury and transplantation

– Preclinical and clinical implementation

Martin Stenlo, MD



LUND
UNIVERSITY

DOCTORAL DISSERTATION

Department of Clinical Sciences, Lund

Anesthesia and Intensive Care

Supervisor: Professor Sandra Lindstedt, MD, PhD

Co-supervisor: Snejana Hyllén, MD, PhD

Co-supervisor: Associate Professor Darcy Wagner, PhD

Co-supervisor: Professor Malin Malmjö, MD, PhD

Cover photo: Alveoli with autofluorescence, taken by Anna Niroomand

Copyright pp 1-119 Martin Stenlo

Paper I © 2020 the American Physiological Society

Paper II © 2021 the Authors. Physiological Reports

Paper III © the Authors (Manuscript unpublished)

Paper IV © the Authors (Manuscript unpublished)

Paper V © 2021 the Authors. ERJ Open Research

Lund University

Faculty of Medicine

Department of Anesthesia and Intensive Care

ISBN 978-91-8021-119-2

ISSN 1652-8220

Printed in Sweden by Media-Tryck, Lund University

Lund 2021



Media-Tryck is a Nordic Swan Ecolabel certified provider of printed material. Read more about our environmental work at www.mediatryck.lu.se

MADE IN SWEDEN 

Dedicated to my wonderful family

Table of Contents

List of publications	8
Populärvetenskaplig sammanfattning (Summary in Swedish)	9
Abbreviations	12
Introduction	14
The respiratory system	14
Anatomy and physiology	14
Mechanical ventilation	16
Ventilation modes	17
Ventilator-induced lung injury (VILI)	18
Cardiopulmonary monitoring	18
Cardiopulmonary circulation	19
Pulmonary artery catheter	19
Acute respiratory distress syndrome (ARDS)	21
Definition	21
Classification	22
Pathophysiology	22
Treatment	23
ECMO	24
Veno-arterial ECMO (V-A ECMO)	25
Veno-venous ECMO (V-V ECMO)	25
Particles in exhaled air (PExA)	26
Exhaled breath as a non-invasive technique	26
PExA analysis in chronic rejection in lung transplant recipients	28
Different methods in the search for biomarkers	29
Proximity extension assay (PEA) technology	30
Animal models of ALI and ARDS	30
Porcine models of ALI and ARDS	31
Lung transplantation	32
Donor organ scarcity	32
<i>Ex vivo</i> lung perfusion	33
Survival after LTx	36

Aims	38
Materials and methods.....	39
PExA	39
ECMO setup.....	40
<i>Ex vivo</i> lung perfusion.....	42
Multiplex	44
Histology	45
Subjects and study design	46
Statistical analysis	51
Results.....	53
Paper I	53
Paper II	58
Paper III.....	67
Paper IV	75
Paper V.....	86
Discussion	90
Paper I	90
Paper II	91
Paper III.....	94
Paper IV	97
Paper V.....	99
Ethical aspects.....	102
Conclusions	103
Future perspectives	105
Acknowledgments.....	106
References	107
Papers I-V	119

List of publications

Paper I

Stenlo M, Hyllén S, Silva IA, Bölükbas DA, Pierre L, Hallgren O, Wagner DE, Lindstedt S. Increased particle flow rate from airways precedes clinical signs of ARDS in a porcine model of LPS-induced acute lung injury.

Am J Physiol Lung Cell Mol Physiol 2020;318(3):L510-17.

Paper II

Stenlo M, Silva IAN, Hyllen S, Bölükbas DA, Niroomand A, Grins E, Ederoth P, Hallgren O, Pierre L, Wagner DE, Lindstedt S Monitoring lung injury with particle flow rate in LPS-and COVID-19- induced ARDS.

Physiol Rep. 2021;9(13):e14802.

Paper III

Stenlo M, Niroomand A, Hirdman G, Edström D, Ghaidan H, Franziska O, Pierre L, Hyllen S, Lindstedt S. Monitoring progression of acute lung injury with particles in exhaled air in three different ARDS models.

Manuscript. 2021.

Paper IV

Ghaidan H, Stenlo M, Gvazava N, Niroomand A, Edstrom D, Silva I, Broberg E, Hallgren O, Olm F, Pierre L, Hyllen S, Lindstedt S. Reduction of primary graft dysfunction using cytokine filtration following acute respiratory distress syndrome in lung transplantation.

Nature Communications. 2021; Under revision.

Paper V

Hallgren F, Stenlo M, Niroomand A, Broberg E, Hyllen S, Malmsjo M, Lindstedt S. Particle flow rate from the airways as fingerprint diagnostics in mechanical ventilation in the intensive care unit: a randomised controlled study.

ERJ Open Res. 2021;7(3):00961-2020.

Populärvetenskaplig sammanfattning (Summary in Swedish)

Generellt sett är mätning av ämnen i utandningsluften fortsatt ett relativt nytt och utforskat område med relativt få kliniska implementeringar. Olika metoder finns beskrivna och de mest etablerade benämns EBC (utandat kondensat) där man kyler utandningsluften till vätska och analyserar vätskan för olika volatila ämnen. Vidare har det gjorts en del forskning på partiklar i utandningsluften där PExA är väl etablerad på vakna spontanandandes patienter med olika typer av lungsjukdomar så som astma och KOL. Partikelflöden i utandningsluft hos respiratorbehandlade individer med lungskada är undersökt i mycket begränsad utsträckning och befinner sig fortsatt i sin linda.

Detta avhandlingsarbete börjar med att undersöka om partikelflödes hastighet (PFR), mätt med en optisk partikelmätare, kan användas som ett diagnostiskt verktyg för akut lungskada (ALI) och akut andningssyndrom (ARDS). Vidare undersöker vi om partiklar i utandningsluft (EBP) kan analyseras för olika protein som kan relateras till lungskada, liknande ett "blodprov" från utandningsluften.

I delarbete 1 implementerade, utvecklade och validerade vi en lungskadmodell på gris med LPS (bakterietoxin) för att undersöka om PFR kunde användas diagnostiskt för ARDS. Alla grisar utvecklade ARDS inom 1–3 timmar. Vi fann att partikelflödet i utandningsluften var signifikant högre hos grisar med ARDS än hos kontrollgrisar samt att PFR förekom andra kliniska tecken på ARDS och därmed har potential att vara ett komplement till redan etablerade undersökningar för lungskada. Artikeln publicerades i American journal of physiology Lung cellular and molecular physiology 2019.

I delarbete 2 tar vi utgångspunkt i resultaten från första arbetet och undersöker vidare om PFR kan användas på ARDS patienter med ECMO behandling. Eftersom Thoraxavdelningen vid Skånes universitetssjukhus i Lund är ett kompetenscentrum för ECMO vet vi att det är problematiskt att mäta omfattningen av lungskada medan patienten har pågående ECMO-behandling dels på grund av säkerhets- och logistikfrågor men också p.g.a. av att ECMO tar över lungans funktion. En icke-invasiv metod som kan mäta omfattningen av lungskada och förlopp (förbättring och försämring av lungfunktionen) under ECMO behandling skulle vara av betydande kliniskt värde. Vi jämförde djurgrupper med ARDS med grupper som

hade ARDS och ECMO behandling. Vi fann att PFR ökade tydligt när ECMO initierades och att dessa hade förvärrad lungskada. PFR skulle därmed också ha potential att mäta omfattningen av lungskada samtidigt med ECMO-behandling.

Vid denna tidpunkt var pandemin ett faktum, och vår intensivvårdsavdelning tog hand om patienter med covid -19 inducerad ARDS som behövde ECMO-stöd. Baserat på våra prekliniska fynd fick vi etiskt godkännande att mäta PFR på Covid -19 patienter med ARDS och ECMO. Patienter med ECMO -stöd är glädjande nog relativt få men vårdas under lång tid och under de första 6 månaderna kunde vi endast inkludera 4 patienter i studien som ett ”proof of concept” då våra resultat visade att PFR kunde användas som ett kliniskt verktyg för långtidsbehandling av ECMO-patienter. Intressant nog fann vi att våra prekliniska fynd kunde översättas till kliniska miljöer. Resultaten kan komma att ha inverkan på lungskadebedömningen på intensivvården. Artikeln publicerades i Physiological Reports.

I delarbete 3 var vi intresserad av att undersöka om PFR kunde användas som ett diagnostiskt verktyg för olika lungskador på sövda grismodeller. Vi ville undersöka om PFR, vid lungskada orsakat av 1) infektion, 2) aspiration och 3) drunkning, skiljdes åt. Vi kontaktade Hedenstiernalaboratoriet vid Uppsala universitet som har en validerad drunkningsmodell på sövda djur och efter etiskt godkännande åkte vi till Uppsala och provade vår PFR-metod i deras djurmodell.

Samtidigt utvecklade vi en aspirationsmodell med flytande maginnehåll som tredje lungskademodell. Vi fann att PFR kunde användas för att diagnostisera ARDS i två av tre modeller. Den starkaste signalen och den mest signifikanta förändringen i PFR sågs i LPS modellen följt av modellen för aspiration av maginnehåll medan drunkningsmodellen inte kunde användas på ett tillfredställande sätt för mätning av PFR. Resultaten är mycket lovande, och nästa steg är att undersöka om resultaten från magaspirationsmodellen också kan översättas till kliniska miljöer.

Då flera av oss i forskningsgruppen arbetar med lungtransplantation i den kliniska vardagen och bristen på organ är ett stort problem och leder till dödsfall på väntelistan för lungtransplanterade så blev det i delarbete 4 intressant att titta på behandling av lungskada i samband med lungtransplantation i en djurmodell. Genom att cirkulera blod genom lungan i en maskin utanför kroppen (EVLP) och samtidigt filtrera blodet så skulle man kunna få skadade lungor att accepteras som donatorlungor istället för att de kasseras. Kliniskt har vi använt ett cytokin-filter för att minska inflammationsgraden i donatorlungan. Cytokiner är att likna vid inflammatoriska signalprotein i blodet som igångsätter och underhåller inflammation. Med tanke på cytokinernas roll i transplantationsbiologi undersökte vi hypotesen om att återställa skadade donatorlungor för att på så sätt öka donatorpoolen. Vi utvecklade, implementerade och validerade en EVLP och lungtransplantationsmodell på grisar som erhållit lungskada med LPS. Endast en annan grupp i världen har en lungstransplantationsmodell för gris som kan utvärdera

lungorna mer än 4 timmar efter transplantationen, och vår modell är den enda transplantationsmodellen som finns med hemodynamisk mätning under de tre dagar som uppföljningen fortlöper.

I denna modell inducerade vi ARDS med LPS hos donatordjuren. Efter en etablerad ARDS tar vi ut lungorna enligt kliniska riktlinjer. Vi utvärderade donatorlungorna i EVLP och därefter transplanterade vi lungorna. En grupp fick behandling med cytokinfilter under EVLP och efter transplantationen. Efter transplantation. Kontrollgruppen fick inte behandling med cytokinfilter. Intressant nog resulterade behandlingen vid både EVLP och efter transplantationen i en förbättrad lungfunktion medan de obehandlade djuren alla utvecklade akut lungskada efter transplantation som beskrivs som primär transplantatdysfunktion (PGD).

Med tanke på resultaten i den prekliniska studien fick vi etiskt godkännande för en klinisk prövning som vi ska börja inom kort. Vi tror att detta kommer att vara av stor betydelse för patienterna.

I delarbete 5 önskade vi att bredda spektrumet av studier i avhandlingen utforskade därför PFR hos sövda, nyopererade och lungfriska patienter i en klinisk randomiserad kontrollerad studie där vi undersökte olika ventilationsinställningar och påverkan på PFR. 30 patienter randomiserade till antingen volymkontrollerad ventilation (VCV) eller tryckkontrollerad ventilation (PCV) i 30 minuter inklusive en rekryteringsmanöver (RM). PFR -mätningar fortsatte när patienterna övergick till tryckreglerad volymkontroll (PRVC) och sedan tryckundersstödd ventilation (PSV) fram till extubation. Fördelningen av partiklar skilde sig mellan de olika ventilationslägena. Vi kan dra slutsatsen att mätning av PFR varierar mellan olika ventilationslägen samt att fördelningen av partiklarna också varierar. Låg PFR under mekanisk ventilation kan korrelera till en skonsam ventilationsstrategi. PFR ökar när patienten övergår från mekanisk ventilation till spontanandning, vilket troligtvis beror på rekrytering av alveoler när diafragman öppnar upp mer distala luftvägar. Artikeln är publicerad i ERJ Open Research.

Abbreviations

ABG	Arterial blood gases
ACT	Activated clotting time
AECC	American-European Consensus Conference
ALI	Acute lung injury
aPTT	Activated partial thromboplastin time
ARDS	Acute respiratory distress syndrome
AVR	Aortic valve replacement
BALF	Bronchoalveolar lavage fluid
BOS	Bronchiolitis obliterans syndrome
CABG	Coronary artery bypass grafting
C _{dyn}	Dynamic compliance
CO ₂	Carbon dioxide
COPD	Chronic obstructive pulmonary disease
DCD	Donation after circulatory death
DLTx	Double lung transplant
DO ₂	Oxygen delivery
EBP	Exhaled breath particles
ECMO	Extra corporeal membrane oxygenation
ELISA	Enzyme-linked immunosorbent assay
ELSO	Extracorporeal Life Support Organization
ET	Endo tracheal
EVLP	<i>Ex vivo</i> lung perfusion
FiO ₂	Fraction of inspired oxygen
H&E	Hematoxylin and eosin
H1N1	Influenza virus (swine flu)
H ₂ O	Water
HCl	Hydrochloric acid
HLTx	Heart and lung transplant
ICU	Intensive care unit
IFN-α	Interferon alpha
IFN-γ	Interferon gamma
IL	Interleukin
IPA	Infusion in pulmonary artery
ISHLT	The International Society for Heart and Lung Transplantation
LPS	Lipopolysaccharide

LTx	Lung transplant
LVEDP	Left ventricular end diastolic pressure
MAP	Mean arterial pressure
MPP	Mean pulmonary pressure
NPX	Normalized protein expression
O ₂	Oxygen
OCS	Organ care system lung protocol
OPC	Optical particle counter
OR	Operating room
PaCO ₂	Partial pressure of arterial carbon dioxide
PAH	Pulmonary arterial hypertension
PaO ₂	Partial pressure of arterial oxygen
PAWP	Pulmonary artery wedge pressure
PCR	Polymerase chain reaction
PCV	Pressure-controlled ventilation
PEA	Proximity extension assay
PEEP	Positive end expiratory pressure
PExA	Particle in exhaled air
PFR	Particle flow rate
PGD	Primary graft dysfunction
PIP	Peak inspiratory pressure
PRVC	Pressure-regulated volume control
PSV	Pressure support ventilation
PVR	Pulmonary vascular resistance
RBC	Red blood cells
RTLF	Respiratory tract lining fluid
SBP	Systolic blood pressure
SEM	Standard error of the mean
SLTx	Single lung transplant
SP-A	Surfactant protein-A
TIMP1	Tissue inhibitor metalloproteinase 1
TNF-a	Tumor necrosis factor alpha
V-A ECMO	Veno-arterial ECMO
VCV	Volume-controlled ventilation
VILI	Ventilator-induced lung injury
VO ₂	Oxygen consumption
V _t	Tidal volume

Introduction

The respiratory system

Anatomy and physiology

The lungs are, together with the gastrointestinal tract, a unique internal organ in the way in which they are in direct contact with the outside world and extremely exposed to the environment. Air entering the lungs is heated, humidified, and filtered from external substances before reaching the alveoli. Once the air reaches the alveoli, the gas exchange of oxygen (O₂) and carbon dioxide (CO₂) takes place between the alveoli and the capillaries. To be able to cope with the body's demands for ventilation, the area of the alveolar surface where gas exchange occurs can reach a size of approximately 70 m², ranging from 30-100 m² depending on the state of inflation, and consists of 300-800 million alveoli (1, 2)

my

The anatomy of the respiratory system begins at the mouth and nostrils and ends in the alveoli. Airways outside the thoracic cage are named the upper airways and inside the thoracic cavity they are the lower airways. From the nasal cavity, nasopharynx, oropharynx, laryngopharynx, trachea, bronchi, bronchioles, and terminal bronchioles there are the conducting airways divided into generations. 0-14, simply passing, humidifying and filtering the air. An intermediate section, 15-18, marks the transition to the respiratory pathway, and 19-23, where the gas-exchange occurs, also known as the Weibel classification (3). Surrounding the lungs there is a stiff cage consisting of 24 costae (12 on each side) originating from the 12 thoracic vertebra and fused together anteriorly with the sternum, protecting the vital organs from external trauma. Inside the thoracic cavity the lungs are covered and separated from each other with the visceral and parietal pleura forming a thin space in between, containing a small amount of fluid to reduce friction (4). In the caudal direction, the cavity consists of the diaphragm which is responsible for the primary respiratory work and which separates the thoracic organs from the abdominal organs (Figure 1).

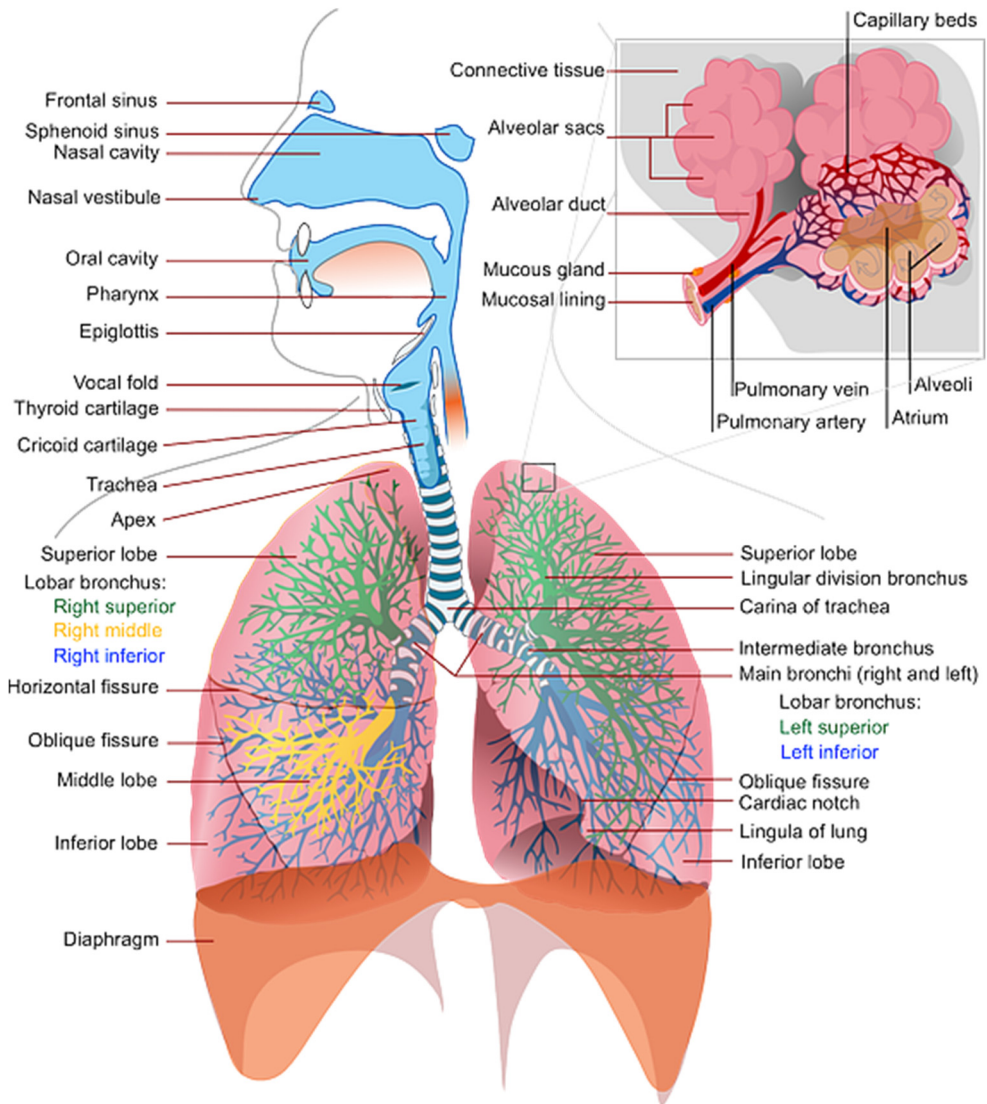


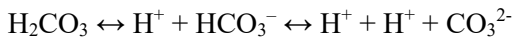
Figure 1. Anatomy of the respiratory system
 Image by Ciker-Free-Vector-Images from Pixabay

As described already in 1963 by Weibel, the distal respiratory tract receives warm, humidified and filtered air from the conducting airways. The respiratory airways contain between 300-800 million alveoli which make up 90% of the entire lung (5). The alveoli consist mainly of two different epithelial cell types, the type 1 pneumocytes which make up most of the alveolar wall where the gas exchange occurs and the type 2 pneumocytes which are responsible for secretion of surfactant which reduces surface tension and prevents the alveoli from collapsing. A smaller

number of neutrophilic cells are also present in the lung and are involved in the initiation of immune response (4).

Physiology

Gas exchange with O₂ and CO₂ takes place over the epithelial-endothelial membrane separating the alveoli and the capillaries. Besides supplying the cells in the body with O₂ and removing CO₂, the lungs also regulate the pH balance in the body almost instantaneously by increasing or decreasing ventilation, thereby altering the CO₂ level:



Respiratory tract lining fluid

Respiratory tract lining fluid (RTLTF) is a fluid mucus layer covering the epithelial surface of the alveoli and is known to protect the most vulnerable parts of the lung from airborne particles and pollutants. Together with the ciliary cells it is responsible for removal of undesired substances in the lungs. RTLTF consists primarily of proteoglycans and mucin glycoproteins secreted from submucosal glands (4, 6).

Phospholipids are one of the main components in the bilayer of cell membrane due to their surface-active properties. A unique substance in the lung, surfactant, as mentioned previously, is secreted from type 2 pneumocytes and is an important component of RTLTF because of its capacity to lower surface tension. Most studies on surfactant have been performed in the neonatal field as a result of its life-saving properties (7, 8)

Proteins are another important component of RTLTF and among several present in the fluid, albumin is important for the distribution of fluid between compartments and for transporting substances (9, 10). It reaches the alveoli by passive transport after being synthesized in the liver.

RTLTF also contains several antioxidants, such as glutathione, as a mechanism of defence in neutralizing gaseous pollutants including ozone and nitrogen dioxide (11).

Mechanical ventilation

Normal breathing is accomplished by the diaphragm as the primary respiratory muscle creating a negative intrathoracic pressure, as a result of which air is sucked into the lungs. The term ‘mechanical ventilation’ refers to an invasive procedure with endotracheal intubation and positive pressure ventilation from a machine to

ensure adequate delivery of O₂ and removal of CO₂. Mechanical ventilation is used for many purposes, such as general anesthesia during and after surgery, for respiratory failure in the intensive care unit (ICU) following pneumonia or acute respiratory distress syndrome (ARDS) and for altered consciousness following intoxication or brain injury. This type of ventilation has revolutionized modern healthcare: looking back to the early 1900s, the iron lung used negative pressure around the body in a closed container making it very hard to manage the patient. In the 1950s, pioneers from Scandinavia made a huge contribution to health care when a polio pandemic forced two Danish physicians at Blegdam Hospital in Copenhagen to set up one of the world's first ICUs with positive pressure ventilation, as a result of which the mortality rate fell from 80% to around 40% (12, 13) and, at the same time, the first modern ventilator was invented, the Engström ventilator.

Ventilation modes

Depending on the manufacturer and model of the ventilator, there are different ventilation modes. The most widely studied modes throughout the world are pressure-controlled ventilation (PCV) and volume-controlled ventilation (VCV) (14). Positive end expiratory pressure (PEEP) is almost mandatory in all forms of mechanical ventilation and prevents the alveoli from collapsing when the patient is in the supine position and thereby also prevents pulmonary shunts of blood flow (15-17). Many studies have shown that PEEP is beneficial in mechanical ventilation, although the optimal level of PEEP is still subject to debate (14, 18, 19).

Pressure-controlled ventilation (PCV)

PCV is a ventilation mode with a target pressure where the ventilator delivers a decelerating flow with a volume that increases until the pre-set inspiratory pressure is reached. The volume of air in each breath, tidal volume (V_t), is then dependent on lung compliance and resistance and may vary depending on the condition of the patient. Exhalation is a passive movement by the recoil of the lungs, muscles and the thoracic cavity.

Volume-controlled ventilation (VCV)

VCV is a ventilation mode with a target volume where the ventilator delivers a constant flow and a volume increase until the pre-set V_t is reached. In contrast to PCV, with VCV the inspiratory pressure is dependent on resistance and compliance and may vary with the condition of the patient.

Pressure-regulated volume control (PRVC)

PRVC is a combined ventilation mode, similar to both VCV and PCV in the way in which a desired V_t is set and the ventilator administers that volume of air with the lowest possible pressure by a decelerating flow. This method ensures adequate V_t and low pressure, which is considered to be gentler to the lungs (18).

Pressure support (PS)

PS is a method that requires a spontaneously breathing patient to initiate his or her own breath and the ventilator senses this by changes in pressure and flow and supports the patient's breathing by additional positive pressure to ensure adequate V_t .

Ventilator-induced lung injury (VILI)

Mechanical ventilation is not without consequences to the lungs. The technique of inflating the lungs with positive pressure can cause injury to them by volutrauma/barotrauma with over-distension of the alveoli, and atelectrauma with deformation of alveoli as a result of their repeated opening and closing (20-22). This interaction of mechanical forces acting on the lung tissue is known to cause ventilator-induced lung injury (VILI). By being aware of pressure, volume and PEEP, studies have shown a lower incidence of postoperative complications and VILI by reducing V_t and using a low-to-moderate PEEP (23). Choice of ventilation mode is still a much-debated topic, even though the evidence may be in favor of PCV (24, 25).

Cardiopulmonary monitoring

Adequate oxygenation to the organs is dependent upon oxygen delivery (DO_2) and the ability of the cells to utilize the O_2 delivered which is called oxygen consumption (VO_2). If there is an imbalance between delivery and consumption, tissue hypoxia can occur. Reasons for insufficient O_2 delivery can be poor pulmonary function, poor cardiac function, or poor transportation capacity (anemia).

Cardiopulmonary monitoring with hemodynamic measurements can be of great value when assessing patients who are at risk of hypoxia, in the ICU or in the operating room (OR) and allows for prompt recognition and the possibility of optimizing tissue oxygenation at the bedside.

Cardiopulmonary circulation

By dividing the circulation into two separate systems, the description can be made easier to visualize:

Left heart

The left heart receives oxygenated blood from the pulmonary circulation to the left atrium, passes it through the mitral valve to the left ventricle, which is a high-pressure pump with a thick wall. The blood is then ejected into the aorta through the aortic valve and into the systemic circulation, which is a high-pressure system. While in the systemic circulation the red blood cells (RBC) deliver O₂ to the tissues as they pass through the small capillaries and simultaneously bind CO₂ that is produced in the cells.

The output from the left ventricle is measurable with an arterial line connected to a pressure transducer, which can convert a physical signal (i.e., arterial or pulmonary pressure) to an amplified and filtered electrical signal displayed on a monitor as a waveform with an additional numeric value.

Right heart

The right heart receives deoxygenated blood from the systemic circulation to the right atrium and passes it through the tricuspid valve into the right ventricle, which is a volume pump with a thin wall. The blood is then ejected into the pulmonary artery through the pulmonic valve into the pulmonary circulation, which is a low-pressure system. While in the pulmonary circulation passing through the capillaries in close proximity to the alveoli, O₂ and CO₂ pass over the membrane and the blood becomes oxygenated again and CO₂ leaves the body through the expired air.

The output from the right ventricle is measurable in a similar fashion, as described above, but the opportunities that arise from using a pulmonary artery catheter are much greater.

Pulmonary artery catheter

The pulmonary artery catheter is known as a PA-catheter or Swan-Ganz catheter after its inventors Dr H.J.C Swan and Dr William Ganz who made the floating balloon catheter accessible at the bedside without fluoroscopy (X-ray) in the 1970s; shortly after the PA-catheter evolved to be able to measure cardiac output with thermodilution.

The catheter is inserted through a central vein and placed into the right atrium where central venous pressure is measurable, and the balloon is inflated and further advanced into the right ventricle. Here the right ventricular pressure can be measured before the catheter is advanced further into the pulmonary artery where

systolic, diastolic, and mean pulmonary pressures are measured constantly. The balloon is then deflated and used for right heart measurements and continuous monitoring of cardiac output.

The balloon can also remain inflated, and the catheter used for left heart monitoring by advancing it further into the pulmonary circulation until the size of the balloon exceeds the diameter of the vessel and a pulmonary artery wedge pressure (PAWP) is obtained. Since the tip of the catheter is located past the balloon, PAWP now reflects the pressure in the left atrium and when the mitral valve opens in diastole, left ventricular end diastolic pressure (LVEDP) can be measured, as seen in Figure 2.

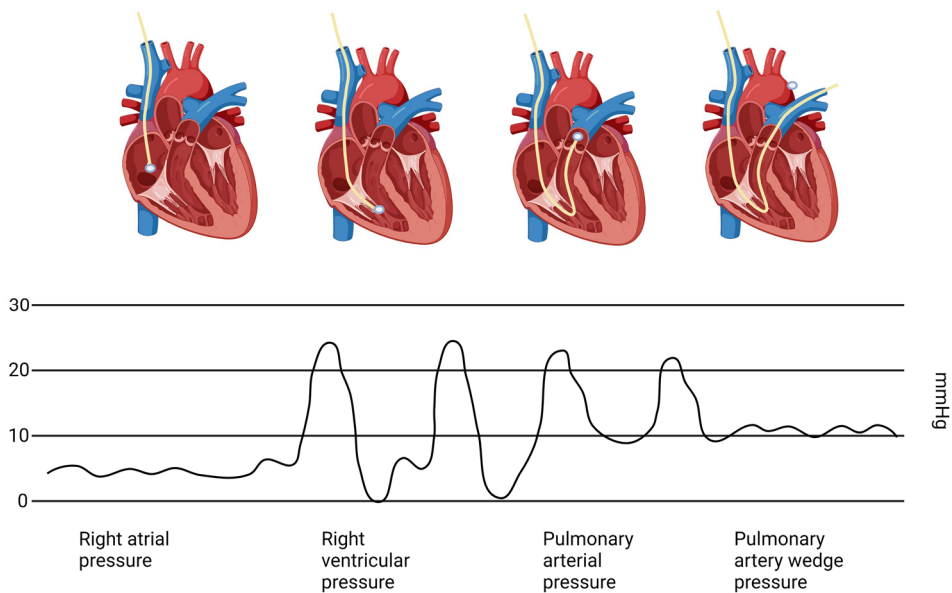


Figure 2. Pressure curves with normal values with a Swan-Ganz catheter

From left: right atrial pressure 2-6 mmHg, right ventricular pressure systolic 15-25 mmHg and diastolic 0-8 mmHg, pulmonary arterial pressure systolic 15-25 mmHg and diastolic 8-15 mmHg, pulmonary artery wedge pressure 8-12 mmHg. Created with BioRender.com

The use of a Swan-Ganz catheter has been subject to debate. Some studies have concluded that the routine use of a Swan-Ganz catheter is not necessary and is associated with increased complications and even death in patients with acute coronary syndrome and in other non-cardiac high-risk patients. However, these findings may be because the catheter has been used by inexperienced personnel and has been subject to overuse as a routine procedure in the intensive care environment.

Other studies have concluded that the use of a Swan-Ganz catheter remains recommended in the hands of trained personnel for patients in cardiogenic shock, those with severe chronic heart failure supported by inotropic and vasopressors, for the differential diagnosis of pulmonary arterial hypertension (PAH), ARDS and in monitoring heart and lung transplant patients (26-28). Just recently, a large retrospective study involving almost 26,000 patients receiving right heart catheterization monitoring due to cardiogenic shock showed improved outcome with respect to lower mortality, lower stroke rate and lower readmission rate compared with patients who did not receive the technique (29).

Acute respiratory distress syndrome (ARDS)

ARDS is a life-threatening condition due to inflammation and impaired gas exchange in the lungs, as a result of which severe hypoxemia occurs. This syndrome, first described in 1967 by Ashbaugh et al. (30), has been studied and debated intensively over the last few decades regarding pathogenesis, classification and treatment. The condition is a syndrome with a multifactorial cause. ARDS might be triggered by direct causes such as pneumonia, aspiration, drowning and inhaled toxic substances, but also from indirect triggers, such as sepsis, trauma, burns and transfusion reactions to name but a few (31, 32). This acute life-threatening lung injury almost always requires mechanical ventilatory support.

Definition

In 1994, the American-European Consensus Conference (AECC) first defined ARDS as acute onset of hypoxemia (partial pressure of arterial oxygen [PaO_2]/fraction of inspired oxygen [FIO_2] ≤ 200 mmHg) with bilateral infiltrates on chest X-ray and without evidence of left heart failure. Acute lung injury (ALI) was defined using similar criteria but with $\text{PaO}_2/\text{FIO}_2 \leq 300$ mmHg (33).

Following doubt regarding the reliability of this definition, a panel of experts assembled in 2011 from the Society of Critical Care Medicine, the American Thoracic Society and the European Society of Intensive Care Medicine and developed the Berlin definition of ARDS using a consensus process, the results of which were published in 2012 (34).

To define ARDS, the Berlin definition requires all four criteria to be present:

Timing:

Respiratory symptoms within 1 week of a known clinical insult, or new or worsening symptoms during the past week.

Chest imaging:

Bilateral opacities not explained fully by pleural effusions, lobar/lung collapse, or pulmonary nodules.

Origin of edema:

Respiratory failure not explained fully by cardiac failure or fluid overload. An objective assessment (e.g. echocardiography) to exclude hydrostatic pulmonary edema is required if no risk factors for ARDS are present.

Oxygenation:

A moderate-to-severe impairment of oxygenation must be present, as defined by the $\text{PaO}_2/\text{FiO}_2$ ratio.

The Berlin definition had a better prediction for mortality with increased percentage of mortality associated with increasing severity of ARDS: mild 27%, moderate 32%, and severe 45% with 95% confidence interval (CI) compared to the AECC definition.

Classification

The severity of the hypoxemia classifies the severity of ARDS as described by the Berlin definition of ARDS.

Mild ARDS:

$200 \text{ mmHg} < \text{PaO}_2/\text{FiO}_2 \leq 300 \text{ mmHg}$, with a PEEP or continuous positive airway pressure $\geq 5 \text{ cm water (H}_2\text{O)}$.

Moderate ARDS:

$100 \text{ mmHg} < \text{PaO}_2/\text{FiO}_2 \leq 200 \text{ mmHg}$, with a PEEP $\geq 5 \text{ cm H}_2\text{O}$.

Severe ARDS:

$\text{PaO}_2/\text{FiO}_2 \leq 100 \text{ mmHg}$ with a PEEP $\geq 5 \text{ cm H}_2\text{O}$.

Pathophysiology

Characteristic of ARDS is an acute inflammatory state with diffuse alveolar injury due to diverse range of causes, as mentioned above, with a release of

proinflammatory cytokines such as tumor necrosis factor alpha (TNF- α), and interleukins IL-1 β , IL-6 and IL-8 which, in turn, recruit polymorphonuclear cells (i.e. neutrophils) with endothelial and epithelial barrier damage and alveolar edema with formation of hyaline membranes (32). This leads to impaired gas exchange and decreased compliance. This stage is also known as the exudative stage and lasts for days to a week and is followed by the proliferative stage after approximately 10-14 days with reabsorption of edema and proliferation of type 2 pneumocytes and collagen deposition. Following this there is a chronic phase with alveolar repair and resolution of edema with some degree of fibrosis (31, 35).

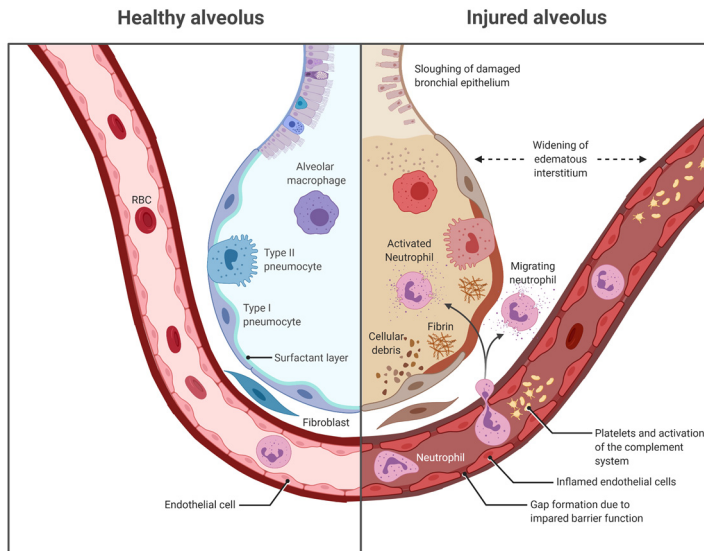


Figure 3. Alveolar changes in acute respiratory distress syndrome (ARDS)

The right side of the Figure shows endothelial and epithelial damage infiltration of immune cells and widening of the tight junctions with gap formation leading to edema. Created with BioRender.com

Treatment

As a result of the high mortality and multifactorial causes, there is a range of treatments available for ARDS which are theoretically appealing, but which have not always proved useful. The following three interventions have earned their place as treatment methods.

Protective ventilation

Protective ventilation means ventilating the patient with low V_t between 4-6 mL/predicted body weight and with low plateau pressures between 25-30 cm H_2O

which have been shown to reduce mortality in ARDS and ALI (36) and reduce proinflammatory cytokines (37, 38). By preventing over-distension of the alveoli, barrier properties between the endothelium and epithelium are preserved, which can prevent VILI (36, 37, 39, 40). The term ‘open lung concept’ refers to the idea of using low V_t and high PEEP to avoid over-distension and, at the same time, reduce the periodic atelectasis during exhalation, but consensus has not been reached regarding levels of PEEP (36, 39).

Prone position

Ventilating patients in the prone position helps restore collapsed areas of the dorsal part of the lung and is also favorable for transpulmonary pressure. The prone position is associated with improved oxygenation and improved survival in patients with ARDS (41, 42).

Extra corporeal membrane oxygenation (ECMO)

Extra corporeal membrane oxygenation (ECMO) is a circulatory and ventilatory support to secure oxygenation while the lungs recover from injury. Used as rescue support in patients with severe ARDS, ECMO has been used with success (43, 44).

Other therapies

High frequency oscillatory ventilation, neuromuscular blocking agents, fluid conservative therapy, corticosteroids and mesenchymal stem cells are treatments that have been proven ineffective or which have still not been evaluated fully.

ECMO

ECMO is a system of life support that circulates and exchanges gases in the blood outside the body. ECMO itself is not a treatment and does not cure the underlying cause but supports the organs with oxygenated blood in order to give the heart, lungs, or both, time to heal.

Historically, ECMO is derived from the heart-lung machine used in cardiopulmonary bypass during cardiac surgery; the first successful cardiac operation with pulmonary bypass was in 1953 by Gibbon. In 1971, Hill reported the first adult survivor on ECMO and in 1976, Bartlett reported the first infant patient to benefit from ECMO support. The first trial of ECMO support in patients with respiratory failure compared to conventional ventilation was initiated by the American National Heart, Lung and Blood Institute and the results that were published showed an overall 90% mortality and no differences between groups (45). Even though the use of ECMO decreased markedly over the following years, some clinicians continued to develop and improve the technique and some success was

found in the pediatric ECMO centers which resulted in the founding of the Extracorporeal Life Support Organization network in 1989. The use of ECMO in adult patients took off again in 2009 with the swine flu (H1N1) pandemic and, at the same time, a large prospective trial was published in the *Lancet* (CESAR trial [Conventional ventilatory support versus extracorporeal membrane oxygenation for severe adult respiratory failure]) showing that transferring patients with ARDS to a specialist center with the ECMO system available improved outcome.

Today, ECMO has several indications ranging from ventilatory support in patients with ARDS and after lung transplantation, and circulatory support after cardiac surgery and heart transplantation. ECMO is now used as extracorporeal cardiopulmonary resuscitation and has gained more acceptance in patients with septic shock.

Managing patients on ECMO requires anticoagulation and the most widely used drug by far is heparin. Heparin prevents coagulation of the blood and is necessary to be able to run the ECMO circuit for several days and even weeks. The patient's coagulation status is monitored by activated clotting time (ACT) and activated partial thromboplastin time (aPTT).

Veno-arterial ECMO (V-A ECMO)

Veno-arterial ECMO (V-A ECMO) is a system whereby blood is taken from a vein and returned to an artery. V-A ECMO can be peripheral or central. In peripheral V-A ECMO, blood is taken from a cannula inserted in the femoral vein, with the tip placed in the inferior vena cava, and returned via a cannula inserted in the femoral artery, with the tip placed in the abdominal aorta. In central V-A ECMO, the patient has an open chest, and cannulas are inserted directly into the inferior vena cava through the right atrium and into the aorta. This modality can offer circulatory support to a failing heart by using a pump and support gas exchange to a failing lung with the use of an oxygenator. V-A ECMO is associated with greater risks. Dislodgement of the arterial cannula will have greater consequences in terms of bleeding. Air embolus in the arterial line can be fatal compared to air in the venous line. In addition, in the case of malfunction of the pump, blood can flow in the opposite direction driven by the patient's own blood pressure.

Veno-venous ECMO (V-V ECMO)

Veno-venous ECMO (V-V ECMO) differs from V-A ECMO in three important ways. Cannulation is made solely on the venous side and in most cases via peripheral cannulation. Blood is usually taken from the cannula in the femoral vein and returned through a cannula in the right jugular vein. Both tips of the catheters are placed in the inferior and superior vena cava, respectively, and particularly the

returning cannula is placed in close proximity to the right atrium. If the tips are placed too close to each other, there is a risk of re-circulation. V-V ECMO offers only gas exchange by passing blood through an oxygenator. Oxygenated blood is returned to the right atrium and mixed with the patient's own blood and passed through the lungs to the systemic circulation.

Particles in exhaled air (PExA)

Exhaled breath as a non-invasive technique

To date, several different techniques have been explored for monitoring the status of the lungs in a non-invasive manner. The technique of sampling exhaled air has emerged as an attractive alternative to conventional techniques because it is non-invasive and allows repeated sampling with ease and at no risk to the patient.

A well-studied procedure is exhaled breath condensate (EBC). EBC is collected from exhaled breath through a refrigerated device that cools exhaled air into liquid. The EBC collection procedure is non-invasive, does not modify airway surface, only requires tidal breathing, and is considered safe without adverse effects (46). Variations in spontaneous breathing pattern may affect EBC collection and composition (47) and it is therefore recommended to use low airflow, normal or large V_t and slow breathing rate because the collection of EBC becomes increasingly inefficient with increasing flow rates (48) with less time to condensate the exhaled air. Low V_t with high dead-space ventilation favors EBC sampling from conducting airways to a greater extent rather than from respiratory parts which results in EBC dilution (49).

Exhaled breath particles (EBPs) contain an aerosol of small particles detectable with an optical particle counter (OPC) or laser. Laser particle counting revealed that micron- and submicron-sized droplet particles are formed in the exhaled breath. Such particles serve as the only evidence of nonvolatile components in the EBC (50). The main components of EBC include condensed water vapor, volatile molecules (such as nitric oxide, carbon monoxide, and hydrocarbons), and nonvolatile molecules (such as urea, glutathione, leukotrienes, prostanoids, and cytokines) (46, 51). However, condensation might be an inefficient method to collect non-volatiles because many particles pass through the condenser without being collected.

However, knowledge of the biomarkers' origin is important in order to understand and interpret the data correctly. To date, both exhaled volatile compounds and EBP have been explored for diagnosing lung diseases, such as asthma, chronic obstructive pulmonary disease (COPD), pulmonary fibrosis and lung cancer.

While volatile compounds can offer some insight into the disease process, exhaled particles may offer more specific knowledge of it since a variety of different biological molecules can be measured.

Exhaled particles are formed in the airways and have been shown to reflect the overall chemical composition of the RTLF. These particles can range from nano- to microscale in size and have been shown previously to differ in their composition, depending on the disease status (52, 53).

A new non-invasive method, particles in exhaled air (PExA), has been shown to be suitable for measuring and collecting the exhaled particles for further compositional analysis. The PExA method has been used previously to measure proteins and lipids non-invasively as biomarkers in RTLF collected from the small airways. Exhaled particle number concentrations in the size interval 0.30-2.0 μm are recorded in real time (54). Thus, PExA might be a suitable tool for monitoring the status of the lung tissue.

Our group has recently modified the PExA device in order to make it capable of measuring EBP in subjects undergoing mechanical ventilation. The modified PExA device was first evaluated pre-clinically using pigs undergoing different ventilation modes and different pressures (55). The method was also used during *ex vivo* lung perfusion (EVLP) and was able to detect different exhaled particles in different ventilation modes in healthy lungs (56). The PExA device was evaluated over several days in preclinical sessions using pigs. The exhaled particles remained stable over the days in pigs without lung injury. One animal developed a significant increase in exhaled particles which began 24 hours before it developed clinical signs of ARDS (55). The results from the pig that showed a different particle pattern even prior to clinical signs of ALI or ARDS was the starting point for my PhD thesis. Could the PExA method be used as a diagnostic tool, as a bedside method in the ICU for patients with ALI or ARDS? And could specific biomarkers for ALI and ARDS be found in the EBP or perhaps also new biomarkers?

The modified PExA device has been investigated in a clinical trial and was shown to be capable of measuring EBP in patients undergoing mechanical ventilation in the first few days following lung transplantation (LTx) (57).

In addition to biomarker identification, the PExA device is also capable of measuring particle flow and particle characteristics (i.e. size distribution) in real time. This could allow for the identification of early markers of ALI.

In proof-of-principle studies, our group has previously collected PExA data from 13 patients on the first 3 days following LTx. In the majority of patients, there was a low amount of EBP which increased slightly over the first 3 days (Figure 4a). Interestingly, in one patient who developed primary graft dysfunction (PGD) within the first 48 hours following LTx, we saw an initial increase in the amount of EBP collected over the same time period during the first day as compared to our larger

pilot cohort (Figure 4b). This case report illustrates the potential power of PEXA technology in mechanically ventilated patients in diagnosing and monitoring PGD development in real time.

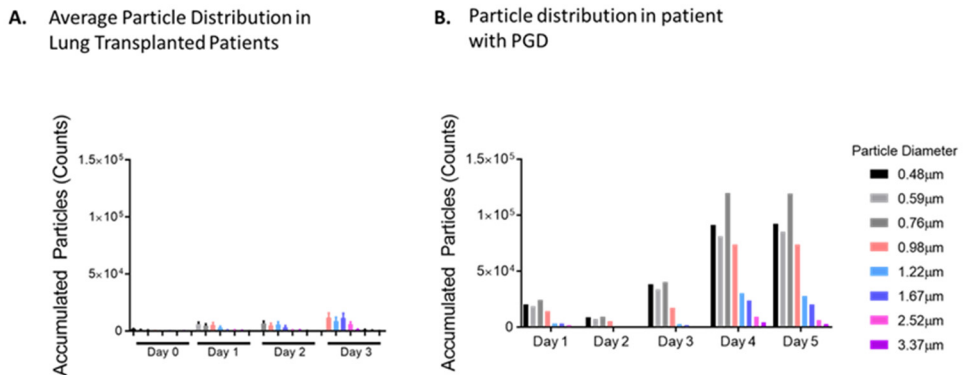


Figure 4. Particles in exhaled air (PEXA) analysis in transplanted patients with primary graft dysfunction (PGD) PEXA analysis on mechanically ventilated patients can be used to monitor PGD development. a) Average particle distribution in lung transplanted (LTx) patients; b) particle distribution in a patient with PGD.

PEXA analysis in chronic rejection in lung transplant recipients

Chronic organ rejection remains the most significant hurdle to the long-term success of LTx. The PEXA device was used previously to sample surfactant protein-A (SP-A) and albumin in the exhaled breath of a small cohort of patients who underwent LTx (PEXA collection at 6 months' post-transplantation) (58). SP-A and albumin were chosen since they are both major components of the distal RTLF. Interestingly, the recipients who developed bronchiolitis obliterans syndrome (BOS) had significantly lower average levels of SP-A compared to recipients who did not develop BOS at a 1-year follow-up. While this study established the feasibility of measuring proteins in exhaled breath which could be relevant for monitoring the status of LTx recipients non-invasively, SP-A levels in four of the seven patients who developed BOS at 18 months' post-transplantation were in the same range as those of healthy controls and of those patients who did not develop BOS. Thus, SP-A might not a suitable biomarker for predicting the development of BOS in a reliable manner. Identification and validation of new biomarkers, which are more accurate for recognizing and predicting the development of acute and chronic allograft dysfunction, are needed urgently.

The modified PEXA device, used in conjunction with mechanical ventilation, is connected between the patient and ventilator in a series circuit with a Y-connector on the endotracheal tube containing a one-way valve, which prevents rebreathing (Figure 5). This modified ventilatory unit has been tested for safety and feasibility

in both the preclinical and clinical settings (55-57, 59). Even though mechanical ventilation is an invasive treatment, PExA itself is non-invasive and it is possible to use it as a bedside tool in the environment of the OR or ICU.

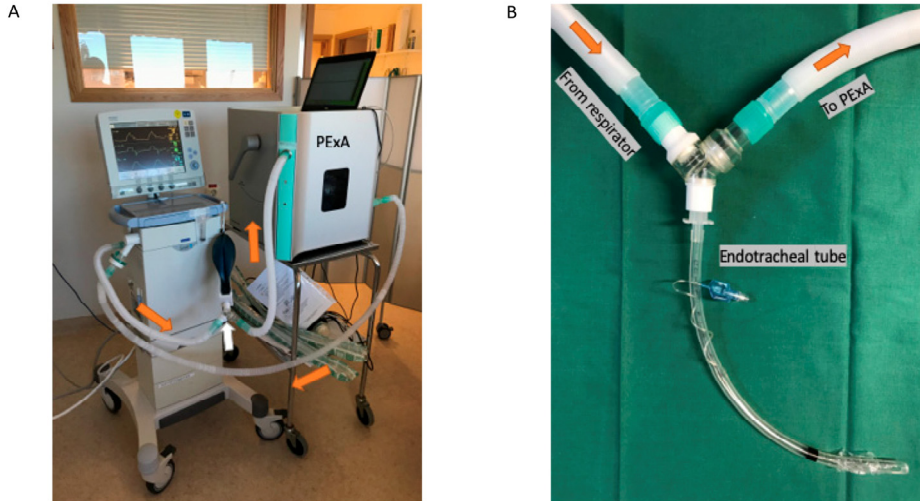


Figure 5. Particles in exhaled air (PExA) device in conjunction with ventilatory circuit

a) Shows the ventilatory circuit connected to PExA with the orange arrows show the direction of airflow. b) Shows the endotracheal tube with the non-rebreathing Y-connector. Copyright Ellen Broberg with permission.

Different methods in the search for biomarkers

PExA were collected using a two-stage inertial impactor, described in previous articles (53, 54, 60-62). Mass spectrometry was used to quantify the phospholipids di-palmitoyl-phosphatidyl-choline and palmitoyl-oleoyl-phosphocholine. The method is described in previous articles (56, 59). Albumin and SP-A were analyzed by enzyme-linked immunosorbent assay (ELISA), described in previous articles (53).

A major problem in analyzing EBP relates to the low number of particles collected. The range of particles collected using the PExA device is in the range of 5-200 ng. To be able to detect proteins with ELISA, relatively large amounts of the protein that are being analyzed are required. Given the small amounts of proteins that we collect, we began to investigate analysis methods that could detect minute amounts.

Proximity extension assay (PEA) technology

As a result of the low number of particles collected, interest in the proximity extension assay (PEA) technology increased. PEA technology has been developed and is executed at Olink[®] proteomics with the headquarters in Uppsala, Sweden. The unique technology behind Olink[®] Target 96 panels enables high-throughput, multiplex immunoassays that measure 92 proteins across 96 samples simultaneously using only 1 μL of serum, plasma, or almost any other type of biological sample. Each one of the 96 oligonucleotide antibody pairs contains unique DNA sequences allowing hybridization only to each other. Subsequent proximity extension will create 96 unique DNA reporter sequences which are amplified by real-time polymerase chain reaction (PCR). A limiting factor of multiplexed immunoassays is the antibody cross-reactivity, which restricts the degree of multiplexing of most assays to below 10-plex. Cross-reactive events will not be detected with Olink's panels since only matched DNA reporter pairs are amplified with real-time PCR. This allows for scalable multiplexing without loss of specificity and sensitivity.

Animal models of ALI and ARDS

Animal models of ALI and ARDS have been used for decades to try to mimic a clinical scenario and for understanding of the underlying pathogenesis. Studies involve different species ranging from rodents, which can be handled by scientists without medical training at a low cost, to expensive large animal models such as pigs or sheep that often require anesthesiological expertise.

Since ALI and ARDS have such a broad spectrum of causes, many different lung injury models have been tested over the years. Direct causes of ARDS can be pneumonia, aspiration, smoke inhalation and drowning, while indirect causes include sepsis, major trauma, pancreatitis, and adverse reactions to transfusion products (transfusion-related acute lung injury) (32, 33).

Clinical data state that pneumonia and gastric aspiration are responsible for most cases of direct lung injury, while sepsis is the major reason for indirect lung injury (32, 63). There is a substantial overlap, and it might be difficult to distinguish between causes, but studies have shown that > 50% of ARDS is caused by a direct lung injury and up to 80% of ARDS patients also have sepsis (63, 64).

Porcine models of ALI and ARDS

Three different large animal models will be described in this thesis and more specifically in the Methods section. They were chosen for their clinical relevance and their common appearance in the literature (65-67).

Lipopolysaccharide (LPS) induced lung injury

Lipopolysaccharide (LPS), also known as endotoxin, is a large molecule found in great numbers in the outer membrane of Gram-negative bacteria, such as *Escherichia coli*, and is known to have barrier properties to protect the bacteria from hydrophobic compounds, such as antibiotics (68). LPS is also the most abundant antigen on the surface of many Gram-negative bacteria and induces a strong inflammatory response by the innate immune system to help the host overcome an infection. However, an imbalance in the immune response with excessive inflammation may be devastating to the host, as seen in septic shock and ARDS. Several studies have used LPS, both intravenously to mimic a sepsis-induced ARDS or/and intratracheal administration to mimic pneumonia (69-71).

After injection of LPS into a central vein, constriction of the pulmonary vascular bed is measurable with an increase in pulmonary artery pressure and pulmonary vascular resistance (PVR) (72). Vascular endothelia show signs of apoptosis (73, 74) and, simultaneously, a strong systemic inflammatory reaction is induced with an increase in cytokines and neutrophils (75).

Saline lavage induced lung injury

Depletion of surfactant by repeated saline lavage is a well-known method to study lung physiology (76). In the absence of surfactant, surface tension increases and makes the alveoli more prone to collapse.

Lavage is performed with warm (37°C) isotonic saline (30-40 mL/kg) and repeated every 10 min until hypoxia has reached the desired level. The number of lavages can differ, depending on how much hypoxemia the animal can tolerate but a mean of eight lavages has been described (65).

By adding harmful ventilation (i.e. barotrauma and atelectrauma) and creating additional VILI, a more sustained lung injury is obtained since only repeated lavage tends to be reversible (77).

Used with lavage alone, this model has little effect on the cytokine response and there is less infiltration of neutrophils.

Gastric-aspiration induced lung injury

Aspiration of gastric contents is not unusual among critically ill patients and gastric aspiration is a well-known risk factor for ALI and ARDS (78, 79). In animal models, it is common to use surrogates such as hydrochloric acid (HCl) to replace actual

gastric acid. Even if the pH can be adjusted to the level that is in the ventricle, which is around 1.5-2, some properties that are in the gastric contents will be lost that might impose additional harm to the lungs in the case of aspiration.

Gastric-aspiration induced lung injury can be performed by instilling gastric juice visually in all lobes of the lung, preferably with the use of a bronchoscope.

Compared to apoptotic cells in the LPS model, this model shows signs of necrosis in the epithelial cell layer and also infiltration of neutrophils and edema.

Pulmonary arterial pressures rise slowly together with PVR, but hemodynamic changes tend to be very modest.

Lung transplantation

During the last couple of decades, improved treatment with immunosuppression, improved surgical technique and advancements in graft preservation have made LTx the golden standard as the final treatment for end-stage pulmonary disease. LTx can be carried out as double-lung transplant (DLTx), single-lung transplant (SLTx) and a combined heart and lung transplant (HLTx). More diagnoses are now being considered for LTx including COPD/pulmonary fibrosis followed by cystic fibrosis, alpha-1 antitrypsin deficiency, pulmonary sarcoidosis and PAH (80).

Donor organ scarcity

As with most organ donation, scarcity of organs is the main limiting factor to the number of transplants performed, and this applies especially to LTx (81). It is estimated that only 15-20% of possible lung donors are harvested for transplant, compared with kidneys and hearts at rates of 80% and 30%, respectively (82). The possible reasons for this low number of lungs suitable for donation is probably due to complications during and after the brain death process, such as neurogenic pulmonary edema, VILI, gastric aspiration, blood transfusions and intravenous fluid while the patient is being treated with mechanical ventilation (83, 84).

According to Eurotransplant, in 2020 only half of the patients with end-stage pulmonary disease on the waiting list received an organ. The remaining 50% of the patients were either re-listed, unfit for LTx and taken off the list or died while waiting. This illustrates the urgent need for increasing the availability of donor lungs.

Donor pool can be expanded

In addition to extended criteria for selecting donors, another indication for LTx that has arisen in recent years is re-transplantation of patients with graft dysfunction. Due to a growing demand and donor scarcity, ethical dilemmas have developed with regard to how to distribute organs (85).

Making more organs available for LTx is of particular interest. One method is donation after circulatory death (DCD) which in some centers accounts for 20% of LTx (86) and refers to retrieval of organs from patients with confirmed death due to circulatory criteria (87).

The other way to make more organs available for LTx is by improving graft preservation and making initially rejected lungs suitable for transplantation.

Ex vivo lung perfusion

Currently *ex vivo* lung perfusion (EVLP) is the preferred machine perfusion method of evaluating whether a donor lung is suitable for transplantation. Lungs from DCD (88, 89) or lungs that were initially rejected due to poor blood gases are the type of situations where EVLP has been used successfully.

The first clinical application of EVLP was performed by Professor Stig Steen in Lund, Sweden, at the beginning of the 21st century resulting in six patients receiving reconditioned lungs. The EVLP technique has been used successfully by other research groups in the world, leading to new modifications and extended protocols, among them the Toronto group in Canada.

Machine perfusion provides a treatment platform to restore damaged organs. The concept behind machine perfusion is dynamic reconditioning and repair through restoring blood flow of the donor organ by connecting it to a pump with the possibility of adding O₂ and therapeutic agents. Besides restoring organs and improving organ quality, machine perfusion has the potential to make initially discarded organs suitable for transplantation.

The second benefit is the possibility of pre-transplantation viability assessment of the donor organ ‘while on pump’ to prevent unnecessary transplantations with an organ that will never function in the recipient.

The third benefit is the possibility of extending the time until transplantation, for example to provide daytime surgery or longer transportations abroad. During EVLP, the donor organ is connected to a perfusion device that pumps perfusate solution continuously through the organ. Machine perfusion can be performed at different temperatures. In contrast to static cold storage, hypothermic machine perfusion may be a more efficient way to cool the donor organ while metabolic and toxic waste products are washed out. During normothermic machine perfusion, the temperature

is within physiologic range, which increases metabolic activity and allows for active repair. Normothermia is often preferred when using machine perfusion as a treatment platform to restore organs. As normothermia leads to metabolic activity, an oxygenated perfusate is essential. Either whole blood-based perfusate (cellular), containing washed and leukocyte-depleted RBC, or acellular perfusion solution can be used. Additional substances, such as antibiotics, vitamins, prostaglandins, bicarbonate and heparin may be added to provide a suitable environment for active repair.

For EVLP there are currently three clinically applied protocols: the Lund protocol, the Toronto protocol and the Organ Care System Lung protocol (OCS) (90).

Table 1. Protocol of ex vivo lung perfusion (EVLP)

Three clinically applied protocols for EVLP: the Toronto protocol, the Lund protocol and the Organ Care System Lung Protocol (OCS).

Protocol of ex vivo lung perfusion			
	Toronto	Lund	OCS
	Perfusion		
Perfusate	Steen solution 2000 mL	Steen solution 2000 mL	OCS lung solution 1500 mL
Red blood cells	No	Yes, hematocrit of 15	Yes, hematocrit of 15-25
Pump	Centrifugal	Roller	Piston
Target flow (L/min)	40% of cardiac output	100% of cardiac output	2-2.5 L/min
Pulmonary artery pressure (mmHg)	≤15 or flow dictated	≤20	≤20
Left atrium pressure (mmHg)	3-5 (left atrium closed)	0 (Left atrium open)	0 (Left atrium open)
	Ventilation		
Mode	VCV	VCV	VCV
PEEP (cmH₂O)	5	5	5
Respiratory rate (b/min)	7	10 - 15	10
Vt (mL/kg)	7	8	6
FiO₂ (%)	21	50	21
	Temperature °C		
Perfusion begins	25	15	32
Ventilation begins	32	32	32-34
Evaluation begins	37	37	37

VCV: volume-controlled ventilation; PEEP: positive end expiratory pressure; Vt: tidal volume; FiO₂: fraction of inspired oxygen.

The main principle of EVLP starts after organ retrieval (where the lung graft is perfused with cold Perfadex[®] and put in cold storage) and involves placing the lung graft in a transparent plastic dome and connecting the pulmonary artery to a circuit of perfusion and the trachea to a ventilator.

The left atrium is left open in the Lund and OCS protocols for the perfusate to drain back into the system reservoir and the atrium is closed and cannulated in the Toronto protocol. A closed left atrium with physiological pressure has been shown to produce superior results with significantly less edema and improved lung physiology when using normothermic EVLP up to 12 hours (91). The perfusate is a hyper-oncotic solution that washes out blood clots, inflammatory cells and waste products.

Whether to add RBC in perfusate is another question that differs between the three protocols. At the current time, the Toronto protocol advocates an acellular regimen. Studies have shown benefits with RBC and, in particular, whole blood in terms of lower pulmonary pressures and PVR together with less volume replacement in the reservoir when extending the EVLP beyond 6 hours (92).

A third difference between the protocols is whether the EVLP is run with high or low flow. The Lund protocol advocates high flow while the Toronto and OCS protocols advocate low flow. Bearing in mind that the Lund protocol was not designed for long-term use, a recent study shows favorable results for low flow perfusate in terms of reduced edema and reduced signs of inflammation, together with improved physiological function (93). While the graft is connected to EVLP, cold static lung preservation of the graft can slow down lung deterioration by active cooling which reduces O₂ demand by slowing down cell metabolism (94). Objective measurements and assessment of the graft can be made over a time period of hours under normothermic conditions where evaluation and maybe also improvement of the graft regarding the PaO₂/FiO₂ ratio can be achieved (94-96).

The different mechanisms that might improve the function of the graft are: (1) resolving pulmonary edema by utilizing high oncotic pressure, (2) removal of harmful substances by adding filters to the circuit, (3) improved matching of ventilation/perfusion by recruitment of atelectatic areas, and (4) prevention or therapy against immunological reactions (90).

Ischemia-reperfusion injury and allo-immune response are of major importance in organ transplantation. During ischemia-reperfusion injury, necrosis in the organs releases damage-associated molecular pattern molecules, leading to immune cell activation. Inflammatory cells produce and release pro-inflammatory cytokines, especially TNF- α , IL-1 β , IL-6 and IL-8 (97, 98), and promote tissue inflammation, infiltration of immune cells and activation of T-cells; the latter contribute to either rejection or tolerance.

Cytokine filtration

There is ongoing research in the field of cytokine filtration and cytokines as therapeutic targets. Cytokines can be released from a large variety of cell identities, including lymphocytes, monocytes, granulocytes, endothelial cells, and synovial cells. They release pro-inflammatory cytokines such as TNF- α , IL-1, IL-2, IL-6, and IL-8 to mediate the immune and inflammatory responses to stress, which can result in anything from sepsis to tissue damage. These cytokines are then responsible for a variety of downstream actions, including the recruitment of inflammatory cells and increasing cell-mediated immunity. IL-1b has been identified as a prognostic indicator of non-recovery during EVLP (99).

Other anti-inflammatory cytokines, such as IL-4, IL-10, IL-11 and IL-13 will then stop inflammatory reactions, which helps maintain a balance between the actions of the pro-inflammatory and the anti-inflammatory molecules.

As a platform for organ repair, EVLP can be combined with a cytokine filtration technique. Cytokine filtration during human kidney perfusion has shown to reduce delayed graft function (100). When cytokine filtration is used during heart transplantation, patients have been found to have reduced need for inotropic support and improved hemodynamic status post-transplantation (101).

Patients going through transplantation surgery and follow-up are known to have increased cytokine levels. PGD and rejection may involve mediation of these cytokines. It can be speculated that a cytokine filter in line with machine perfusion or cytokines used as therapeutic targets could be a promising method to repair donor organs during machine perfusion.

Survival after LTx

Another factor affecting the availability of organs is the short survival rate of lung grafts. Despite the fact that Sweden has one of the highest survival rates in the world, when considering the last 25 years, the overall survival time at 20 years for all lung grafts was only 19%. DLTx has a better outcome than SLTx with an almost twice as high survival rate at 10 years' post-transplant (102).

The main reasons for death after LTx are due to either acute rejection, named PGD or chronic rejection, named chronic lung allograft dysfunction. Since this thesis focuses on acute lung injury, only PGD will be described.

Primary graft dysfunction (PGD)

PGD is the major cause of death when looking at 30-day mortality after LTx and is a syndrome resembling ARDS that develops within 72 hours after LTx (103, 104). The symptoms are related very closely to those of ARDS with edema seen on chest X-ray and a decrease in ratio of PaO₂/FiO₂ with a grading system that differs slightly

from that of ARDS. The incidence of PGD is 10-50% with an average of 30% and is both linked to increased short- and long-term mortality (105-107) and to the duration of days spent under mechanical ventilation (108, 109).

The International Society for Heart and Lung Transplantation (ISHLT) grades PGD according to the oxygenation ratio and presence or absence of edema. Their 2016 guidelines state:

PGD grade 0 has no visible edema on chest X-ray.

PGD grades 1-3 have edema present on X-ray and a ratio of $\text{PaO}_2/\text{FiO}_2$ as follows: grade 1, > 300 mmHg, grade 2, 200-300 mmHg, and grade 3, < 200 mmHg.

Grading is performed every 24 hours in the first 72-hour period and ideally with a PEEP of 5 and an FiO_2 of 1.0.

There are several risk factors for developing PGD, for example the use of cardiopulmonary bypass during transplant surgery, SLTx, PAH, large volume of transfusion products and a history of smoking in the donor (105).

Aims

Paper I

To explore the hypothesis that alterations in particle flow rate (PFR) can be used as a diagnostic tool for early detection of ARDS in a preclinical ARDS model with mechanical ventilation using a customized PExA device.

Paper II

To explore the hypothesis that alterations in PFR can be used as a diagnostic tool for early detection of ARDS and as a diagnostic tool over time to monitor progression or recovery from ARDS when ECMO treatment is initiated in both a preclinical model and in patients. We also aimed to investigate whether collected particles on membranes could be analyzed for potential biomarkers.

Paper III

To explore the hypothesis that alterations in PFR can be used as a diagnostic tool for early detection of ALI and ARDS in different animal models of lung injury and that EBP collected on membranes could be analyzed to identify potential biomarkers of lung disease.

Paper IV

To explore the hypothesis that cytokine filtration before LTx, during EVLP, and extracorporeal cytokine hemofiltration post-transplant would restore pulmonary function and reduce the incidence of PGD.

Paper V

To explore the hypothesis that different ventilator settings resulted in different PFR patterns in postoperative patients on mechanical ventilation without lung pathology. Furthermore, the effect of recruitment maneuver during different ventilation modes was investigated.

Materials and methods

PExA

In Papers I-III and V, all subjects were put on mechanical ventilation after being anesthetized and a customized PExA 2.0 device (PExA, Gothenburg, Sweden) was connected to the expiratory limb of the respiratory circuit on the ventilator. A Y-piece containing a one-way valve was used to prevent the mixture of inspiratory and expiratory air. PFR was measured continuously from the airways by the PExA device for the entire period, during the experimental setup with the pigs in Papers I-III, and as long as the patients were intubated in the ICU in Paper V. In Paper II the measurements on patients on ECMO were made for 1 hour on a weekly basis.

The PExA device conducts measurements using an OPC and by impaction on a membrane measured as total accumulated mass (ng). EBP samples were kept frozen at -80°C until analysis.

The OPC can analyze exhaled particle flow and exhaled particle size distribution, as described in Paper V and also in detail in previous studies (55). The PExA device measures particles in the size range 0.41 µm to 4.55 µm by the OPC and divides them into eight different size groups, as follows: particle 1: 0.48 (0.41–0.55) µm; particle 2: 0.59 (0.55–0.70) µm; particle 3: 0.75 (0.70–0.92) µm; particle 4: 0.98 (0.92–1.14) µm; particle 5: 1.22 (1.14–1.44) µm; particle 6: 1.67 (1.44–2.36) µm; particle 7: 2.52 (2.36–2.98) µm; and particle 8: 3.37 (2.98–4.55) µm (56). Measured particles were in the range of 0.41–4.55 µm in Papers I-II and V and in range of 0.33–3.67 µm in diameter in Paper III due to a newer version of PExA.

Proximity extension assay (PEA) technology

EBP on membranes from PExA were analyzed in Papers II and III using the Olink Multiplex Cardiometabolic and Inflammatory panel (Olink Proteomics, Uppsala, Sweden [<https://www.olink.com/>]). The panel contains 92 antibody probe pairs that bind target proteins in the sample. A proximity-dependent deoxyribonucleic acid polymerization event leads to the formation of a PCR reporter sequence quantified by real-time PCR. Internal, extension, and detection controls monitored deviation. Proteins detected in more than 15% of samples were included in the statistical analysis. Normalized protein expression (NPX) was calculated by subtracting out an external inter-plate control. The values were set relative to a correction factor

determined by Olink and generated on a log₂ scale with the background level set at 0. Normalization due to the amount of nanogram (ng) on the membranes was calculated in order to be able to compare the different animal cohorts in Paper III.

ECMO setup

Animals

The ECMO equipment used was Medtronic Bio-Medicus[®] 560 centrifugal pump console, an Affinity[®] CP magnetic centrifugal blood pump and the TX50 Bio-Probe[®] Flow Transducer for measurement of the blood flow by conductivity. The circuit comprised a microporous polypropylene hollow fiber oxygenator with a surface of 2.5 m², Affinity Fusion[™], a polyvinyl chloride 3/8-inch tubing set and a low prime centrifugal pump head AP40[®]. All components were coated with Cortiva[®] surface which is an endpoint attached heparin surface (Medtronic Inc., Minneapolis, USA).

Heparin 1000 IU/mL was administered intravenously prior to cannulation and onset of ECMO. The heparin effect was monitored with ACT targeting 180-220 sec. to avoid thrombotic events using a Hemochron Signature Elite[®] (Accriva Diagnostics Inc., San Diego, USA).

Cannulation was performed with a 32 Fr venous cannula (DLP[®] Dual Lumen Aortic Root Cannula with Vent Line single-stage venous cannula, Medtronic Inc., Minneapolis, USA) placed in the right atrium and the arterial cannula, 20 Fr (EOPA[®] Elongated One Piece Arterial cannula, Medtronic Inc., Minneapolis, USA), in the ascending aorta. ECMO flow was adjusted to 75% of estimated cardiac output. V-A ECMO was chosen over V-V ECMO due to hemodynamic instability (Figure 6).

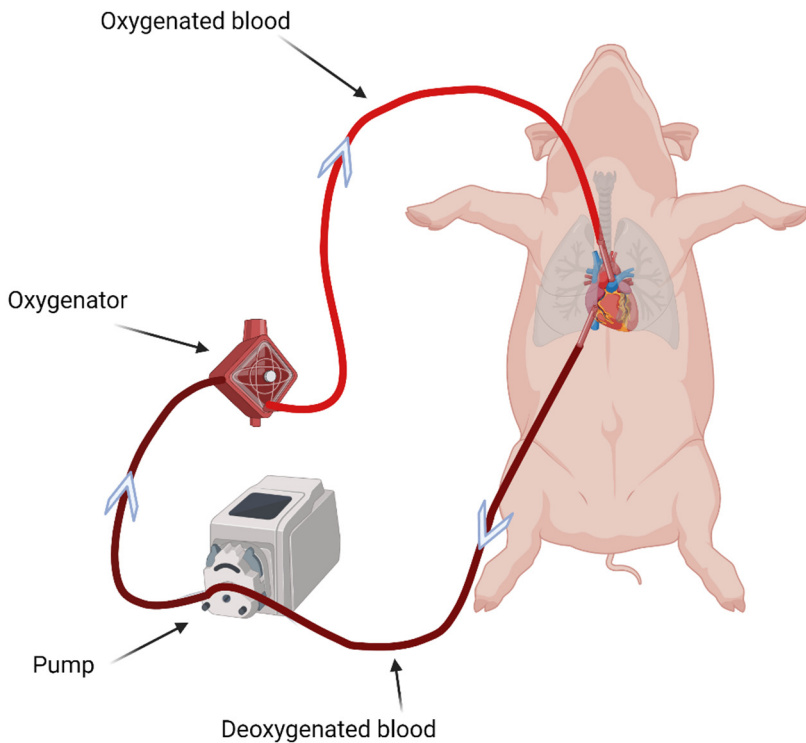


Figure 6. Central veno-arterial extra corporeal membrane oxygenation (V-A ECMO) in a pig

Cannulation in the right atrium and ascending aorta. Deoxygenated blood is drawn from the superior and inferior vena cava by a roller pump and oxygenated before being returned in the aortic cannula. Created with BioRender.com

Patients

The ECMO equipment and single-use equipment for V-V ECMO was Cardiohelp ECMO System (Maquet, Getinge Sweden) and HLS ECMO circuit (Maquet, Getinge, Sweden).

Before cannulation the patient was given heparin 100 IE/kg bodyweight and monitored with ACT and aPTT. Cannulation was performed in the femoral vein using a Biomedicus Next Generation 21-25 Fr outflow cannula and a Biomedicus Next Generation 19-23 Fr inflow cannula in the internal jugular vein (Medtronic Inc, Minneapolis, USA). The choice of cannulas was based on patient body surface area and anatomy. A distance between the tip of the cannulas was kept at 10-15 cm apart, confirmed by echocardiography, to avoid recirculation.

Target flow on ECMO was adjusted to 50 mL/kg/min and was maintained at a flow rate, no less than 2.5 L/min, to deliver full ECMO support. FiO_2 was initially kept at 100% and sweep gas flow was regulated depending on PaCO_2 (Figure 7).

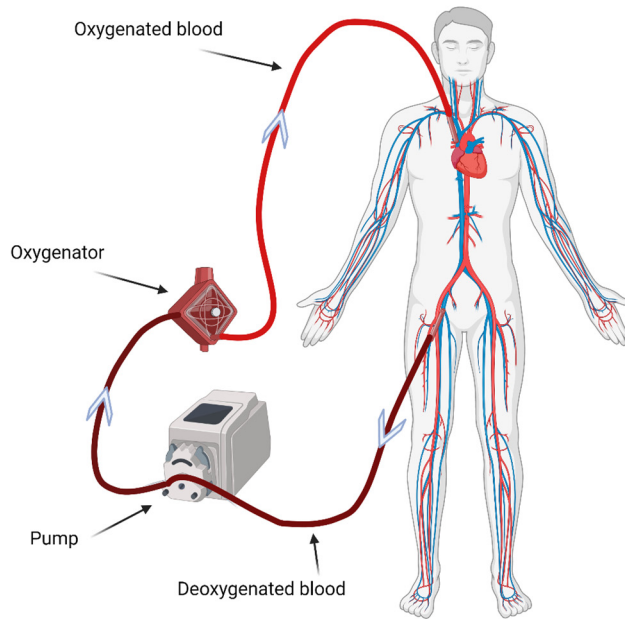


Figure 7. Peripheral veno-venous extra corporeal membrane oxygenation (V-V ECMO) in a human
Cannulation in the right femoral vein and right internal jugular vein. Deoxygenated blood is drawn from the inferior vena cava by a roller pump and oxygenated before being returned in the superior vena cava. Created with BioRender.com

Ex vivo lung perfusion

Currently there are three EVLP protocols in clinical use worldwide with small differences and modifications between them regarding pressure, ventilatory settings and target flow. In this thesis, a modified Toronto protocol was used in Paper IV.

Preparation of donor

When the lungs were being harvested from the donor animal the pulmonary artery was cannulated with a 28 Fr cannula and secured by a purse string suture. A clamp was put on the superior vena cava, the inferior vena cava, and on the ascending aorta and cardiac fibrillation is induced. The left atrium was left open and followed by antegrade perfusion of the lungs with 4 L of cold Perfadex[®] PLUS solution (XVIVO, Gothenburg, Sweden) distributed at a low perfusion pressure (< 20

mmHg). The lungs were then harvested *en bloc* and immersed in cold Perfadex[®] solution for cold storage at 4°C for 2 hours.

Ex vivo lung perfusion (EVLP)

EVLP was performed using Vivoline LS1 (XVIVO Perfusion, Gothenburg, Sweden) and the Toronto protocol with a target perfusion of 40% of cardiac output, a Vt of 7 mL/kg body weight of the donor, respiratory rate of 7 b/min, PEEP of 5 cm H₂O and 21% FiO₂ for 4 hours after reaching 32°C. The system was primed with Steen[™] Solution (XVIVO Perfusion, Gothenburg, Sweden) and with RBC from the donor animal, drawn prior to LPS treatment, to reach a hematocrit level of approximately 15% in the EVLP circuit. If the perfusate level dropped below 300 mL in the reservoir, additional Steen[™] solution (XVIVO Perfusion, Gothenburg, Sweden) was added to compensate for the loss. Physiological parameters were recorded hourly during the 4-hour perfusion period. After 4 hours of EVLP, the lungs were cooled down to 8-12°C for approximately 45 min before transplantation (Figure 8).

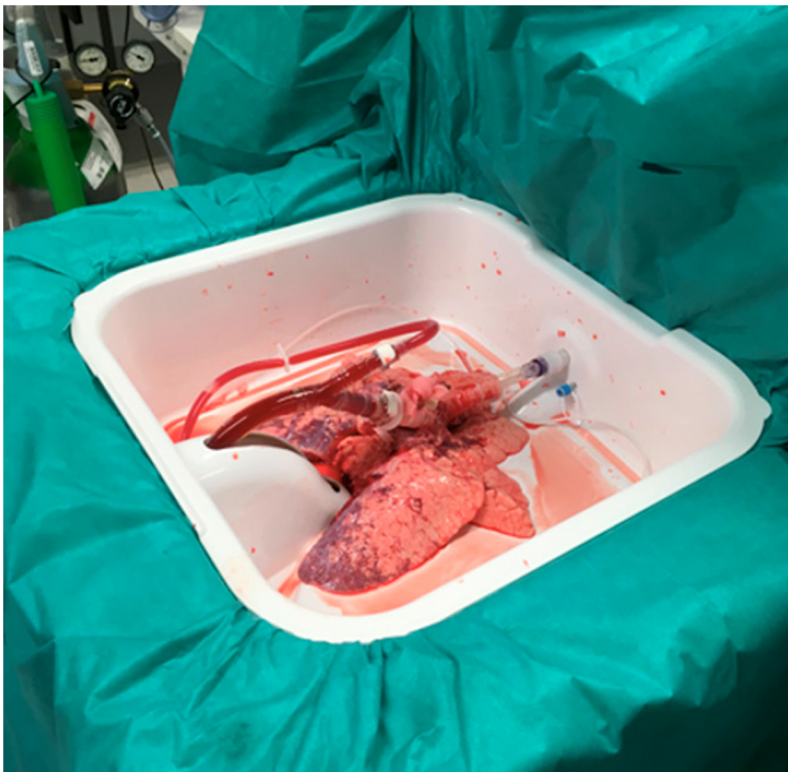


Figure 8. *Ex vivo* lung perfusion (EVLP) setup

Lungs connected to *ex vivo* lung perfusion (EVLP). Copyright Ellen Broberg with permission.

Cytokine filtration during EVLP

Cytokine filtration has recently been evaluated in conjunction with EVLP in pre-clinical settings and has rejuvenated healthy lungs from extended cold ischemic storage (110, 111). The question is whether cytokine filtration during reconditioning with EVLP can restore previously rejected lungs and thereby increase the donor pool.

During EVLP, in the treated group of animals, the perfusate was filtered continuously through an absorbent filter (CytoSorb[®], CytoSorbents Europe GmbH, Berlin, Germany) through a veno-venous shunt from the reservoir at a rate of 300 mL/min.

Extracorporeal hemofiltration after transplantation

The group of animals that received cytokine filtration during EVLP then received a further 12 hours of extracorporeal hemofiltration following transplantation using a roller pump, equipped with the cytokine filter, at a rate of 300 mL/min. This was accomplished through a veno-venous shunt using a hemodialysis catheter (Power-Trials[®] Slim-Cath[™], Becton, Dickinson and Company, New Jersey, USA) inserted in the right jugular vein.

Multiplex

Analyzing cytokines in plasma

In Papers I-II plasma samples were taken at baseline, at 30 min and every 60 min until the end of the experiment. In Papers III and IV, plasma samples were taken at baseline and every 60 min. In the donor animals in Paper IV, plasma samples were also taken every hour during EVLP, and every 4th hour in the recipient animals. From plasma, cytokine levels were analyzed with the multiplex kit Cytokine & Chemokine 9-Plex Porcine ProcartaPlex[™] Panel 1 (Thermo Fisher Scientific Cat. No. EPX090-60829-901) according to the manufacturer's instructions. The kit was run using a Bioplex-200 system (BioRad, Hercules, CA, USA). Nine cytokines were analyzed: IL-1b, IL-4, IL-6, IL-8, IL-10, IL-12p40, interferon alpha (IFN-a), interferon gamma (IFN-g) and TNF-a. Blood samples were centrifuged, and plasma separated and frozen at -80°C until analysis.

Analyzing cytokines in bronchoalveolar lavage fluid (BALF)

To see if and how cytokines produced in the lung tissue correlate with plasma, bronchoalveolar lavage fluid (BALF) was taken at baseline and at the end of the experiment in Papers II and III. In Paper IV BALF was also obtained in the donor animals before lung harvest, at the end of EVLP, and at the end of the experiment in the donated lungs of the recipient. BALF was frozen at -80°C until analysis.

The multiplex kit, specifically designed for the porcine model, is an immunoassay based on the principles of a sandwich ELISA, which uses two layers of specific antibodies binding to different epitopes of one antigen (i.e. target molecule). The detection of an antigen is visualized with fluorescence using a Luminex instrument, creating a spectral signature using laser, to quantitate all protein targets simultaneously.

Blood cell counts

Leukocytes, neutrophils, and total white blood cell counts were measured in Paper IV using a Sysmex KX-21N automated hematology analyzer (Sysmex, Milton Keynes, UK) in plasma every 30 min in the donor animals, every hour during EVLP, and every 1-6th hour after LTx. Blood samples anti-coagulated with ethylene diamine tetra-acetic acid were kept at 4°C until analysis.

Histology

In Papers I-IV, baseline lung biopsies were taken from the right lower lobe through a right-sided thoracotomy in the anesthetized pigs before lung injury, and biopsies were taken again at the termination of the experiments through a midline sternotomy from all lobes in both lungs. Biopsies were placed in 10% neutral buffered formalin solution (Sigma Aldrich, Germany) and left at 4°C overnight for fixation. Formalin-fixed tissues were then subjected to a graded ethanol series and isopropanol (both Fisher Scientific, UK) prior to paraffin embedding (Histolab, Sweden). Tissue sections (4-5 µm wide) were cut and placed on microscope slides (Thermo Scientific, Germany) and after deparaffinization, the sections were stained with hematoxylin and eosin (H&E; Merck Millipore, Germany), followed by dehydration in consecutively graded ethanol and xylene solutions. Dried sections were mounted with Pertex (Histolab, Sweden). Bright-field images were acquired with a Nikon Eclipse Ts2R microscope (Nikon, Japan) and Olympus VS120-S5 slide scanning system.

In Paper II, after the end of the experiments with LPS and ECMO, the lungs were additionally assessed for signs of hemorrhage. Using ImageJ (version 1.53a, NIH), both the area of hemorrhage and the area of the entire lung were defined and measured. The percentage area of hemorrhage of the total lung was then recorded.

In Paper IV, biopsies were also taken from the right lower lobe just before lung harvest after confirmed ARDS. When the lung was connected to EVLP, biopsies were taken from the right lower lobe at start and then every hour during the EVLP session. Biopsies were taken from the transplanted left lung at the end of the experiment at 48 hours' post-transplant.

Wet-to-dry weight ratio

The possible presence of pulmonary edema was examined in Papers I, II and IV by measuring the wet-to-dry weight ratio in lung tissue from the right lower lobe at baseline before lung injury was induced and from both the left and the right lower lobes at the end of the experiment. Lung tissue pieces harvested from the lower lobes in both left and right lungs were weighed, lyophilized for 24 hours, and then weighed again. The ratio between the wet and dry weight was then calculated. Two separate lung tissue pieces were analyzed from each location and time point, and each data point is shown as the mean.

In Paper IV, the wet-to-dry weight ratio in lung tissue from the lower lobe was also measured after EVLP in the left lung and after 48 hours of transplantation in both the left (transplanted) lung and right (native) lung.

Scoring

To be able to grade the lung injury that occurred after LPS administration in Paper IV, and the progression/regression of lung injury that followed after EVLP and LTx, with or without cytokine filtration, histological images with H&E staining from each animal were scored independently. Three blinded scorers with experience in porcine lung injury models scored for lung injury on the basis of the number of inflammatory cells, presence of hyaline membranes, level of proteinaceous debris, thickening of the alveolar wall, enhanced injury, hemorrhage and atelectasis using a modification of a previously described scoring methodology (112). Scores were given on a scale of 0 to 8 for each feature and reported as the average of the sum of the characteristic scores.

PGD

Recipients were followed for a minimum of 48 hours. All animals were immunosuppressed daily with tacrolimus, 0.15 mg/kg, sub-lingually and methylprednisolone, 1 mg/kg, twice daily, intravenously to prevent acute rejection. Before ending the experiment, a right thoracotomy was performed, and the right native lung was clamped in order to be able to evaluate the left transplanted lung alone for 4 hours. PGD occurring after transplantation was graded according to the ratio of PaO₂/FiO₂ following the guidelines of ISHLT (updated 2016) (107).

Subjects and study design

Paper I

This preclinical study is a proof of concept and an experimental interventional study with a case-control group based on a previous study by Broberg et al. (55) in which

a pig unexpectedly developed ARDS and had a significant increase in exhaled particles.

Ten Swedish domestic pigs with a mean weight of 60 kg were anesthetized according to local protocols and kept on mechanical ventilation. Seven pigs received LPS, both endotracheally and intravenously, with the intention of causing ARDS, and three pigs received sham treatment with saline.

Hemodynamic measurements, ventilatory parameters and blood gases were taken every 30 min and measurements were recorded continuously during the 6-hour experiment together with plasma samples and biopsies.

Paper II

The design of Paper II is based on the LPS-induced ARDS pig model we used in Paper I. In this preclinical study we aimed to see if PFR could be used as a diagnostic tool to measure lung injury while the animal was on ECMO. It is also an experimental interventional study with case controls. A total of 21 Swedish domestic pigs (of which information on 10 pigs was published earlier in Paper I), with a mean weight of 62 kg each, were anesthetized according to local protocols and maintained with mechanical ventilation and divided into four different groups of intervention according to the timeline in Figure 9:

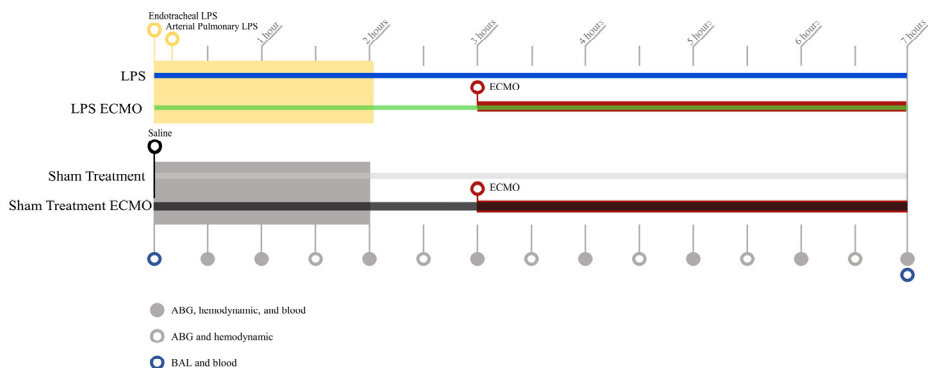


Figure 9. Experimental timeline in Paper II

LPS: seven pigs receiving LPS, LPS ECMO; eight pigs receiving LPS and ECMO, Sham treatment; three pigs receiving saline, Sham treatment ECMO; three pigs receiving saline and ECMO. LPS: lipopolysaccharide; ECMO: extracorporeal membrane oxygenation; ABG: arterial blood gas; BAL: bronchoalveolar lavage.

A total of 21 pigs were divided into four groups. Fifteen pigs received LPS both endotracheally (0.33 mg/kg) and intravenously through a Swan-Ganz catheter (2 µg/kg/min) and were given mechanical ventilation for 7 hours. Eight of these pigs were started on V-A ECMO after 2-3 hours and continued for 4 hours and named

‘LPS ECMO animals’. The other seven pigs were referred to as ‘LPS animals’. Six pigs received sham treatment with saline infusion and mechanical ventilation for 7 hours. Three of these pigs were started on V-A ECMO after 2-3 hours and continued for 4 hours and named ‘sham-treated ECMO animals’. The other three pigs were referred to as ‘sham-treated animals’. Hemodynamic measurements, ventilatory parameters and blood gases were taken every 30 min and PFR measurements were recorded continuously during the 6-hour experiment together with plasma samples, BALF and biopsies. Four patients with ARDS and V-V ECMO treatment were included in this study as a proof of concept.

Paper III

Paper III was a preclinical study in which three different animal models of acute lung injury were compared with regard to PFR. There were seven domestic pigs in each group. The groups were named after their respective lung injury: LPS (LPS-induced lung injury), lavage (repeated lavage-induced lung injury) and gastric (gastric-aspiration induced lung injury). A total of 21 domestic pigs with a mean weight of 34 kg were anesthetized according to local protocols and maintained under mechanical ventilation. The different lung injury models are described in the Introduction. The PExA devices were connected in the LPS group before the LPS was administered. The PExA devices were connected after the lavage process in the lavage group and after the aspiration phase in the gastric group. Hemodynamic measurements, ventilatory parameters and blood gases were taken every 30 min and PFR measurements were recorded continuously during the 6-hour experiment together with plasma samples, BALF and biopsies.

Paper IV

This was a pre-clinical prospective, randomized study involving 24 domestic pigs, with a mean weight of 50 kg each. Twelve pigs with LPS-induced ARDS were used as donors and 12 pigs were used as recipients. After ARDS was established with LPS administered intravenously as an infusion (2 µg/kg/min) for 1 hour, and reduced by 50% for another hour, randomization was made to 4 hours of EVLP with or without treatment with cytokine filtration and a following left lung transplantation with or without 12 hours of cytokine filtration with six pigs in each group. The intention was to restore pulmonary function to make the lungs suitable for LTx and reduce the postoperative risk of PGD (Figure 10).

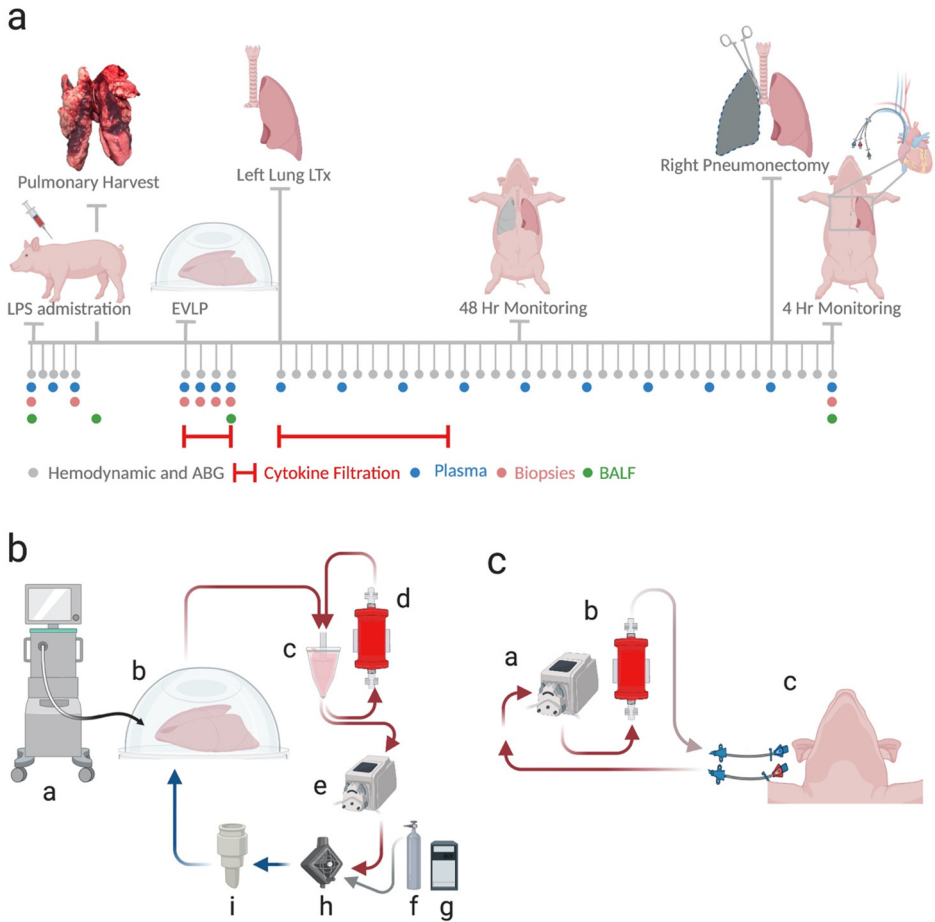


Figure 10. Experimental setup

a Timeline of LPS-induced acute respiratory distress syndrome (ARDS) and lung recovery by therapeutic interventions during *ex vivo* lung perfusion (EVL) and transplantation follow-up. Pulmonary harvest was conducted after confirmation of ARDS and the lungs were then placed on EVLP. The recipient was monitored for 48 hours after left lung transplantation with a mid-sternotomy followed by a right pneumonectomy in the last 4 hours which allowed for isolated monitoring of the transplanted lung. A Swan-Ganz catheter was placed in this monitoring period. **b** Setup of cytokine filtration during EVLP. A mechanical ventilator (a) was connected to the lungs in the dome (b). Flow continued into the reservoir (c) which fed into the cytokine filter (d) that then directed filtered perfusate back into the reservoir. Flow continues as per established methodology using a peristaltic pump (e) into a deoxygenator (h) connected to a gas supply (f) and heater (g). Following the leukocyte filter (i), the perfusate returns to the lungs. **c** Setup of cytokine filtration post-transplantation. A veno-venous shunt using a hemodialysis catheter was inserted into the jugular vein. This facilitated flow through a pump (a) that was in line with the cytokine filter (b). After filtration, flow returned to circulation via the hemodialysis catheter in the jugular vein (c). LPS: lipopolysaccharide; ABG: arterial blood gases; BALF: bronchoalveolar lavage fluid.

Paper V

This was a clinical randomized study where 30 patients without lung pathology were randomized to either VCV or PCV including a recruitment maneuver, with the intention to study PFR during their postoperative care in the thoracic ICU after heart surgery.

The aim of the study was to investigate if different ventilation modes gave rise to differences in PFR.

Upon arrival into the ICU, patients were randomized to either VCV or PCV during the first 30 min after arrival at the ICU including a recruitment maneuver 15 min after initiation of ventilation. The recruitment maneuver was performed over 1 minute using a PEEP of 10 cm H₂O, a respiratory rate of 4 breaths/min and an inspiratory-expiratory ratio of 2:1. All other settings were kept unchanged during the recruitment maneuver. A representative measurement of 3 min before and 3 min after the recruitment maneuver was chosen for statistical analysis of PFR during the recruitment maneuver. PFR was measured during VCV and PCV at two time periods: before and after the recruitment maneuver to obtain a representative value.

Patients were excluded if they had COPD stages 1-4, pulmonary fibrosis, or other types of lung pathology. They were also excluded if they were currently a smoker or a recent smoker (< 6 months ago). Other exclusion criteria included an ejection fraction < 45%, chronic renal failure or chronic liver failure. Patient demographics are shown in Table 2.

Table 2. Patient demographics

CABG: coronary artery bypass grafting; AVR: aortic valve replacement.

	Volume controlled ventilation (VCV)	Pressure controlled ventilation (PCV)	Total
Patients	n = 15	n = 15	n = 30
Sex M/F n (%)	13 (87)/2 (13)	9 (60)/6 (40)	22 (73)/8 (27)
Type of surgery:			
CABG	n = 8	n = 7	n = 15
AVR	n = 6	n = 4	n = 10
CABG and AVR	n = 1	n = 4	n = 5
Age (year)	70.3 ± 11.1	67.5 ± 9.4	68.9 ± 10.2
Smoking	No	No	No
Normal chest radiograph	Yes	Yes	Yes
Normal renal function	Yes	Yes	Yes
Ejection fraction > 55%	Yes	Yes	Yes

Statistical analysis

Paper I

Descriptive statistics, in the form of mean, and \pm standard error of the mean (SEM) for the number of animals, PFR, mechanical ventilation parameters, blood gases parameters, and hemodynamic parameters, were analyzed. Statistically significant differences between the different groups were tested with the Student's t-test when data were distributed normally and with the Mann-Whitney test when data were distributed abnormally. All statistical analysis was performed using GraphPad Prism Software (San Diego, CA, USA). Significance was defined as $p < 0.001$ (***), $p < 0.01$ (**), $p < 0.05$ (*), and $p > 0.05$ (not significant).

Paper II

Continuous variables were reported as mean and \pm SEM. For histological variables and the wet-dry ratios, values were reported graphically as mean, minimum, and maximum. Statistically significant differences between groups were tested with the Student's t-test and within groups with ANOVA when data were distributed normally. The Mann-Whitney test and the Wilcoxon test were used when data were distributed abnormally. All statistical analysis was performed using GraphPad Prism Software version 9.0 (San Diego, CA, USA). Significance was defined as: $p < 0.001$ (***), $p < 0.01$ (**), $p < 0.05$ (*), and $p > 0.05$ (not significant).

Paper III

Continuous variables were reported as mean \pm SEM. Statistically significant differences within groups were tested with the Student's t-test when data were distributed normally and the Mann-Whitney test when data were distributed abnormally. The Kruskal-Wallis test, Friedman and mixed effect analyses with multiple comparisons were performed to compare groups. Simple linear regression was used for correlation using Pearson's r . Heatmaps were generated in RStudio Version 1.4.1717 using the 'gplots' package. All statistical analysis was performed using GraphPad Prism Software version 9.0 (San Diego, CA, USA). Significance was defined as: $p < 0.001$ (***), $p < 0.01$ (**), $p < 0.05$ (*), and $p > 0.05$ (not significant).

Paper IV

Continuous variables were reported as mean \pm SEM. Statistically significant differences between groups were tested with the Student's t-test and within groups with analysis of variance when data were distributed normally. The Mann-Whitney test and the Wilcoxon test were used when data were not distributed normally. A Chi-Squared test was performed to analyze observed frequencies of categorical variables. All statistical analysis was performed using GraphPad Prism Software

version 8, (San Diego, CA, USA). Significance was defined as: $p < 0.001$ (***), $p < 0.01$ (**), $p < 0.05$ (*), and $p > 0.05$ (not significant).

Paper V

A power analysis was performed prior to the study. Descriptive statistics with mean \pm SEM were used in results and figures. The Mann-Whitney test and the Kruskal-Wallis test were performed (depending on data distribution) to analyze whether a statistically significant difference was achieved among particles in exhaled air. GraphPad Prism version 8 (San Diego, CA, USA) was used for statistical analysis. Statistical significance was defined as $p < 0.0001$ (****), $p < 0.001$ (***), $p < 0.01$ (**), $p < 0.05$ (*) and $p > 0.05$ (not significant).

Results

Paper I

Animals

Seven animals received LPS both endotracheally (0.33 mg/kg) and intravenously through a Swan-Ganz catheter (2 µg/kg/min). Three animals received only saline. No anatomical anomalies were found at the final autopsy.

Increased PFR after LPS administration

PFR at baseline (BL) was 60 ± 28 particles/minute. Immediately after baseline, the animals received LPS endotracheally and shortly afterwards, the first infusion with LPS was given. After 30 min, PFR started to increase and after 60 min there was a significant increase with a PFR of 1511 ± 638 particles/minute ($p = 0.0012$). PFR remained unchanged in the control group that received saline during the experimental timeline. The results are shown in Figure 11.

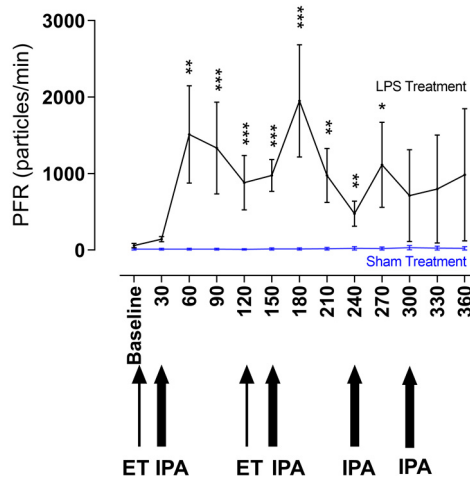


Figure 11. Particle flow rate (PFR) during experimental timeline

PFR after lipopolysaccharide (LPS) administration compared to baseline. Sham-treated animals are shown in blue to visualize the difference. ET: endotracheal installation; IPA: infusion in pulmonary artery. Copyright Am J Physiol Lung Cell Mol Physiol 318: L510-L517, 2020.

All animals developed ARDS within 90 min after the experiment began, according to the PaO₂/FiO₂ ratio in the Berlin definition (34). In order to see if PFR could be used as an early indicator of ARDS and correlate with different levels of ARDS, we compared PFR at baseline with different ARDS states: pre-ARDS, mild ARDS, moderate ARDS and severe ARDS. All ARDS states had significantly increased PFR, even pre-ARDS, which is noticeable from the perspective as PFR might be used as an early indicator. The results are shown in Figure 12.

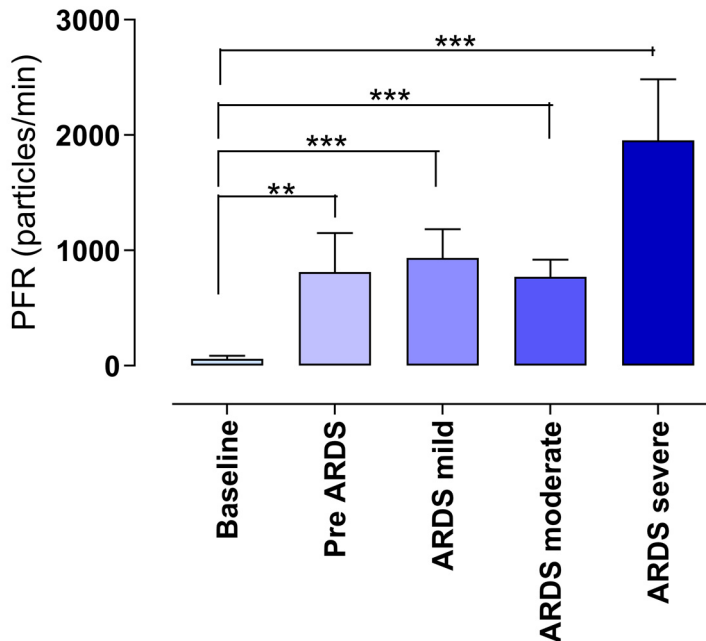


Figure 12. Particle flow rate at different acute respiratory distress syndrome (ARDS) time points
 Particle flow rate (PFR) at baseline compared to: PFR after lipopolysaccharide (LPS) was administered but before reaching mild acute respiratory distress syndrome (ARDS) (pre-ARDS), PFR at mild ARDS, PFR at moderate ARDS and PFR at severe ARDS. Copyright Am J Physiol Lung Cell Mol Physiol 318: L510-L517, 2020.

Changes in physiological parameters

LPS-treated animals had a PaO₂/FiO₂ ratio of 504 ± 31 mmHg at baseline which deteriorated to 209 ± 37 mmHg at 90 min. At the end of the experiment PaO₂/FiO₂ decreased to 144 ± 6 mmHg at which time all LPS-treated animals reached a moderate to severe ARDS. Sham-treated animals remained at a normal ratio of 493 ± 35 mmHg.

Mean arterial pressure (MAP) decreased as a sign of vasodilation: cardiac output and PVR and both had an s-shaped course with a dramatic increase in PVR between 30-60 min with 494 ± 143 DS/cm⁵ when capillary reaction to LPS was fully

developed and at the same time there was a dip in cardiac output due to right ventricular hypertension. These findings all confirm that our LPS-induced ARDS model was associated with significantly increased hemodynamic instability and pulmonary vasoconstriction compared to baseline.

Arterial blood gases (ABG) also showed a significant decrease in PaO₂ and pH with hypoxia and acidosis and simultaneously an increase in partial pressure of arterial carbon dioxide (PaCO₂) and lactate. These results illustrate the ventilatory changes occurring in an LPS-induced ARDS model. Results are shown in Figure 13.

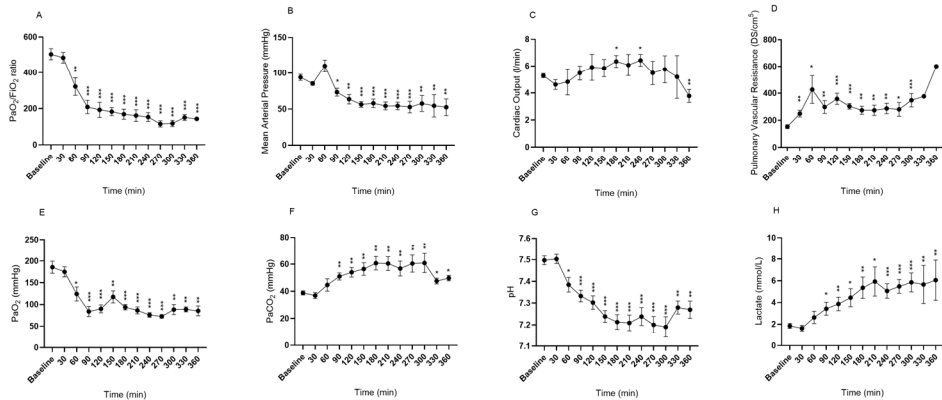


Figure 13. Physiological parameters during the experimental timeline

a: Partial pressure of arterial oxygen/fraction of inspired oxygen (PaO₂/FIO₂) ratio decreased significantly over time compared to baseline. Note that acute respiratory distress syndrome (ARDS) (ratio < 300 mmHg) occurred after 90 min. b-d: hemodynamic parameters with mean arterial pressure (b), cardiac output (c), pulmonary vascular resistance (d). e-h: arterial blood gas shown as: partial pressure of arterial oxygen (PaO₂) (e), partial pressure of arterial carbon dioxide (PaCO₂) (f), pH (g) and lactate (h). Copyright Am J Physiol Lung Cell Mol Physiol 318: L510-L517, 2020.

Cytokine expression in plasma after LPS administration

Of nine cytokines analyzed, six were increased significantly compared to baseline during the experimental timeline with TNF-α and IL-10 at 120 min and IL-1β, IL-6, IL-8 and IL-12 at 180 min. After its peak at 120 min, IL-10 decreased rapidly followed by TNF-α after 180 min. In comparison, the cytokines that peaked at 180 min remained elevated during the experimental timeline. The levels of IL-4, IFN-α and IFN-γ were below the detection limits at all time points. The results are shown in Figure 14.

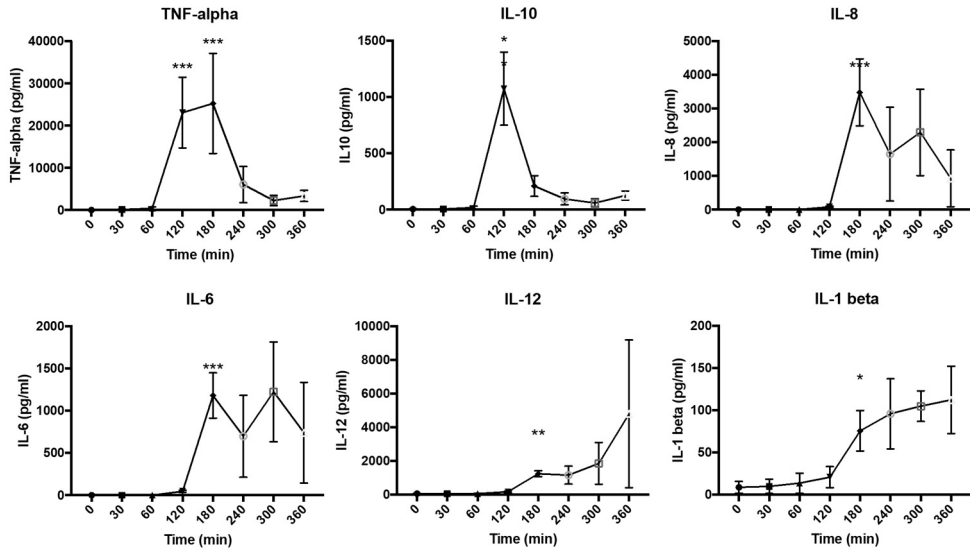


Figure 14. Cytokine response in plasma

Concentration of tumor necrosis factor-alpha (TNF-a), interleukin (IL)-10, IL-6, IL-8, IL-12 and IL-1b in plasma measured by multiplex after lipopolysaccharide (LPS) administration over the experimental timeline and compared with baseline. Copyright Am J Physiol Lung Cell Mol Physiol 318: L510-L517, 2020.

Histological changes after LPS administration

A baseline biopsy of lung tissue from the right lower lobe was taken before LPS administration and compared to lung tissue taken at the end of the experiment. In the seven pigs that received LPS and mechanical ventilation for approximately 6 hours, H&E staining revealed signs of diffuse alveolar damage, infiltration of immune cells, intra-alveolar hemorrhage, thickening of the alveolar-capillary barrier and edema, confirming severe lung injury in our model as seen in Figure 15a. In contrast to the LPS group, the sham-treated animals that received saline and mechanical ventilation for 6 hours demonstrated no signs of lung injury compared to baseline as seen in Figure 15b.

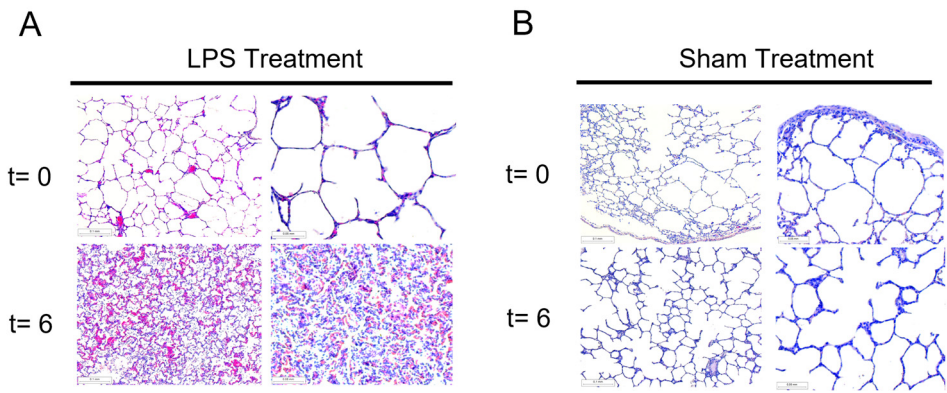


Figure 15. Lung biopsies with hematoxylin and eosin staining

a: Baseline biopsy at timepoint 0 showing normal lung tissue compared to biopsy with LPS treatment and mechanical ventilation 6 hours later. The morphological structure of the lung is deformed and signs of diffuse alveolar damage such as thickening of the alveolar-capillary wall, infiltration of immune cells, intra-alveolar hemorrhage and edema are now present. b: Baseline biopsy at timepoint 0 showing normal lung tissue compared to biopsy with sham treatment and 6 hours of mechanical ventilation still showing normal lung tissue. LPS: lipopolysaccharide. Copyright Am J Physiol Lung Cell Mol Physiol 318: L510-L517, 2020.

Increased wet-to-dry weight ratio after LPS administration

By measuring wet-to-dry weight ratios from biopsies taken at baseline and comparing them with biopsies taken at the end of the experiment, there was a significant increase in weight after LPS treatment compared to baseline. This confirms the histological findings and the results are shown in Figure 16.

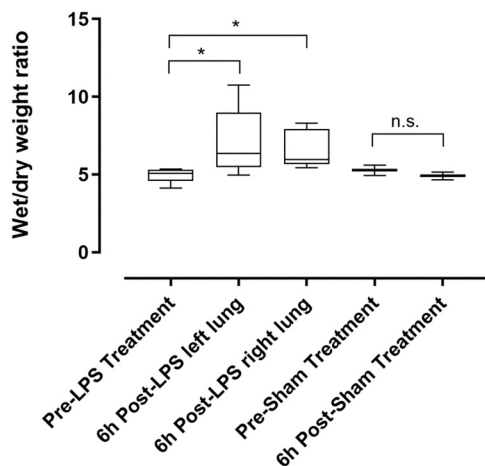


Figure 16. Wet-to-dry weight ratio in lung tissue

Wet-to-dry ratio measured at baseline and after 6 hours at the end of the experiment. The results show a significant difference in weight in the lipopolysaccharide (LPS) group compared to baseline while no difference was seen in the sham-treated group. Copyright Am J Physiol Lung Cell Mol Physiol 318: L510-L517, 2020.

Paper II

Animals

The animals comprised 21 pigs in total, divided into four groups. Fifteen pigs received LPS both endotracheally (0.33 mg/kg) and intravenously through a Swan-Ganz catheter (2 µg/kg/min) and were put under mechanical ventilation for 7 hours. Eight of these pigs were started on V-A ECMO after 2-3 hours which was continued for 4 hours; this group was called LPS ECMO animals. The other seven pigs were referred to as LPS animals. Six pigs received sham treatment with saline infusion and mechanical ventilation for 7 hours. Three of these pigs were started on V-A ECMO after 2-3 hours which was continued for 4 hours and they were named sham-treated ECMO animals. The other three pigs were referred to as sham-treated animals, as seen in the timeline in the Methods section. No significant anatomical anomalies were found at the final autopsy.

PFR increases following LPS and ECMO

All LPS-treated pigs developed ARDS within 180 min, as defined by two separate arterial blood gases within a 15-min interval. PFR in LPS-treated animals was 324 ± 114 particles/min when ECMO was initiated. PFR continued to increase significantly over time and reached 688 ± 187 particles/min ($p = 0.0030$) 30 min after the onset of ECMO. The LPS animals had a PFR significantly higher than that of the sham-treated animals at all time points. The LPS animals had a lower PFR than the LPS ECMO animals, as seen in Figure 17a.

PFR was compared between the four animal groups; a significant increase in PFR was observed not only between the sham-treated animals with and without ECMO, but also between LPS animals with and without ECMO, as seen in Figure 17b.

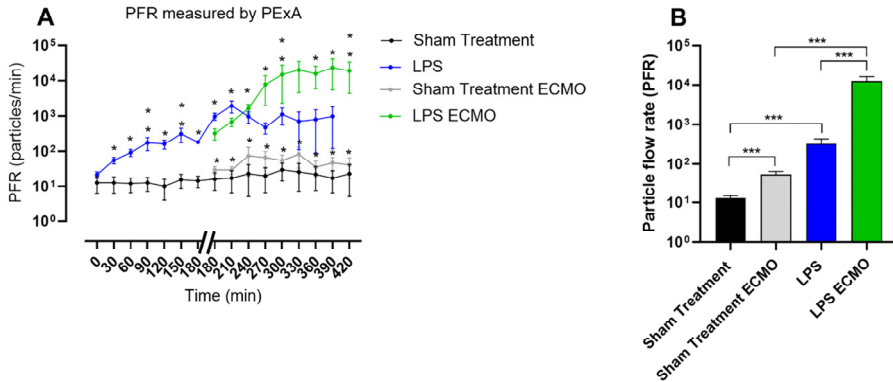


Figure 17. Particle flow rate (PFR) measured in different animal groups

a) Particle flow rate (PFR) from the airways in four different groups: LPS, LPS ECMO, sham treatment ECMO and sham treatment during experimental timeline. Note how PFR increased significantly after only 30 min following LPS treatment. There was a dramatic increase in PFR after the establishment of ECMO in LPS-treated animals. b) The mean values of the PFR between the different treatments. We observed a significant increase in PFR between the sham treatment groups but also a striking increase in PFR between LPS treatment and LPS and ECMO treatment. LPS: lipopolysaccharide; ECMO: extra corporeal membrane oxidation; PFR: particle flow rate; PEXA: particles in exhaled air.

Measuring possible biomarkers in EBP

EBPs were collected on a membrane from baseline, during ARDS development and ECMO treatment over the entire timeline. EBPs were analyzed using Olink proteomics due to the method's sensitivity to small amounts of protein. Many of the proteins detected in the LPS animals and LPS ECMO animals including FAS ligand, vascular endothelial growth factor-A (VEGF-A), MCP-1, C-X-C motif chemokine 10 (CXCL10), and MMP-1 are all recognized biomarkers for ALI and ARDS.

The number of proteins detected in each cohort is shown in Figure 18.

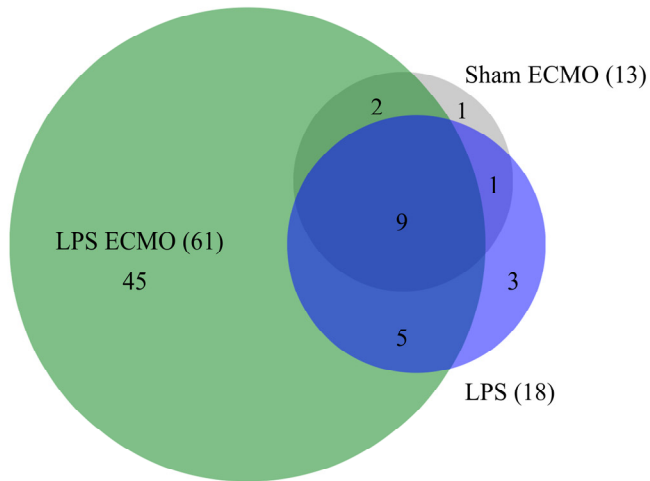


Figure 18. Proteins detected in exhaled breath particles (EBP) using Olink proteomics

Protein detected in the different animal groups and total numbers in parenthesis regardless of overlap. LPS: lipopolysaccharide; ECMO: extra corporeal membrane oxygenation.

Cytokine response in plasma during LPS and ECMO treatment

Cytokine concentrations were measured in plasma, collected hourly to monitor the inflammatory response after LPS administration and ECMO treatment and to see if changes in cytokine levels coincided with increased PFR. Significant increases in pro-inflammatory cytokines IL-6, IL-12, and TNF- α were seen in the LPS ECMO animals compared to the LPS ones. IL-10 was elevated early in both LPS animals and LPS ECMO animals (around 100 min) but reached higher peak levels in the LPS animals. The sham-treated animals had significantly lower cytokine levels at all time points compared to both LPS and LPS ECMO animals, except for IL-1 β , as seen in Figure 19.

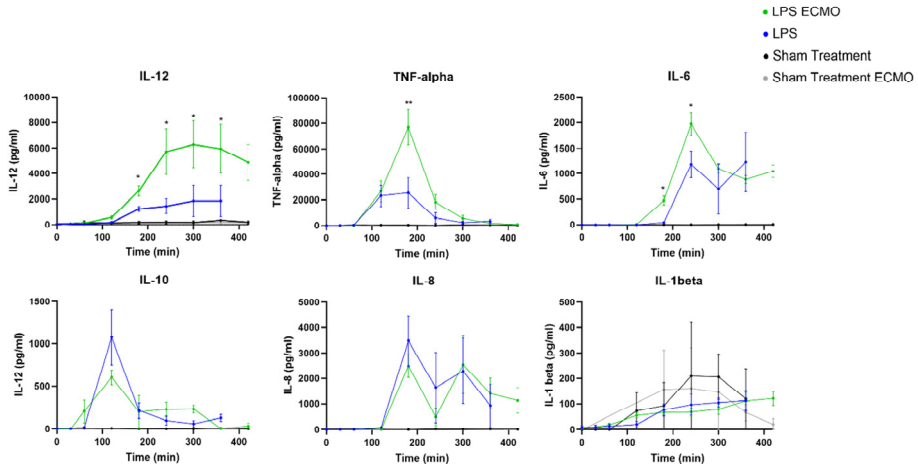


Figure 19. Cytokine response in plasma measured by Multiplex

The concentration of interleukin (IL)-1b, IL-10, IL-12, IL-8, IL-6, and tumor necrosis factor-alpha (TNF-a), in plasma measured at baseline and at different time points after LPS or saline administration and compared between LPS and LPS ECMO group. LPS: lipopolysaccharide; ECMO: extra corporeal membrane oxygenation.

Cytokine response in BALF during LPS and ECMO treatment

Bronchoscopy with BALF was performed at baseline and the end of the experiment in all four groups. In both LPS animals and LPS ECMO animals, the concentration of all cytokines increased significantly compared to the levels at both baseline and in sham-treated animals.

The concentrations of IL-6 and IL-12 increased significantly in the LPS ECMO animals compared to the LPS animals as seen in Figure 20. Between sham-treated groups, there was a significant rise in IL-6 in the sham-treated ECMO animals compared to those who had not undergone ECMO.

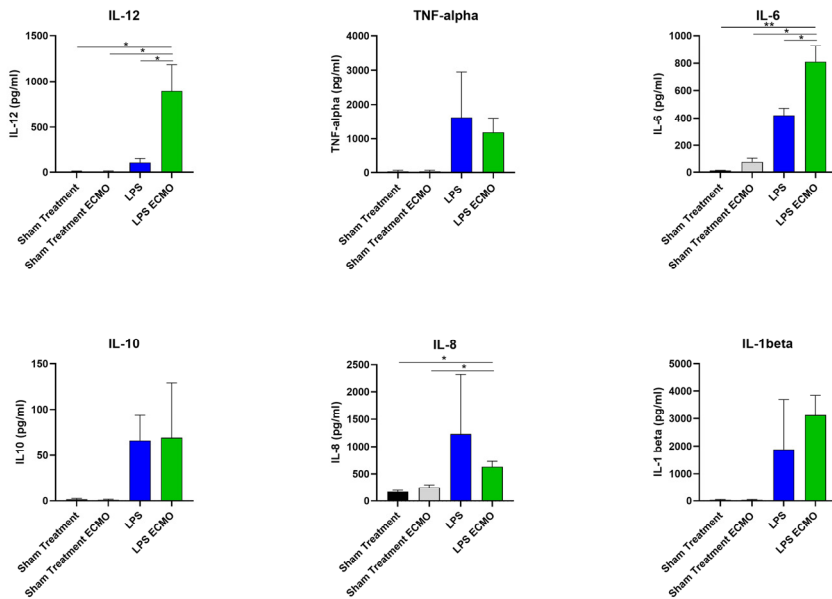


Figure 20. Cytokine response in bronchoalveolar lavage fluid (BALF)

The concentration of cytokines with interleukin (IL)-1b, IL-10, IL-12, IL-8, IL-6, and tumor necrosis factor-alpha (TNF-a), in bronchoalveolar lavage fluid (BALF) measured by multiplex at baseline and at the end of the experiment. LPS: lipopolysaccharide; ECMO: extra corporeal membrane oxygenation.

Histological changes after LPS and ECMO

H&E-stained lung tissue taken at baseline appeared healthy. Lung biopsies from the lower lobes at the end of the experiment confirmed the development of severe lung injury and ARDS with signs of diffuse alveolar damage, infiltration of immune cells and thickening of the alveolar-capillary barrier with intra-alveolar hemorrhage and edema. Significantly worse lung damage was observed in LPS animals and LPS ECMO animals compared to sham-treated animals, assessed by using histological scoring. No significant differences in histological scoring were observed between sham-treated animals and sham-treated ECMO animals, nor between LPS animals and LPS ECMO animals (Figure 21).

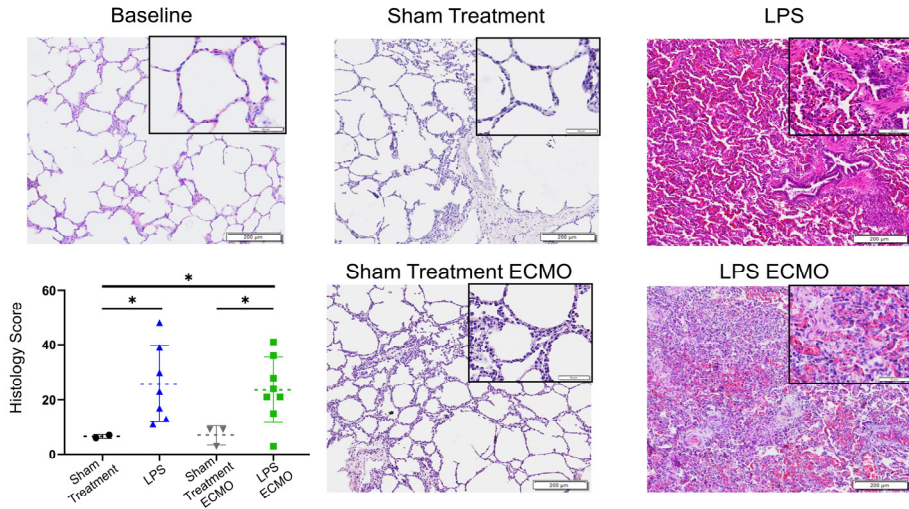


Figure 21. Hematoxylin and eosin (H&E) staining of lung tissue and histological scoring

Baseline tissue at the start of the experiment and after approximately 7 hours at the end of experiment. Sham-treated animals: sham treatment with mechanical ventilation did not show any structural damage. LPS animals: LPS administration with mechanical ventilation showed evidence of hemorrhage, presence of inflammatory cells and structural damage. Sham-treated ECMO animals: sham treatment with saline and mechanical ventilation including 4 hours of ECMO showing a mild thickening of the alveolar wall. LPS ECMO animals: LPS including mechanical ventilation and 4 hours of ECMO showing evidence of severe hemorrhage, presence of inflammatory cells, and structural damage. Significantly worse lung damage was observed in LPS animals and LPS ECMO animals compared to sham-treated animals, assessed through histological scoring. LPS: lipopolysaccharide; ECMO: extra corporeal membrane oxygenation.

Macroscopic assessment of hemorrhage in lung parenchyma

At the end of the experiment, the parenchyma of the lungs was assessed macroscopically for areas of hemorrhage and thrombosis. In sham-treated animals, no areas of hemorrhage or thrombosis were found, whereas large areas of these were found in the lung parenchyma of both LPS and LPS ECMO animals. The LPS ECMO animals had significantly more macroscopic hemorrhage, with an average of $66.6 \pm 2.8\%$ hemorrhage (max. 75.6%, min. 54.0%) than the LPS animals, which had $43.3 \pm 3.4\%$ hemorrhage (max. 58.6%, min. 27.2%; $p = 0.0002$) as seen in Figure 22. Using ImageJ (version 1.53a, NIH)

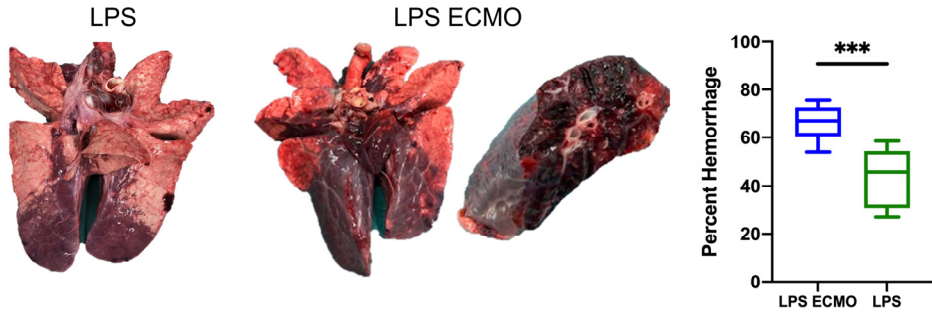


Figure 22. Macroscopic assesment of the lung

Macroscopic changes in lung tissue obtained 7 hours after LPS administration and after 4 hours of ECMO following LPS. The LPS ECMO lungs showed greater evidence of widespread areas of severe hemorrhage, as quantified macroscopically using ImageJ (version 1.53a, NIH). LPS: lipopolysaccharide; ECMO: extra corporeal membrane oxygenation.

Increased wet-to-dry weight ratio after LPS administration and ECMO

Wet/dry weight ratios for lung tissue in all four groups were calculated at baseline and at the end of the experiment. There were significant increases in edema in LPS animals and LPS ECMO animals compared to baseline biopsies and sham-treated animals with and without ECMO. There was also a tendency towards increased edema in sham-treated ECMO animals compared to sham-treated animals, and this tendency was also seen in LPS ECMO animals compared to LPS animals; however, the difference was not significant, as seen in Figure 23.

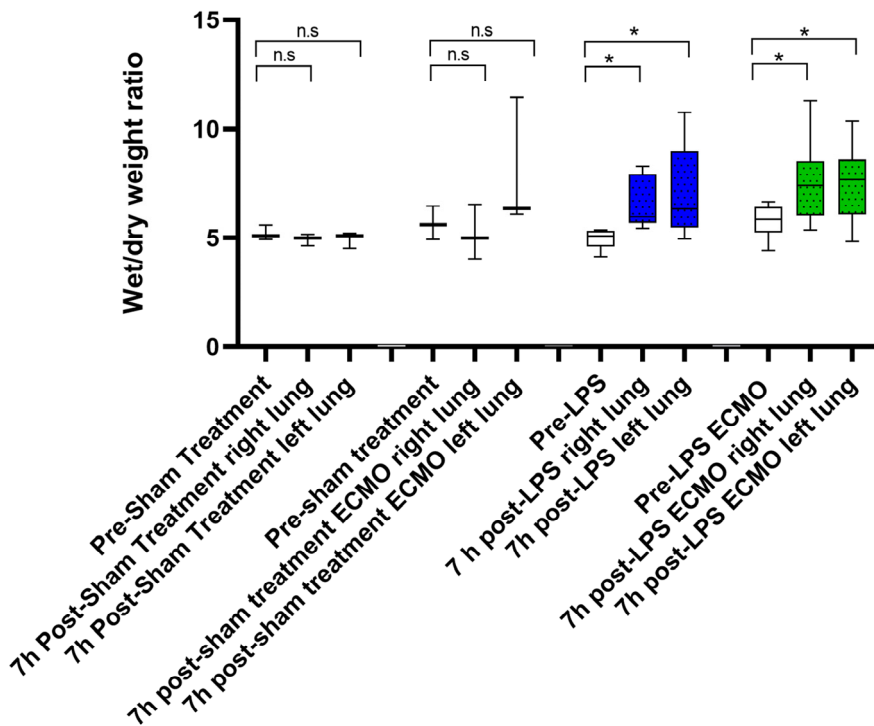


Figure 23. Wet/dry weight ratio

The Figure shows wet/dry weight ratio from lung tissue at baseline and at 7 hours' post-LPS, sham and ECMO treatment. Wet/dry weight ratio showed a significant increase in edema in LPS and LPS ECMO animals compared to baseline biopsies and levels in sham-treated animals. Even though animals treated with ECMO (both sham and LPS treated) showed a tendency towards more edema compared to animals not treated in ECMO, the differences were not significant. LPS: lipopolysaccharide; ECMO: extra corporeal membrane oxygenation.

Demographic characteristics of the patients with ARDS receiving ECMO

Having confirmed that PFR monitoring could be used in a porcine model of ARDS and ECMO, we enrolled a small cohort of patients to test the clinical application of this approach. The cohort comprised four patients from the cardiothoracic ICU receiving V-V ECMO due to ARDS with a mean age of 58 years (range 50–63). All patients were male. Three of the patients had COVID-19- induced ARDS confirmed via PCR testing of nasopharyngeal and bronchoalveolar lavage. The fourth patient had confirmed bacterial-induced ARDS. The patients had developed symptoms of upper respiratory tract infection 8 ± 1 days prior to hospital admission. The patients spent 3.6 ± 1.5 days in the hospital prior to admission to the ICU and 6.3 ± 3.3 days on mechanical ventilation before requiring ECMO.

PFR measurements were begun during the first 2 days of ECMO treatment and repeated weekly during a period of approximately 3 weeks. All patients had a V-V

ECMO inserted in the superior vena cava, and femoral vein and chest X-rays were performed regularly.

All four patients had a similar PFR at the initiation of ECMO treatment (Figure 24a). However, two patients recovered and could be weaned from ECMO, over which time they showed a decrease in PFR, together with an increase in V_t and lung compliance along with improved gas-exchange and improvement in their chest X-rays (Figure 24b).

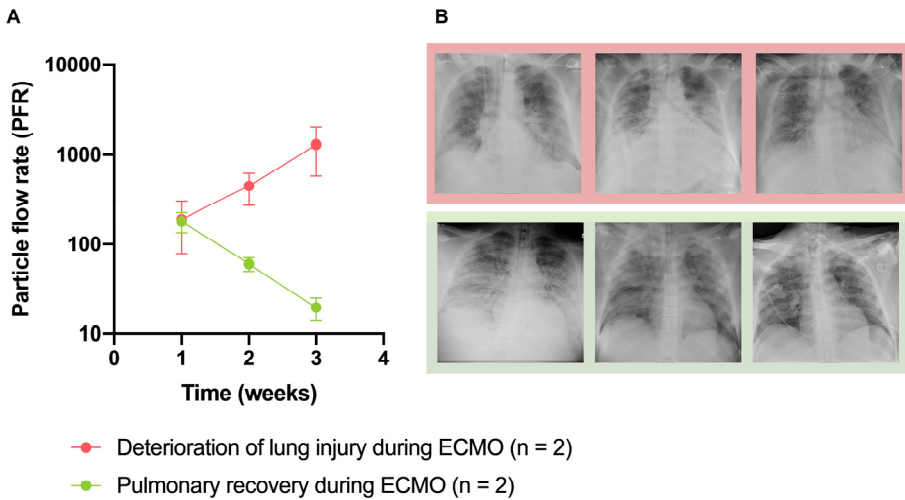


Figure 24. Patients on extra corporeal membrane oxygenation (ECMO) treatment

A) PFR. B) X-ray. PFR: particle flow rate.

Two patients deteriorated in lung function during the ECMO treatment and showed an increase in PFR over time (Figure 24a). Simultaneously, there was a deterioration in their gas-exchange and overall pulmonary function together with a visual deterioration on chest X-rays (Figure 24b).

One patient died after 3 weeks on ECMO, and one patient was still treated with ECMO after 8 weeks without any signs of recovery of lung function.

Paper III

Animals

This study consisted of three different lung injury models using domestic pigs with a mean weight each of 34 kg. The different animal models are described in detail in the Introduction and Methods sections. The model groups are named after their respective genesis for lung injury: LPS group, Lavage group and Gastric group after LPS-induced lung injury, repetitive saline lavage-induced lung injury and gastric aspiration, respectively.

Changes in physiological parameters between different lung injury models

Throughout the experiments, blood gases, hemodynamic parameters and ventilatory parameters were recorded. A decline in pH and pO₂ and a simultaneous increase in pCO₂ corresponding to the increasingly worsening pulmonary function was seen in all three animal cohorts and supported the fact that acute lung injury had developed.

Along with a deterioration in pulmonary function, hemodynamic changes occurred in cardiac output, mean pulmonary pressure (MPP) and PVR, which are shown in Figure 25.

MPP increased significantly over time in all three groups compared to baseline. The LPS group ($p = 0.0014$), the lavage group ($p < 0.0001$) and the gastric group ($p = 0.0092$). A comparison of the three endpoint values between each group showed a significant difference between the lavage and gastric groups ($p = 0.0127$).

PVR increased significantly between baseline and endpoint in all three groups: the LPS group ($p = 0.0201$), the lavage group ($p = 0.0003$) and the gastric group ($p = 0.0007$). Among the three end-point values, there was a significant difference between the LPS and lavage groups ($p = 0.0455$).

Ventilatory parameters showed a gradual decrease in dynamic compliance (C_{dyn}) and a simultaneous increase in respiratory rate and peak inspiratory pressure (PIP) in all models, as shown in Figure 25.

C_{dyn} decreased significantly between baseline and end point in the LPS group ($p = 0.016$) and in the lavage group ($p = 0.0001$), but the decrease in the gastric group was not significant ($p = 0.0992$). Again, a significant difference was seen between the end-point values for the LPS and lavage groups ($p = 0.0015$) and also between the lavage and gastric groups ($p = 0.0238$).

PIP increased significantly over time in all three groups: $p = 0.0168$ in the LPS group, $p < 0.0001$ in the lavage group and $p = 0.0452$ in the gastric group. Among the end-point values, the LPS and lavage groups had a significant difference between them ($p = 0.0004$), which was also seen between the lavage and the gastric groups ($p = 0.0097$).

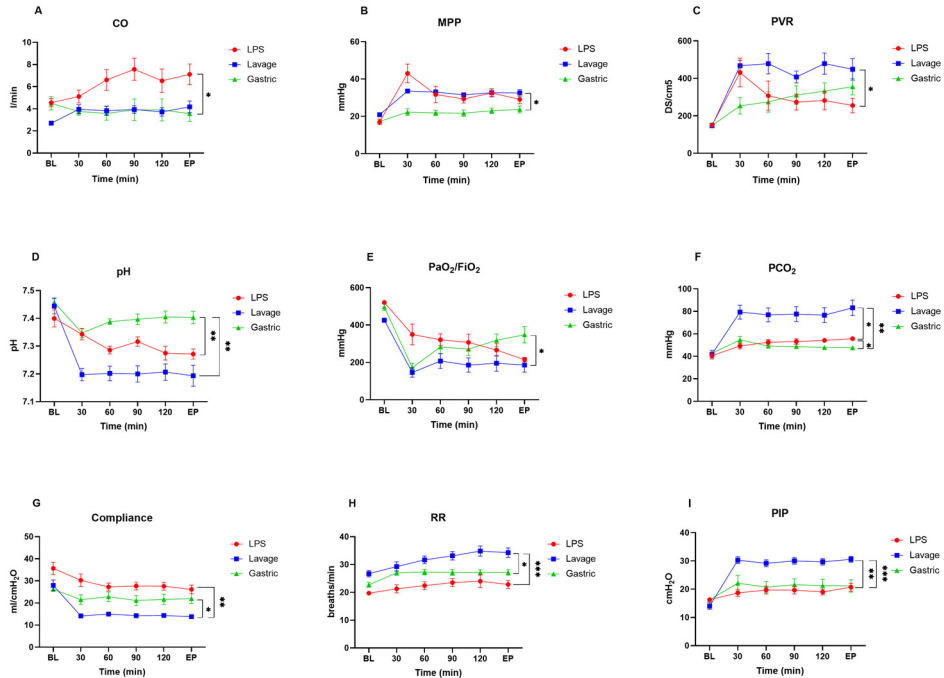


Figure 25. Physiological changes in three different animal models

Results of hemodynamic parameters, blood gases and ventilatory measurements during the timeline of the experiment confirming acute lung injury in the three animal models. Hemodynamics are shown as follows: a) cardiac output (CO), b) mean pulmonary pressure (MPP), c) pulmonary vascular resistance (PVR). Blood gases are shown as follows: d) pH, e) partial pressure of oxygen in arterial blood/fraction of inspired oxygen (PaO₂/FIO₂), f) partial pressure of carbon dioxide in arterial blood (PaCO₂). Ventilatory parameters are presented as follows: g) dynamic compliance (C_{dyn}), h) respiratory rate (RR), i) peak inspiratory pressure (PIP).

PFR in different lung injury models

In order to see whether PFR correlated with the onset of acute lung injury, PFR was measured continuously over time as particles per minute (p/min). PFR increased significantly after the induction of lung injury in the LPS group from a baseline value of 31.84 ± 18.76 p/min to 213.6 ± 92.8 p/min at the 60-min timepoint ($p = 0.0111$) and increased further to 512.2 ± 164.3 p/min ($p = 0.0023$) by the end point (Figure 26a).

In the lavage group, a non-significant increase was seen after 60 min; however, the PFR levels returned to near-baseline values at the end of the experiment (Figure 26b).

In the gastric group, the PFR increased from 9.94 ± 1.48 p/min at baseline to 71.51 ± 19.66 p/min ($p = 0.0043$) at 60 min after the induction of lung injury. The further increase in PFR remained significant from baseline until the end of the experiment ($p = 0.0022$), as seen in Figure 26c.

To investigate further whether PFR correlated with the onset of acute lung injury, the percentage change in PFR from baseline was compared to the PaO₂/FiO₂ ratio. A significant correlation was seen between the PaO₂/FiO₂ ratio and PFR levels in the LPS group ($r^2 = 0.5213$, $p = 0.0035$) and in the gastric group ($r^2 = 0.7768$, $p = 0.0002$), but not in the lavage group ($r^2 = 0.1247$, $p = 0.21552$) (Figure 26d).

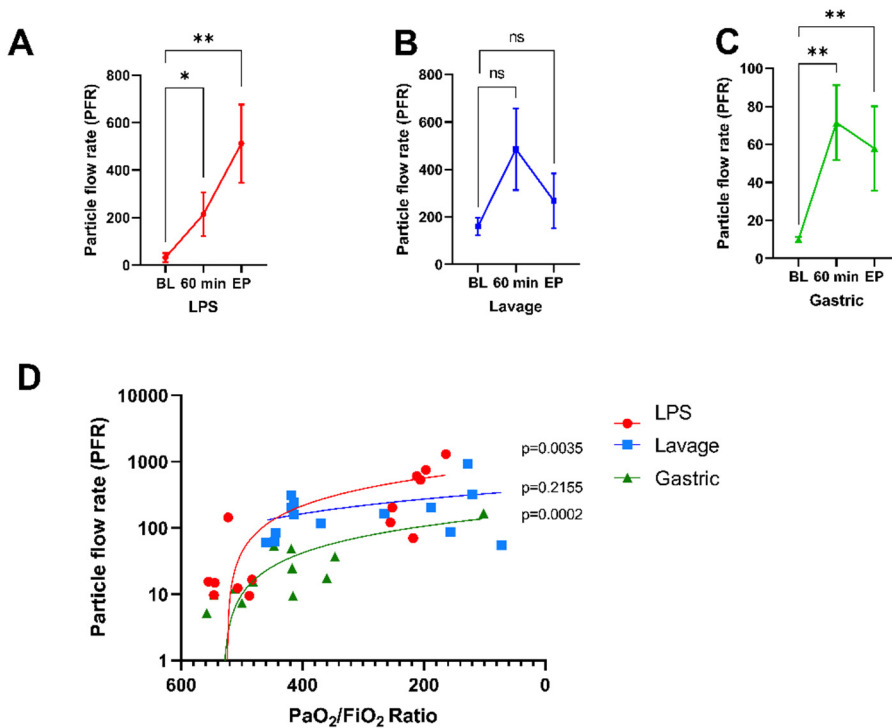


Figure 26. Particle flow rate (PFR) in different lung injury models

Particle flow rate (PFR) is shown from the airways during the experimental timeline and development of acute lung injury. In the LPS group, PFR increased significantly after 60 min and remained significantly elevated at the endpoint (EP) of the experiment. In the lavage group there was a non-significant increase in PFR at 60 min and end point compared to baseline. In the Gastric group a significant increase in PFR was seen after 60 min and at end point compared to baseline. A significant correlation, using simple linear regression, was seen between the PaO₂/FiO₂ ratio and PFR levels in the LPS group and in the gastric group, but not in the lavage group. LPS: lipopolysaccharide; BL: baseline; PaO₂/FiO₂: partial pressure of arterial oxygen/fraction of inspired oxygen.

Measurements of proteins in EBP from different lung injury models

EBPs were collected from all three groups and measured using a proximity extension assay (Olink Proteomics). Of the 92 proteins analyzed, 35 proteins were detected in all three groups. The gastric group generally expressed higher concentrations of proteins in comparison to the LPS and the lavage groups, as visualized in the heatmap (Figure 27a).

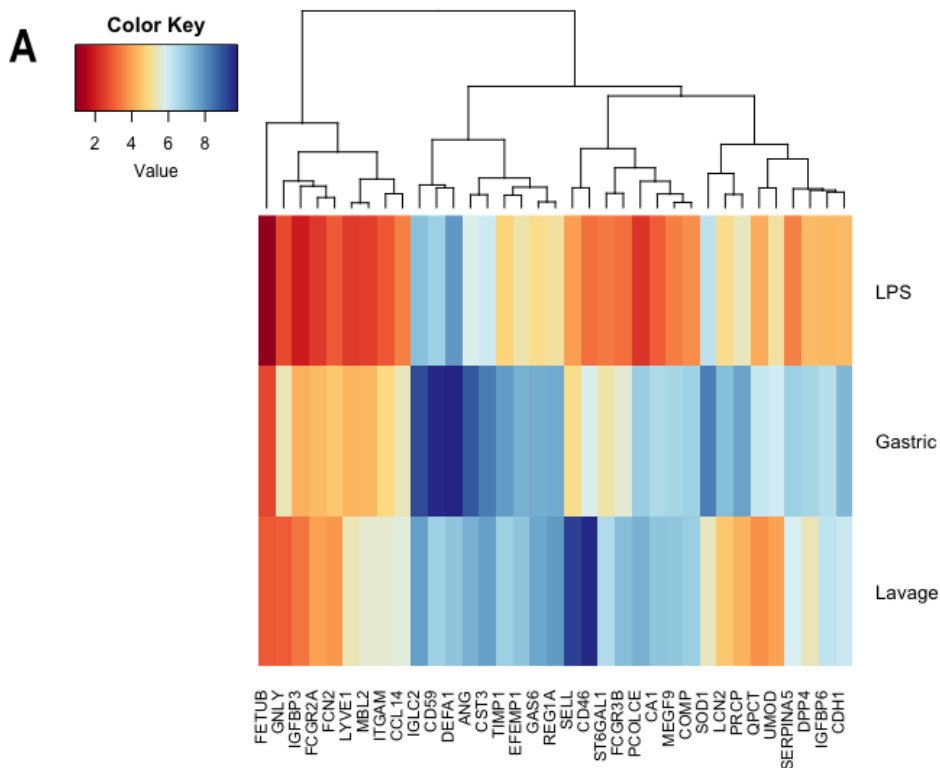


Figure 27a. Heatmap of proteins detected in exhaled breath particles (EBP)

Thirty-five proteins could be detected in exhaled breath particles (EBP) in all three animal groups using the proximity extension assay. Proteins were placed on a logarithmic scale and NPX values were set to zero. Positive values indicate NPX levels above detection and increased compared to the average-scaled NPX value and are shown in the Heatmap. LPS: lipopolysaccharide; NPX: normalized protein expression.

Eight proteins, known to correlate with lung injury, were singled out and analyzed separately. These proteins included dipeptidyl peptidase 4 (DPP4), insulin-like growth factor-binding protein 3 (IGFBP3), metalloproteinase inhibitor 1 (TIMP1), EGF-containing fibulin-like extracellular matrix protein 1 (EFEMP1), neutrophil defensin 1 (DEFA-1), CD59 glycoprotein (CD59), neutrophil gelatinase-associated lipocalin (LCN2) and growth arrest-specific protein 6 (GAS6). Comparison revealed no significant differences in the quantification of the proteins between the three lung injury groups (Figure 27b).

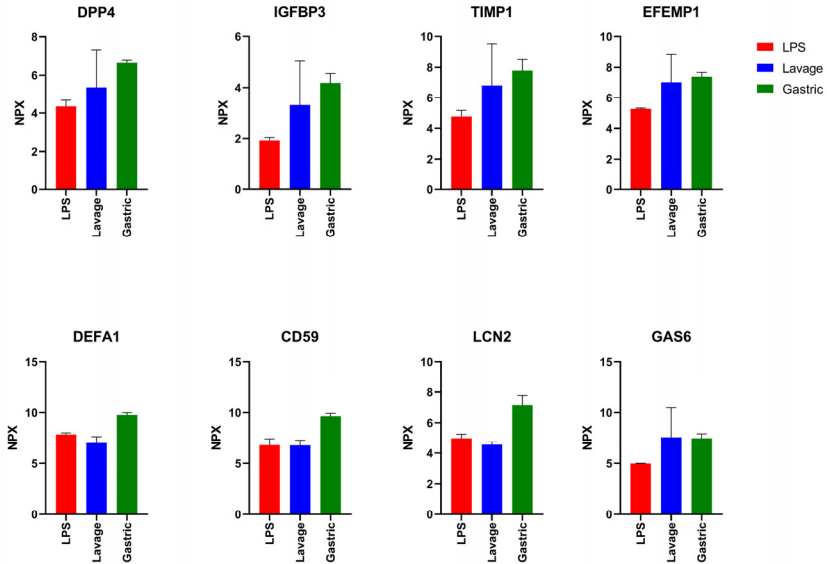
B

Figure 27b. Proteins in exhaled breath particles (EBP) associated with lung injury

Eight proteins known to be associated with lung injury were selected and are shown in Figure 27B. These are Dipeptidyl peptidase 4 (DPP4), Insulin-like growth factor-binding protein 3 (IGFBP3), Metalloproteinase inhibitor 1 (TIMP1), EGF-containing fibulin-like extracellular matrix protein 1 (EFEMP1), neutrophil defensin 1 (DEFA-1), CD59 glycoprotein (CD59), neutrophil gelatinase-associated lipocalin (LCN2) and growth arrest-specific protein 6 (GAS6). There were no significant differences among the three groups. LPS: lipopolysaccharide.

Cytokine response in plasma and BALF in different lung injury models

To monitor the inflammatory response after the induction of lung injury and correlate plasma marker changes to the concurrent measures of PFR in the airways, cytokine concentrations were assessed in plasma and in BALF over the experimental time course.

Cytokine concentrations were measured in plasma at baseline, 1 hour after injury induction, 2 hours after induction, and at the end of the experiment hereafter referred to as the end point.

A significant increase in plasma cytokine concentrations from baseline to end point was seen in the LPS animals for most of the cytokines. In comparison, only IL-6 increased significantly over time in plasma in the lavage and in the gastric groups, suggestive of the systemic effects seen in LPS in comparison with the mostly localized injury of the lavage and the gastric groups. The levels of TNF- α clearly

demonstrated this difference in the LPS model compared to the lavage and the gastric groups.

In the LPS group, TNF-a concentration in plasma increased from 114.44 ± 71.55 pg/mL at baseline to $18,727.12 \pm 2878.56$ pg/mL at end point ($p = 0.0005$) and in comparison, the lavage group TNF-a concentration in plasma increased from 111.68 ± 36.94 pg/mL to 148.77 ± 42.36 ($p = 0.4784$) pg/mL. The gastric group TNF-a concentration in plasma increased from 107.38 ± 104.75 pg/mL to 285.45 ± 245.32 pg/mL ($p = 0.5967$).

Accordingly, IL-6 increased from 5.46 ± 1.28 pg/mL at baseline in the LPS group to 113.24 ± 32.37 pg/mL ($p = 0.0006$) at the end point while IL-6 in the lavage group increased from 3.81 ± 1.16 pg/mL to 36.30 ± 7.86 pg/mL ($p = 0.0006$). The gastric group also showed an increase in IL-6, with values rising from 2.66 ± 2.56 pg/mL to 104.46 ± 56.52 pg/mL ($p = 0.0285$).

Comparing the groups as percentage change from baseline, as seen in Figure 28a, TNF-a differed significantly at the end point in the LPS group compared to the lavage and gastric groups ($p = 0.0040$ and $p = 0.0082$ respectively). Similarly, the LPS and the lavage groups differed significantly at their end points in IL-10 and IFN-a ($p = 0.0263$ and $p = 0.0047$, respectively).

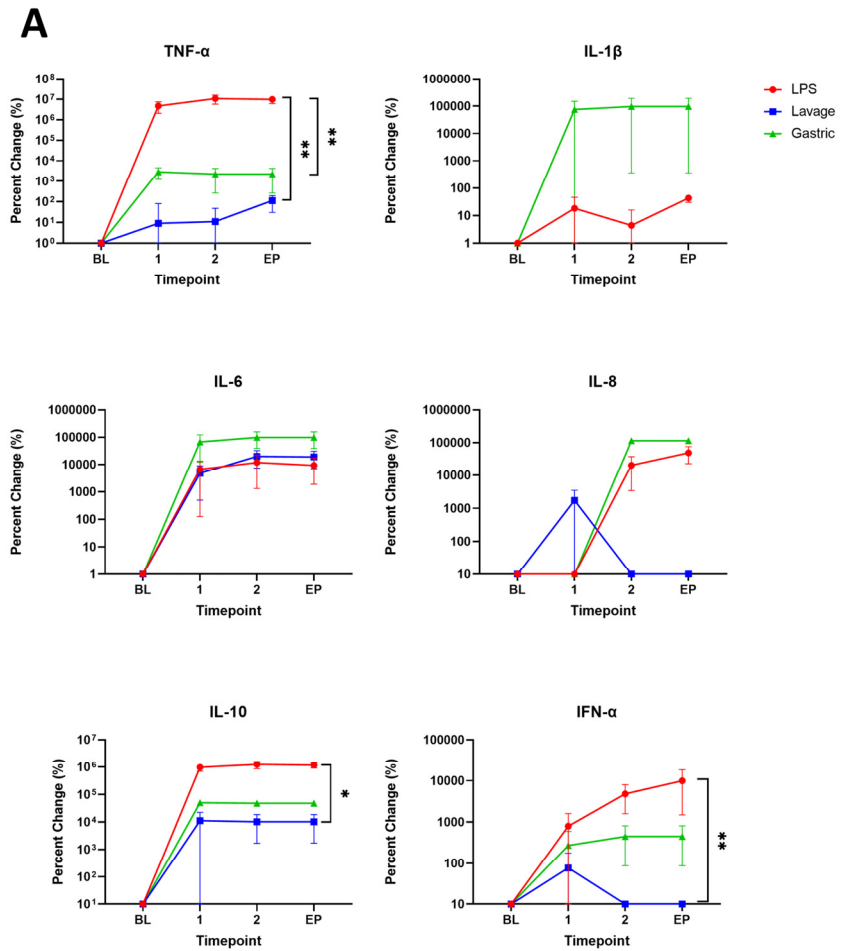


Figure 28a. Cytokine response in plasma in different lung injury models

Concentrations of different cytokines expressed as percent change from baseline (BL) and at different time points until end point (EP). Tumor necrosis factor- α (TNF- α), interleukin (IL)-1b, IL-10, IL-6, IL-8 and interferon alpha (INF-a) in plasma measured by multiplex at baseline before induction of lung injury, 1 and 2 hours after induction of lung injury and end point of the experiment.

In BALF, cytokine concentrations were measured at baseline and at end point. Only IL-6 increased significantly in the LPS and the lavage groups. In the LPS group, it increased from 3.43 ± 1.36 pg/mL to 54.87 ± 19.07 pg/mL ($p = 0.0116$). In the

lavage group, it increased from 11.45 ± 5.13 pg/mL to 137.63 ± 35.51 pg/mL ($p = 0.0075$). IL-6 in the gastric group increased from 17.75 ± 16.27 pg/mL to 939.28 ± 545.86 pg/mL from baseline to end point ($p = 0.3333$).

There were no significant differences between cytokine concentrations in percentage change from baseline to end point between the three different groups, as seen in Figure 28b.

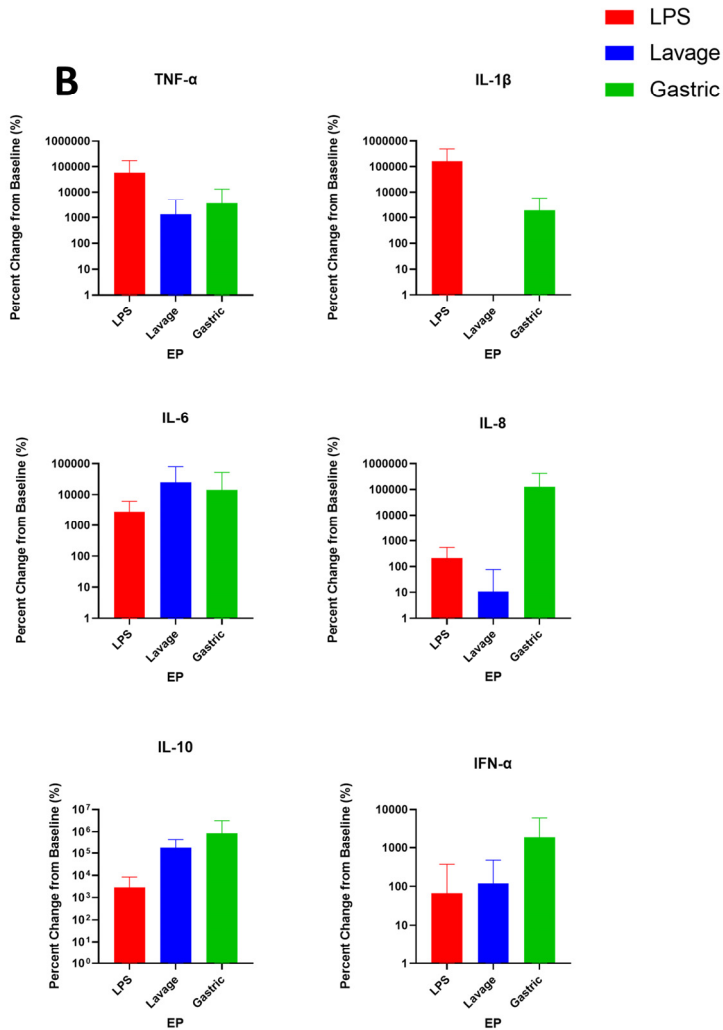


Figure 28b. Cytokine response in bronchoalveolar lavage fluid (BALF) in different lung injury models
 Concentrations of different cytokines expressed as percent change from baseline (BL) to endpoint (EP) of the experiment. Tumor necrosis factor-alpha (TNF-a), interleukin (IL)-1b, IL-10, IL-6, IL-8 and interferon alpha (INF-a) in BALF measured by multiplex. LPS: lipopolysaccharide.

Histological changes in different lung injury models

Histological evaluation with H&E staining of lung biopsies taken from the lower lobes at baseline (Figure 29) demonstrated normal lung tissue without anomalies exemplified by open airspaces, normal distribution of cells, and normal alveolar wall thickness. The lung biopsies at the endpoint of all three groups demonstrated signs of lung injury including infiltration of immune cells and diffuse alveolar damage with thickening of the alveolar-capillary barriers, intra-alveolar hemorrhage, and edema. The LPS and gastric groups showed increased levels of atelectasis and greater wall thickening. The lavage group showed accumulation of hemorrhage within the alveolar space but otherwise more preserved alveolar structure. Scale bar in the larger image represents 0.5 mm and the callout shows a magnified view of the tissue with the scale bar representing 0.2 mm.

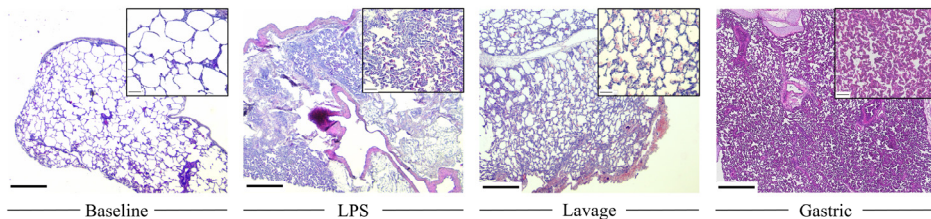


Figure 29. Hematoxylin and eosin (H&E) staining of lung tissue in different lung injury models

Histological evaluation of lung biopsies with hematoxylin and eosin (H&E) staining taken at baseline and after LPS administration at endpoint, the endpoint of lavage procedure, and at the endpoint of gastric aspiration. The baseline demonstrates normal lung histology exemplified by open airspaces. Scale bar in the larger image represents 0.5 mm and the callout shows a magnified view of the tissue with the scale bar representing 0.2 mm. LPS: lipopolysaccharide.

Paper IV

Establishment of ARDS in donor lungs

Donor pigs were given LPS intravenously and developed mild-to-moderate ARDS within 120 ± 30 min, as defined by two separate arterial blood gases within a 15-min interval, making the donor lungs unsuitable for transplantation. There was no significant difference in the severity of ARDS between donors that would go on to receive treatment ($\text{PaO}_2/\text{FiO}_2$ ratio = 281.9 ± 73.2 mmHg) compared to those assigned to the non-treated group (ratio = 294.5 ± 72.1 mmHg, $p = 0.139$). All donors showed hemodynamic instability after LPS administration and required inotropic support (norepinephrine, dobutamine or epinephrine) with the clinical purpose of maintaining hemodynamic stability, as seen in Table 3.

Table 3. Physiological changes during lipopolysaccharide (LPS)-induced acute respiratory syndrome (ARDS)

Clinical measurements for all pigs: oxygen saturation (Sat), heart rate (HR), systolic blood pressure (SBP), diastolic blood pressure (DBP), mean arterial pressure (MAP), central venous pressure (CVP), temperature (Temp); hemodynamic variables: systolic pulmonary pressure (SPP), diastolic pulmonary pressure (DPP), mean pulmonary pressure (MPP), pulmonary artery wedge pressure (Wedge), cardiac output (CO), systemic vascular resistance (SVR); blood gas parameters: pH, partial pressure of oxygen (PaO₂), partial pressure of carbon dioxide (PaCO₂), hemoglobin (Hb), lactate, base excess (BE), partial pressure of oxygen divided by fraction of inspired oxygen (PaO₂/FIO₂); mechanical ventilator settings with volume-controlled ventilation: minute volume (MV), peak inspiratory pressure (PIP), peak inspiratory pressure, positive end-expiratory pressure (PEEP), tidal volume (Vt), dynamic compliance (C_{dyn}), respiratory rate (RR), fraction of inspired oxygen (FIO₂).

	Baseline	Confirmed ARDS
Sat (%)	98.4 ± 0.4	96.2 ± 1.5
HR (bpm)	67.25 ± 2.9	125.6 ± 7.4
SBP (mmHg)	100.8 ± 3.1	98.0 ± 7.1
DBP (mmHg)	70.7 ± 3.1	50.4 ± 6.9
MAP (mmHg)	83.0 ± 3.3	64.4 ± 7.2
CVP (mmHg)	6.3 ± 0.8	6.0 ± 1.3
Temp (C°)	37.7 ± 0.3	36.5 ± 0.5
SPP (mmHg)	25.6 ± 1.5	39.6 ± 3.1
DPP (mmHg)	15.3 ± 2.5	26.4 ± 2.7
MPP (mmHg)	18.8 ± 1.3	34.3 ± 2.5
Wedge (mmHg)	9.9 ± 0.8	9.8 ± 1.3
CO (L/min)	4.2 ± 0.3	4.7 ± 0.5
SVR (DS/cm ⁵)	1372.6 ± 128.0	1024.3 ± 225.9
PVR (DS/cm ⁵)	167.9 ± 23.2	412.0 ± 142.2
CI	2.7 ± 0.1	3.8 ± 0.4
pH	7.4 ± 0.0	7.2 ± 0.0
PaCO ₂ (mmHg)	5.5 ± 0.3	7.3 ± 0.4
PaO ₂ (mmHg)	34.7 ± 1.1	19.7 ± 3.4
Hb (g/L)	89.0 ± 6.0	95.5 ± 1.2
Lactate (mmol/L)	1.5 ± 0.1	3.0 ± 0.4
BE (mmol/L)	4.4 ± 0.8	1.7 ± 0.6
MV (L/min)	8.0 ± 0.4	7.0 ± 1.0
Max. Pressure (cmH ₂ O)	16.7 ± 0.9	19.0 ± 2.1
PEEP (cmH ₂ O)	4.9 ± 0.2	5.0 ± 0.0
Vt (ml)	389.0 ± 14.1	350.5 ± 9.5
C _{dyn} (mL/cmH ₂ O)	35.6 ± 3.4	25.7 ± 4.3
RR (breaths/min)	19.8 ± 0.5	22.0 ± 2.0
PaO ₂ /FIO ₂ (mmHg)	517.1 ± 7.9	233.3 ± 22.7

A significant increase in cytokines, including IL-1b, IL-6, IL-8, IL-10, IL-12, and TNF-a was seen during induction of ARDS in plasma and in BALF, confirming the disease model (Figures 30a, 30b).

In plasma, TNF-a values increased from a baseline of 103.4 ± 42.0 pg/mL to $14,346.1 \pm 3734.0$ pg/mL at the time of confirmed ARDS ($p < 0.0001$). In a similar manner, IL-1b increased from 96.8 ± 52.2 pg/mL to 194.6 ± 96.6 pg/mL ($p = 0.008$). IL-6 increased from baseline 6.7 ± 1.3 pg/mL to 140.2 ± 33.5 pg/mL at confirmed ARDS ($p = 0.003$). IL-8 increased from 0.6 ± 0.2 pg/mL to 454.2 ± 231.1 ($p = 0.002$) and IL-10 from non-detected to $10,30.5 \pm 102.1$ pg/mL ($p = 0.001$). Lastly, an increase in IL-12 was found from 120.7 ± 22.2 pg/mL to 525.4 ± 184.0 pg/mL ($p = 0.007$).

Cell counts were measured every 30 min in the donor animals to investigate the relative amounts of white blood cell types. A dramatic decrease in intravascular white blood cells following LPS administration was noted (Figure 30c). Neutrophils decreased from 11.9 ± 1.7 cells at baseline to 1.3 ± 0.3 cells at the time of confirmed ARDS ($p < 0.001$), together with a decrease in lymphocytes from 11.2 ± 1.4 to 3.3 ± 0.4 ($p < 0.001$).

Lung tissue biopsies (H&E staining) taken prior to LPS administration appeared normal (Figure 30d). After establishment of ARDS, there was significant infiltration by immune cells of the alveolar spaces and notable atelectasis which affected most alveolar spaces. Erythrocytes were also found in abundance within the alveolar space with the occasional appearance of early hyaline membrane formation. Furthermore, vasodilation was visible within the capillaries where there was also hemorrhage and aggregation of neutrophils.

Blinded scoring was performed on all pigs at baseline, post-ARDS, post-EVLP and post-transplantation by three independent observers. Significant increases in a cumulative lung injury score were observed, accounting for multiple signs of lung injury following ARDS onset via LPS administration (baseline mean score = 5.3 ± 0.6 , LPS mean score = 12.8 ± 1.8 ($p = 0.047$), Figure 30e). No significant differences were seen between the treated and non-treated groups at baseline (treated mean score of 4.44 ± 1.8 , non-treated mean score of 6.1 ± 2.3 , $p = 0.21$). Following ARDS, lungs were harvested *en bloc* approximately 1 hour after ARDS was confirmed.

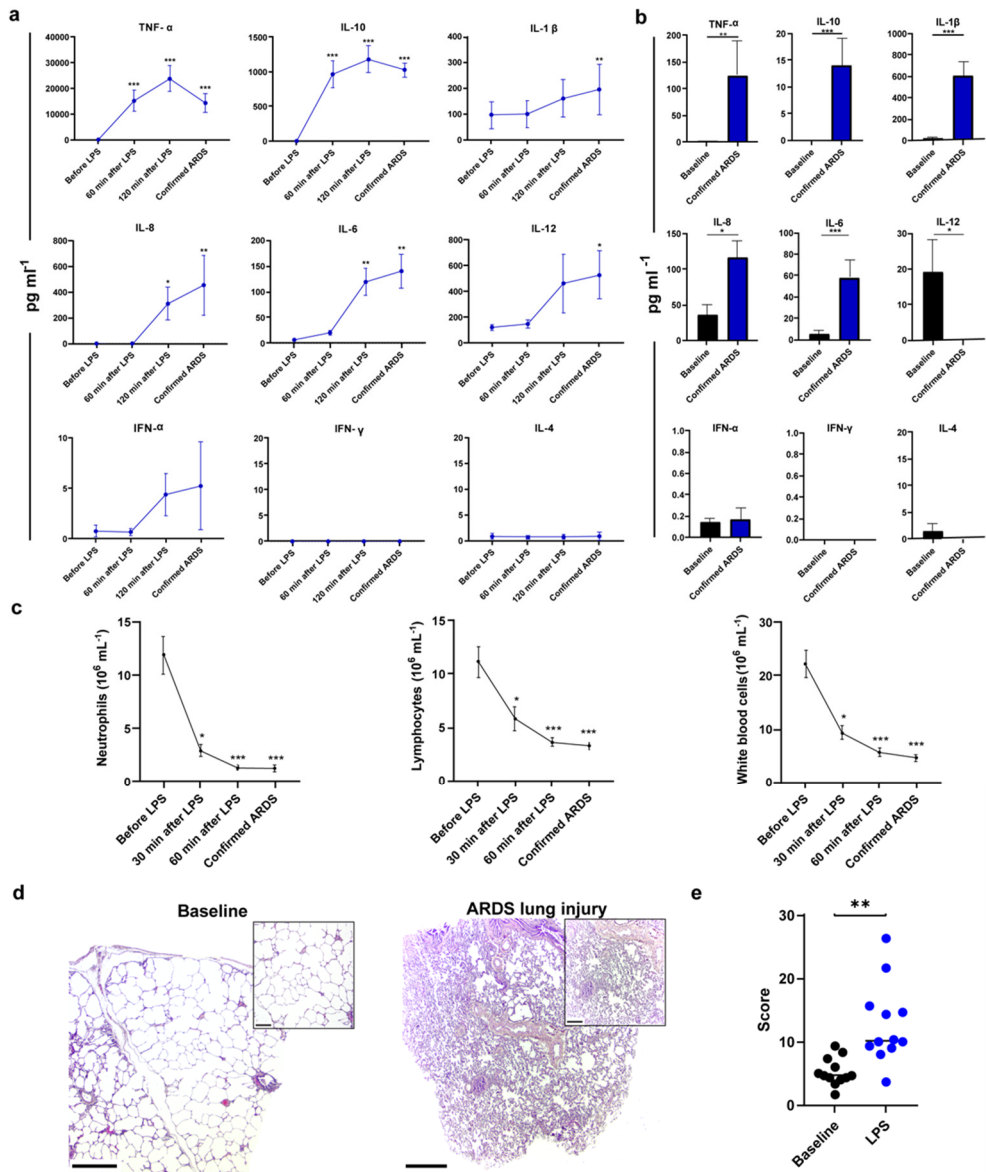


Figure 30. Lipopolysaccharide (LPS)-induced acute respiratory distress syndrome (ARDS) in donor animals
a Cytokine measurement in plasma in the donor before LPS was administered and then 60 and 120 min after LPS was given. Cytokines were also measured in the plasma at the time of confirmed ARDS. **b** Cytokine measurement in bronchoalveolar lavage fluid (BALF) at baseline and again at confirmed ARDS. **c** Neutrophils, lymphocytes, and white blood cell counts were recorded at baseline, 30 and 60 min after LPS, and at confirmed ARDS. **d** Baseline (left) and ARDS lung injury (right) hematoxylin and eosin (H&E) staining. Scale bar in the larger image represents 0.5 mm. The callout shows a magnified portion of the tissue where the scale bar represents 0.2 mm. **e** Scoring of lung injury of baseline biopsies and biopsies taken at pulmonary harvest after ARDS confirmation. All graphs represent data from all donors ($n = 12$).

Recovery of pulmonary function and inflammation following cytokine filtration in ex vivo lung perfusion (EVLP)

After harvesting, the lungs were submerged in Perfadex® PLUS solution (XVIVO Perfusion, Gothenburg, Sweden) and put in cold storage for 2 hours before being subjected to EVLP for 4 hours. All pulmonary grafts had ARDS according to the Berlin ARDS definition using the PaO₂/FiO₂ ratio at the initiation of EVLP. In this definition, the distinguishing criteria of ARDS severity is the PaO₂/FiO₂ ratio such that mild ARDS falls between 201-300 mmHg, moderate between 101-200 mmHg, and severe as ≤ 100 mmHg. The cytokine filter-treated lungs increased their gas exchange capacity and reached a PaO₂/FiO₂ ratio of 324 ± 25 ($p = 0.03$) and met the threshold of clinical acceptance for transplantation. The non-treated lungs did not pass clinical acceptance as they had a PaO₂/FiO₂ ratio of 263.0 ± 15. No significant differences could be seen between the two groups ($p = 0.31$).

All lungs increased in PVR during the EVLP; however, this increase was not significant within each group or between the groups. The airway pressure increased significantly in the non-treated group and the pulmonary compliance decreased significantly in the non-treated group; however, the difference was not significant between groups (Figure 31a).

This change in pulmonary function is reflected on a macroscopic level, as the gross morphology of the treated lungs also showed decreased hemorrhage compared to non-treated donors (Figure 31b). Both groups required additional Steen solution in the EVLP circuit over the 4 hours. Two pairs of lungs in the non-treated group and two in the treated group had acute pulmonary edema after 2 hours in EVLP with fluid withdrawal in the main bronchus. The addition of supplementary Steen solution, a procedural measure taken when perfusate levels dropped below 300 mL/hours in the EVLP reservoir, is a sign of pulmonary edema.

To monitor the inflammatory response during EVLP, cytokine concentrations were measured in the perfusate each hour. A significant decrease in the pro-inflammatory cytokine IL-1b was seen in the cytokine-filtrated lungs both in the perfusate and in BALF. This was exemplified by the 4th hour of EVLP which showed a decrease from 282.9 ± 72.4 pg/mL in the non-treated perfusate to 75.6 ± 27.1 pg/mL in the treated perfusate and a decrease from 362.4 ± 280.3 pg/mL in non-treated BALF to 15.3 ± 15.3 pg/mL in treated BALF. A generally lower level of remaining cytokines could be detected in the treated lungs; however, none reached significance (Figures 31c-d).

Cell counts were measured every hour during EVLP. No significant change in the number of neutrophils, leukocytes, and total white blood count could be found within the 4-hour period in both donor groups (Figure 31e).

Following EVLP, the histology of the tissue showed a significant difference between the treated lung and the non-treated lung with regard to morphology and

lung injury (Figure 31f). Treated lungs had fewer immune cells, erythrocytes, and atelectasis compared to the non-treated lungs.

Histological scoring revealed a significant improvement between the treated (average score of 5.4 ± 1.2) and the non-treated donors (score of 12.4 ± 2.8) ($p = 0.044$) following EVLP (Figure 31g).

According to the wet/dry ratio, an index of accumulated fluid in the lungs, there was no significant difference between the groups at the end of EVLP (Figure 31g, $p = 0.07$).

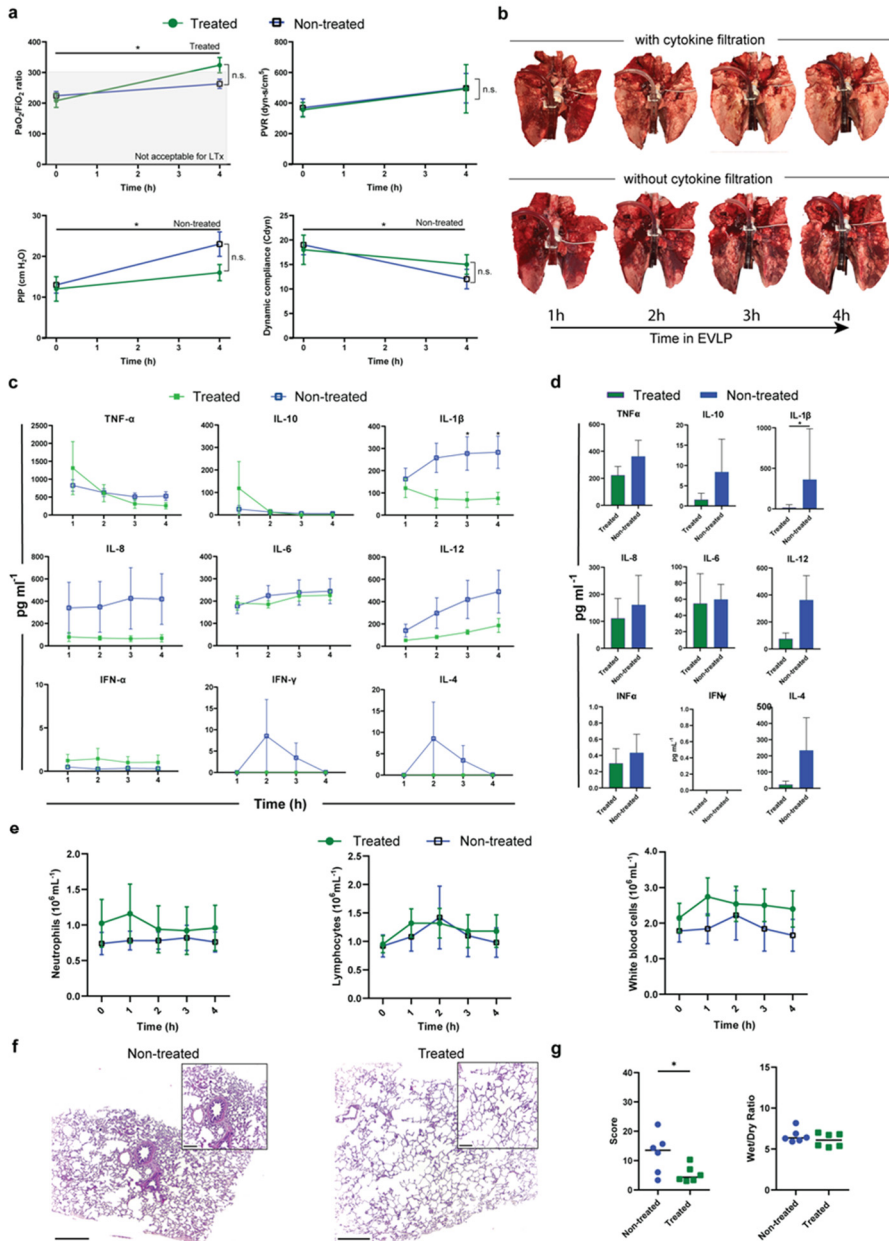


Figure 31. Improvement of pulmonary function following cytokine filtration during ex vivo lung perfusion (EVLV)

Donor lungs connected to an ex vivo lung perfusion (EVLV) circuit and assigned to either non-treated ($n = 6$) or treated ($n = 6$) group wherein treatment consisted of continuous cytokine filtration during the 4 hours of EVLP. **a** Measures of pulmonary gas exchange including the arterial oxygen partial pressure/fractional inspired oxygen (PaO₂/FiO₂) ratio, pulmonary vascular resistance (PVR), peak inspiratory pressure (PIP), and dynamic compliance (C_{dyn}) were recorded throughout EVLP. **b** Gross morphology of the treated lungs (top) and the non-treated lungs (bottom) throughout the 4-hour period of EVLP. **c** Cytokines in plasma with samples taken every hour during EVLP.

d Bronchoalveolar lavage fluid (BALF) was tested at the end of EVLP for cytokine levels. **e** Cell counts of neutrophils, lymphocytes, and white blood cells taken every hour. **f** Images of H&E histology of non-treated lungs (left) and treated lungs (right). Scale bar in the larger image represents 0.5 mm. The callout shows a magnified portion of the tissue where the scale bar represents 0.2 mm. **g** The scores of the histology on the left compare cytokine filtration groups. Right graph shows wet/dry ratios of lung biopsy tissue obtained at the end of EVLP. All graphs represent data from either the treated donor lungs ($n = 6$) or non-treated lungs ($n = 6$).

Restoration of pulmonary function and reduced inflammation after 48 hours of transplantation in treated recipients

After 4 hours of EVLP, a left thoracotomy in the recipient was followed by a left pneumonectomy and a left LTx. Once the lung was transplanted, an extracorporeal hemoperfusion with cytokine filtration in the circuit was placed in the treated recipients for the first 12 postoperative hours. The treated group required significantly less inotropic support post-transplantation, showing improved hemodynamic stability compared to the non-treated group.

To track the inflammatory response post-transplantation, cytokine concentrations were measured in plasma and collected at multiple time points post-transplantation. All measured cytokines were generally decreased post-transplantation in the cytokine filtration-treated group; however, none of these reached statistical significance (Figures 32a-b).

When looking at the blood cell count post-transplantation, a significant decrease in both neutrophils and total white blood cells was observed in the treated group during the transplantation follow up, especially after the right pneumonectomy. At the end of the observation, neutrophils were reduced from 11.7 ± 3.0 (non-treated) to 5.6 ± 1.3 cells (treated) ($p < 0.05$), while lymphocyte counts were significantly lower in the treated group at the majority of time points studied, showing a decrease from 6.4 ± 1.2 (non-treated) to 3.7 ± 0.2 (treated) ($p < 0.001$). Furthermore, total white cell counts dropped from 18.1 ± 3.4 (non-treated) to 9.8 ± 1.2 (treated) ($p < 0.001$) after 4 hours following right pneumonectomy (Figure 32c).

Regarding histology, in the non-treated group, there were significant morphological characteristic changes in ARDS which remained, including the accumulation of immune cells, intra-alveolar hemorrhage, and the collapse of most alveolar spaces after transplantation (Figure 32d). In the treated animals, an immune response was still seen, exemplified by the infiltration of immune cells, as expected in transplanted lungs, but the alveolar spaces were mostly open, and respiratory bronchioles and blood vessels appeared without major visible damage.

The lung tissue wet/dry weight ratios were measured after 4 hours of EVLP, and at 48 hours' post-transplantation. While the ratios between the treated and non-treated groups were not statistically significant (Figure 32e), there was a decrease in the treated lungs' average wet/dry ratio from the time of EVLP (a ratio of 8.55 ± 1.8) to the end of LTx (a ratio of 6.10 ± 0.8) ($p = 0.0196$).

There was a lower score in treated lungs relative to non-treated ones at 48 hours' post-transplantation where the treated recipients had a significantly lower lung injury score of 10.9 ± 1.8 compared to the non-treated group with a score of 21.4 ± 4.1 ($p = 0.041$), (Figure 32e).

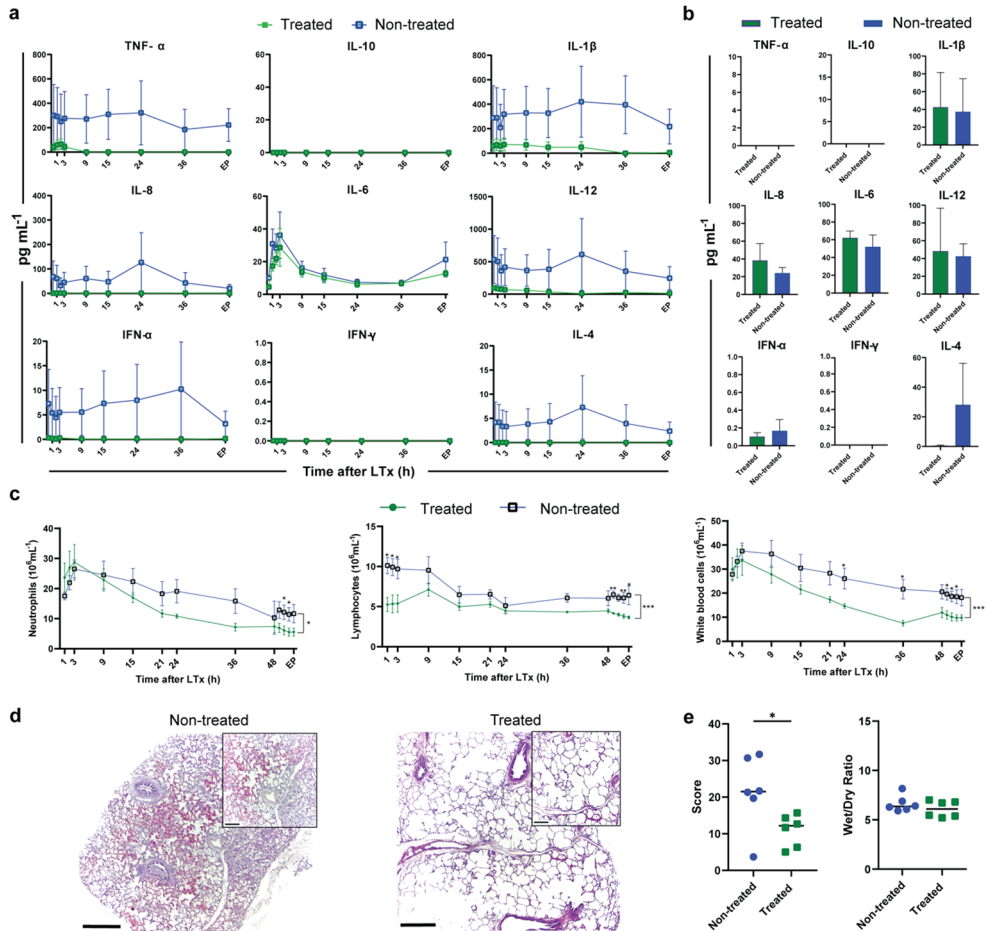


Figure 32. Reduced inflammation during follow-up after lung transplant (LTx)

a Cytokine levels in plasma were monitored throughout the 48-hour period following transplantation. **b** Bronchoalveolar lavage fluid (BALF) was tested for cytokine concentrations at the termination of the experiment. **c** Cell counts including neutrophils, lymphocytes, and total white blood cells were tracked. **d** Hematoxylin and eosin (H&E) staining of non-treated (left) and treated (right) biopsies taken at the end, following 4 hours of isolated transplanted lung function. **e** Quantification of the lung damage seen in H&E staining (left) and wet/dry ratio of tissue (right) were obtained for both groups. All graphs represent data from either the treated recipient lungs ($n = 6$) or non-treated lungs ($n = 6$).

Reduction of primary graft dysfunction (PGD) in treated recipients

Both treated and non-treated recipients were monitored for 48 hours' post-transplantation, with the last 4 hours encompassing single transplanted left lung function following a right pneumonectomy.

The overview of clinical vital measurements during these 4 hours are shown in Table 4 and Figure 33, which demonstrate improved oxygenation capacity of the lung and improved pulmonary vascular resistance upon reliance on the transplanted lung alone. Pulmonary compliance was generally improved in the treated group compared to the non-treated group ($p = 0.001$). Lactate levels were generally lower in the treated group ($p = 0.001$, Figure 33a).

Table 4. Overview of physiological measurements during the last 4 hours of the experiment

Oxygen saturation (Sat), heart rate (HR), systolic blood pressure (SBP), diastolic blood pressure (DBP), mean arterial pressure (MAP), central venous pressure (CVP), temperature (Temp); Hemodynamic variables: systolic pulmonary pressure (SPP), diastolic pulmonary pressure (DPP), mean pulmonary pressure (MPP), cardiac output (CO), systemic vascular resistance (SVR), pulmonary vascular resistance (PVR); Blood gas parameters: hemoglobin (Hb), lactate, base excess (BE); Mechanical ventilator settings with volume-controlled ventilation: minute volume (MV), peak inspiratory pressure (PIP), positive end-expiratory pressure (PEEP), tidal volume (Vt), respiratory rate (RR). The values for the treated recipients are on the left and the non-treated on the right.

	Before Pulmectomy		4 hours' Post-Pulmectomy	
	Treated	Non-Treated	Treated	Non-Treated
Sat (%)	96.2 ± 1.4	96.8 ± 0.70	95.5 ± 1.8	95.2 ± 1.9
HR (bpm)	91 ± 7.0	79 ± 7.6	83.3 ± 7.7	89.8 ± 15.0
SBP (mmHg)	106.6 ± 6.0	109.4 ± 4.0	101.6 ± 3.0	105.0 ± 5.6
DBP (mmHg)	63 ± 8.5	72 ± 3.9	47.4 ± 7.8	65.6 ± 1.4
MAP (mmHg)	80.2 ± 9.0	87.8 ± 5.1	64.8 ± 9.5	80.4 ± 2.7
CVP (mmHg)	6.8 ± 1.0	7.6 ± 1.5	7.0 ± 1.1	6.0 ± 1.4
Temp (C°)	38.6 ± 0.2	39.5 ± 0.2	38 ± 0.3	38.4 ± 0.6
CO (l/min)	4.3 ± 0.7	4.5 ± 0.5	3.7 ± 0.5	5.3 ± 0.5
SVR (DS/cm ⁵)	1730 ± 12	1180 ± 10	1385.0 ± 6.0	1030.0 ± 13.0
PVR (DS/cm ⁵)	196 ± 37	238 ± 39	244.0 ± 36.0	427.0 ± 68.0
pH	7.4 ± 0.1	7.4 ± 0.1	7.3 ± 0.0	7.3 ± 0.1
Hb (g/L)	72 ± 4.0	83 ± 1.5	69.4 ± 4.7	82.6 ± 4.5
BE (mmol/L)	6.4 ± 1.7	6.9 ± 1.8	8.7 ± 1.2	8.4 ± 0.8
MV (L/min)	9.7 ± 1.3	24.6 ± 14.0	11.8 ± 1.7	26.4 ± 15.0
Max. pressure (cmH ₂ O)	22 ± 1.3	22.4 ± 1.5	24.0 ± 1.5	25.4 ± 1.3
PEEP (cmH ₂ O)	6.4 ± 1.0	6.2 ± 0.7	6.0 ± 1.0	5.6 ± 0.6
Vt (mL)	407.0 ± 2.03	429.0 ± 23.5	396.5 ± 14	385.2 ± 10.0
Cdyn (mL/cmH ₂ O)	26.4 ± 0.7	27.1 ± 2.2	22.7 ± 1.0	20.4 ± 1.5
RR (breaths/min)	26.4 ± 0.7	23.8 ± 1.8	22.7 ± 1.0	29.8 ± 2.2
SPP (mmHg)	27.0 ± 2.7	26.0 ± 2.1	38.0 ± 1.5	38.0 ± 4.9
DPP (mmHg)	18.0 ± 11.0	15.0 ± 3.6	23.5 ± 1.5	27.4 ± 9.8
MPP (mmHg)	24.0 ± 1.0	24.0 ± 1.7	31.0 ± 1.0	30.0 ± 4.0

During the first day post-transplantation, no significant difference could be seen in the gas exchange between the groups ($p = 0.122$). During the second day, however,

and especially after the right pneumonectomy, a significant increase in gas exchange could be seen in the treated compared to the non-treated group with $p < 0.0001$ (Figure 33b).

In the non-treated group, five recipients developed PGD grade 3, while one developed PGD grade 2. In the treated group, only one recipient developed PGD grade 2 while the rest of the treated recipients had PGD grade 0. This represented a significance difference in the number of recipients developing PGD in either treatment group ($p = 0.007$, Figure 33c)

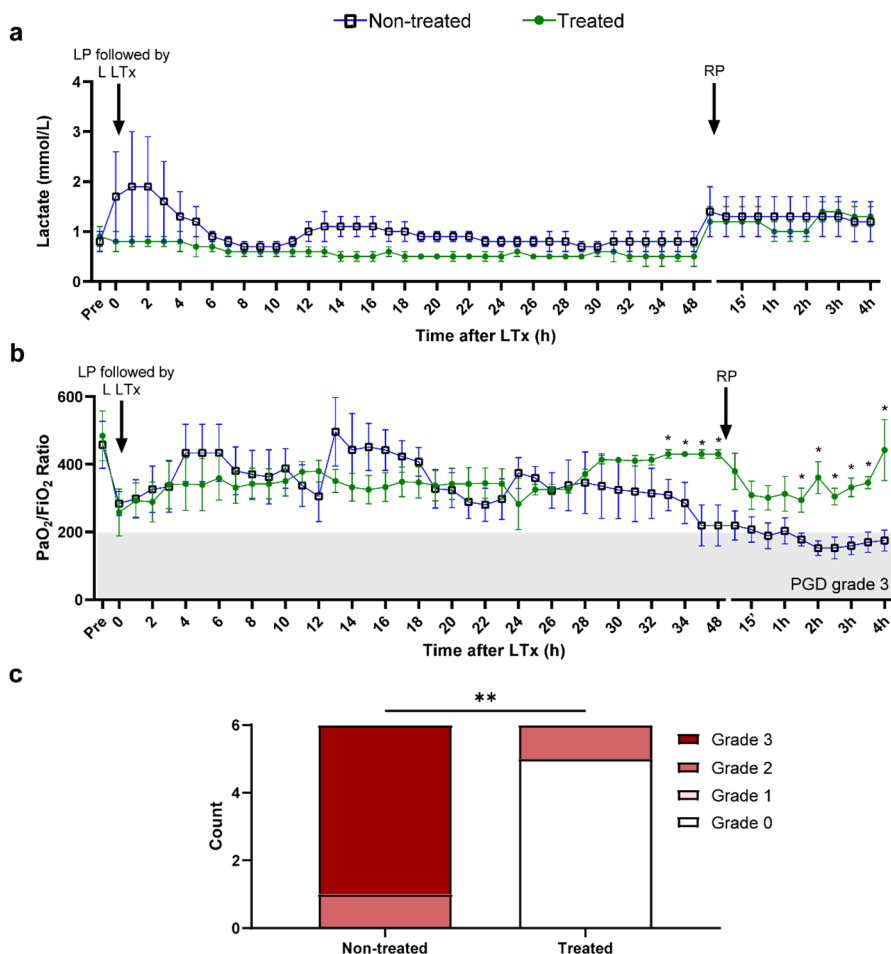


Figure 33. Reduced primary graft dysfunction (PGD) in treated recipients

Both graphs show a first arrow indicating left pneumonectomy (LP) followed by left lung transplantation (LP followed by LLTx) and a second arrow describes the time of right pneumonectomy (RP) a Lactate levels recorded throughout the transplantation follow-up. b Arterial oxygen partial pressure/fractional inspired oxygen (PaO₂/FiO₂) ratios for both groups were followed from before transplantation in the recipient to 48 hours of follow-up. c Comparison of primary graft dysfunction (PGD) grades following transplantation. All graphs represent data from either the treated recipient lungs ($n = 6$) or non-treated lungs ($n = 6$). LLTx: left lung transplantation.

Paper V

Demographic characteristics of the patients

Of 36 patients assessed for eligibility, six patients did not meet the criteria and were excluded. The remaining 30 patients, 22 males and eight females with a mean age of 69 years, were randomized to either VCV or PCV during the first 30 min upon arrival at the ICU. After this 30-min period, which included a recruitment maneuver at 15 min, patients were placed on PRVC until they gained consciousness and they were then placed on pressure-support ventilation (PSV) until extubation as seen in Figure 34.

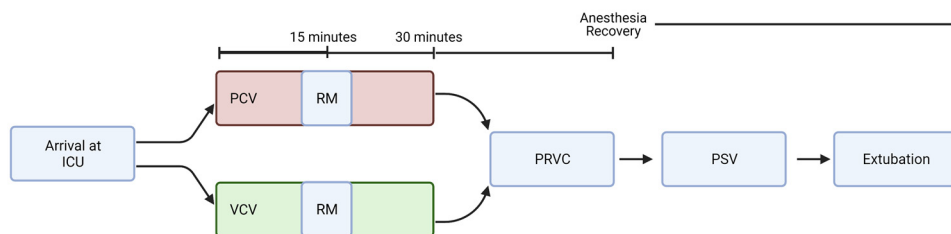


Figure 34. Flowchart with mechanical ventilation in the intensive care unit (ICU)

After randomization to either volume-controlled ventilation (VCV) or pressure-controlled ventilation (PCV) including a recruitment maneuver (RM) as the first line of treatment at arrival at the ICU. The mechanical ventilation was thereafter set to pressure-regulated volume control (PRVC) in all patients until recovery from anesthesia when the ventilator was switched to pressure-support ventilation (PSV) to facilitate spontaneous breathing. Figure created with BioRender.com.

All randomized patients received given interventions. No patients were lost to follow-up.

Particle flow rate (PFR) in different ventilation modes

When comparing different ventilation modes, PRVC produced the lowest PFR at a rate of 77.2 ± 34.4 particles/min compared to VCV 83.7 ± 16.8 particles/min ($p = 0.0285$) and PCV 439.1 ± 153 particles/min ($p = 0.0149$). However, there were no significant differences between the VCV and PCV group ($p = 0.3980$). During recovery from anesthesia, the ventilator mode was set to PSV to allow spontaneous breathing. The PFR increased significantly during PSV compared to all other ventilation modes studied. The PFR during PSV was 2249 ± 426 particles/min compared to PFR during PRVC 77.2 ± 43.4 particles/min ($p < 0.0001$) (Figure 35).

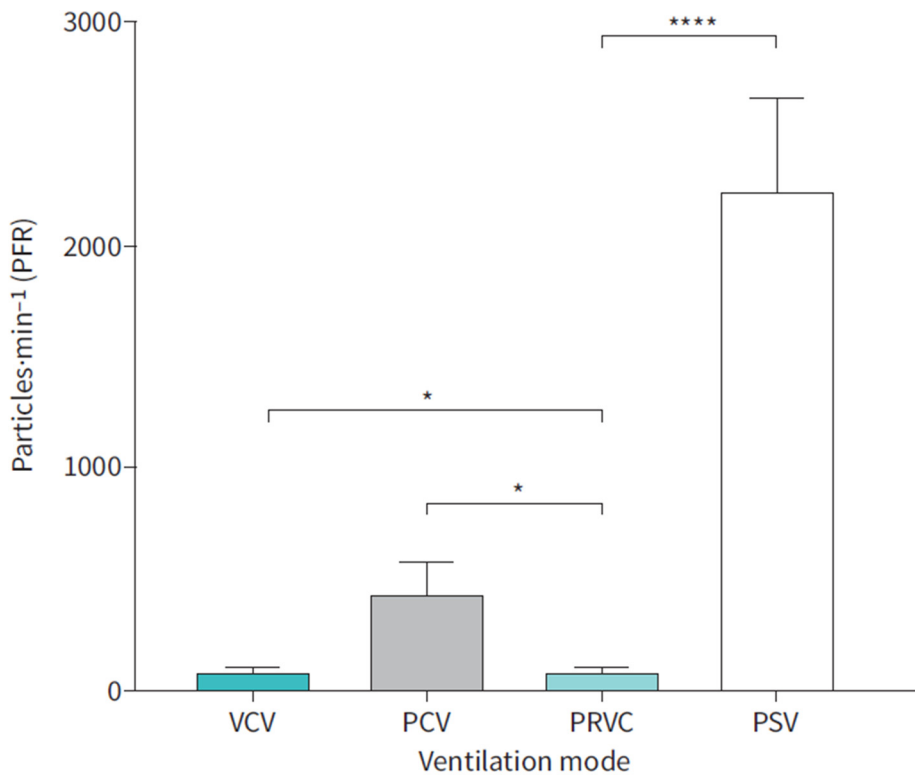


Figure 35. Different ventilation modes

Particle flow rate (PFR) was significantly lower when using pressure-regulated volume control (PRVC) compared to volume-controlled ventilation (VCV) and pressure-controlled ventilation (PCV). Ventilation with pressure support ventilation (PSV) resulted in significantly higher PFR compared to PRVC.

The impact of a recruitment maneuver on particle flow rate (PFR)

A recruitment maneuver was performed in patients after 15 min in both the VCV and PCV modes, but did not result in any significant changes in PFR either before or after. To clarify, PFR in VCV before the recruitment maneuver was 77.6 ± 19.3 particles/min and after it was 89.8 ± 28 particles/min ($p = 0.6529$) (Figure 36).

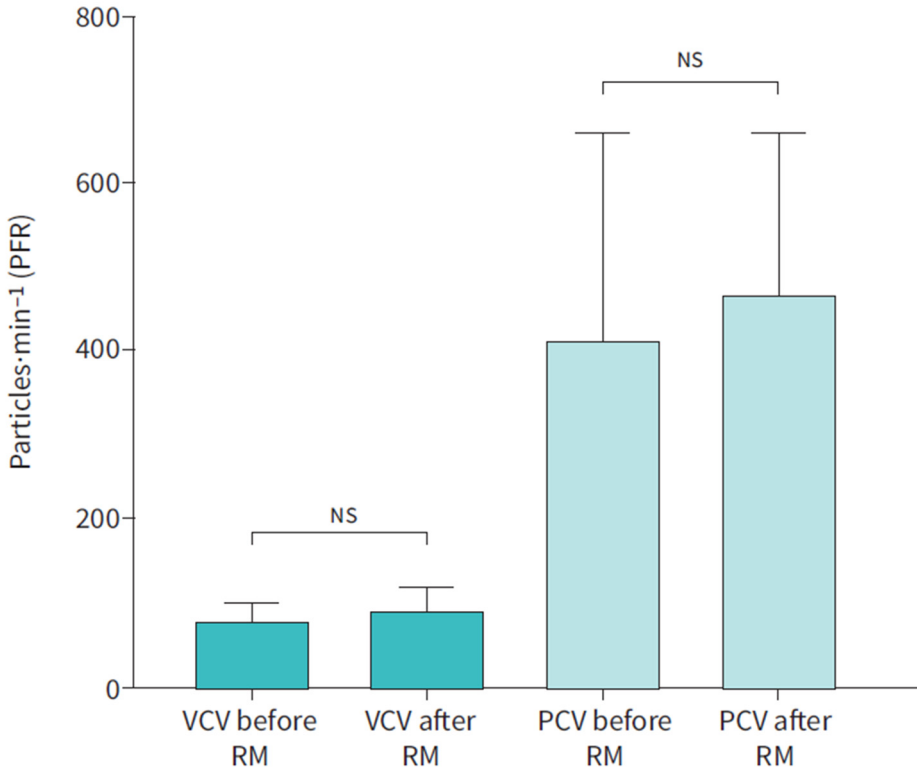


Figure 36. Recruitment maneuver in different ventilation modes

No significant difference was found in either ventilator mode when comparing particle flow rate (PFR) before and after the recruitment maneuver (RM).

Distribution of particles in different ventilation modes

The PExA device analyzes particle size and divides them into eight different size groups or bins according to particle impaction.

We discovered a significantly higher number of particles in PSV for all particle size groups (1-8) compared to the other ventilation modes ($p < 0.0001$) (Figure 37a).

When analyzing particle size separately, we found a significantly lower PFR in particle size groups 1-4 when PRVC was compared to PCV and a significantly lower PFR in particle size groups 1-3 when PRVC was compared to VCV. No difference was found when comparing VCV to PCV for particle sizes 1-4, nor did we find any difference for particle size groups 5-8 (Figure 37b).

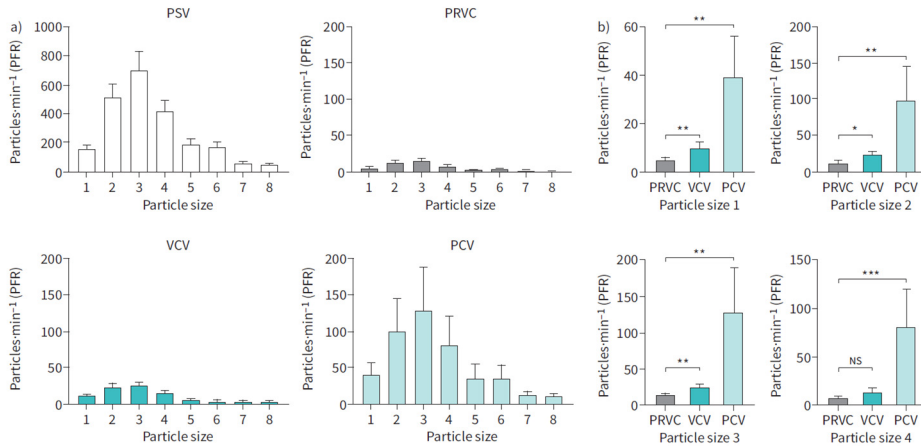


Figure 37. Distribution of particles in different ventilation modes

a) Distribution of particles according to size in the different ventilation modes. In pressure support ventilation (PSV), there was a significantly higher particle flow rate (PFR) for all particle sizes (1-8) compared to the other ventilation modes. b) PFR for particle sizes 1-4 in the different ventilation modes. A significant difference was found between pressure-regulated volume control (PRVC) and pressure-controlled ventilation (PCV) for particle sizes 1-4. A significant difference between PRVC and volume-controlled ventilation (VCV) was found for particle sizes 1-3. No difference was found when comparing VCV to PCV for particle sizes 1-4.

Discussion

Paper I

Critically ill patients with ARDS are difficult to care for. They are frail and prone to deterioration when moved or treated with invasive methods. Regarding treatment and prognosis, it is crucial to identify as soon as possible the patients who will develop ARDS. The identification of an early biomarker or clinical parameter specific for ARDS would facilitate the detection of patients at risk and help to optimize or personalize their therapy at an early stage. Furthermore, this could also reduce the need for time-consuming and difficult in-hospital transports for imaging diagnostics and invasive diagnostics.

In Paper I, we used a large porcine LPS model of acute lung injury to mimic a clinical situation with patients developing ARDS. In clinical settings, ARDS develops over days. In pre-clinical settings the time to develop ARDS may be shortened due to controlled infusion of concentrated LPS. In this particular model, we used a dual hit strategy by applying LPS both intravascularly and endotracheally. According to the Berlin definition (34), all animals that received LPS developed ARDS within a time frame of only 90 min. Lung injury was confirmed using histology that showed characteristic changes in the lung parenchyma and airways with immune cell infiltration, septal thickening, airway constriction and intra-alveolar hemorrhage. Sepsis-like changes in physiological parameters were expected after LPS administration, with a drop in systemic blood pressure, pH, and PaO₂ and, at the same time, an increase in cardiac output, lactate, and PaCO₂.

The interesting part in Paper I is that a significant increase in PFR from the airways was detected in the animals before a mild ARDS stage (according to blood gas analyses) was reached and before any significant changes in traditional parameters, such as ventilator settings, occurred. The result suggests that the PFR could be used as an early indicator of lung injury.

The pathology of ARDS involves inflammation leading to loss of endothelial and epithelial barrier functions, with increased leakage and movement of protein and fluid into the RTLF (32, 113). This results in diffuse alveolar damage, with release of proinflammatory cytokines such as TNF- α , IL-1, and IL-6, high levels of which are hallmarks in ARDS (114, 115). Proinflammatory cytokines recruit neutrophils to the lungs, leading to further inflammation and oxidative cell damage that results

in changes in the RTLf and might also be reflected in increased PFR, as indicated in Paper I. The significant increase in cytokines (TNF- α , IL-1, IL-6, IL-8, and IL-10) in animals that developed ARDS, is similar to cytokine profiles in other porcine models of ALI and ARDS (116) and has been linked to mortality in ARDS patients (117). Notably, 60-120 min before an increase in cytokines could be detected in the animals, PFR increased significantly, indicating that monitoring of PFR may be a new, complementary approach in the clinic for early detection of ARDS.

The PExA device can be used in conjunction with mechanical ventilation (57, 59). It is connected to the expiratory limb on the ventilator and could be connected to the patient in the OR or ICU without interference with existing medical devices. An OPC might therefore be used as a continuous, real-time measurement of PFR in the ICU and would not hinder or complicate the normal standard of care for the patient. While this study included a relatively small number of animals and was limited to one mode of injury, our results indicate the potential of measuring PFR as a complementary technique to those currently used in the clinic to generate further important knowledge on the pathophysiology of the lungs.

Paper II

ECMO support is often used to enable lung-protective ventilation in patients with severe ARDS (118, 119) and when used with protective ventilation, ECMO can improve outcome. (45, 119, 120). Since the pandemic outbreak of the COVID-19 pneumonia, as many as 1752 COVID-19 patients have been treated with ECMO with a discharge from ECMO/survival rate of 55% according to the Extracorporeal Life Support Organization (ELSO) Register (July 2020) (<https://www.else.org/COVID19.aspx>). However, previous studies have shown that ECMO may worsen an existing lung injury and has the potential to lead to complications such as pulmonary hemorrhage, thromboembolic complications, and hemorrhagic infarction (121-123). Its use in ARDS with septic shock has at times not been recommended as a standard course of therapy (124, 125) but this is about to change.

ECMO is not a treatment for underlying lung injury. Its use simply transfers the responsibility of oxygenation from native lung tissue to an extracorporeal membrane, providing the injured lung with an opportunity to recover as a life-prolonging measure. A method to measure the condition of the native lung is needed until weaning from ECMO is possible according to current standards (55, 56, 126). A bedside measure of pulmonary state would be of great clinical value given the significant risks of transporting the patient to different departments for imaging or diagnostics.

In Paper II, PFR measurements were obtained continuously during the LPS porcine model and measured on a weekly basis in human patients to determine the clinical relevancy of using PFR as a measure of change in pulmonary status. We were able to show that PFR increases following the initiation of ECMO in an LPS porcine model to a greater extent than ECMO in a sham-treated animal and furthermore demonstrate that human patients who improved on ECMO had lower PFRs and those who deteriorated had higher PFRs. The motivation for this work was to investigate whether PFR could serve as a tool to measure the progress of lung injury and recovery over time during ECMO treatment. Previously, we have shown that PFR could be used as an early indicator of ARDS (127), and that alterations in pulmonary blood flow alter PFR (56). We also showed that LTx patients with PGD, a form of acute lung injury resembling ARDS, exhibit increased PFR compared to patients without PGD (57).

To explore the relationship of ECMO and PFR specifically, this study placed animals on ECMO after confirmed ARDS. PFR was significantly increased following ECMO establishment despite previous results of decreased PFR when pulmonary blood flow was reduced in an *ex vivo* model (56). When comparing LPS ECMO animals to those given LPS alone, PFR was increased along with the amount of hemorrhage observed macroscopically in the lungs. The coexistence of high PFR with greater lung injury demonstrates that the flow rate can reflect the deteriorating condition of the lungs. This increase in PFR was also seen following the start of ECMO in sham ECMO animals relative to their non-ECMO correlates, but PFR was significantly greater in LPS ECMO animals compared to sham-treated ECMO animals. From this, it can be inferred that the induced ARDS state correlates with a higher PFR that can be monitored during ECMO treatment.

In plasma, we found significant increases in TNF- α , IL-6, and IL-12 between 60 and 180 min in all animals who received LPS and an increase in PFR 30-90 min before cytokines could be detected, which is similar to the cytokine profiles in other porcine models of ARDS shown by us and by others (116, 127). Elevated IL-6 concentrations during ECMO treatment have been associated with parenchymal damage in animal models (128), and also associated with worse outcomes in ECMO patients (129). There is a significant increase in IL-6 concentrations in plasma and BALF in LPS ECMO animals compared to sham-treated ECMO animals. This matches the increased PFR seen in LPS ECMO animals relative to sham-treated ECMO animals. Furthermore, IL-6 was significantly increased in LPS ECMO animals compared to LPS animals as well as IL-12 and TNF- α , indicating a correlation with ECMO itself with an inflammatory response in the lung known to occur when blood comes in contact with foreign material (122). The increase in these inflammatory markers is important given the association between the cytokines and ARDS, as stated in the literature (130, 131). TNF- α , when studied in the context of ARDS, has been cited as expressing higher levels in non-survivors of LTx, which has led to it being postulated as a potential biomarker (130). TNF- α

specifically reflects lung injury severity rather than diagnosis as it is higher in patients with ARDS even compared to those with severe pneumonia, as reported by Bauer (132). IL-6 has also been postulated as a promising biomarker when predicting both mortality and morbidity in ARDS. In clinical studies, it has been increased in both plasma and BALF samples in non-survivors (130). Moreover, it has been correlated with a poorer oxygenation index and more days spent on a ventilator (133, 134). Alveolar M1 macrophages secrete pro-inflammatory cytokines including IL-12 (135). Macrophages also produce TNF- α to activate neutrophils and recruit more inflammatory cells to the alveoli. Given the role that these cytokines play in lung injury and the relationship we have demonstrated between the pattern of PFR increasing as the number of cytokines increase in LPS-induced lung injury, we believe that PFR could be a measure of severity of lung damage as PFR increases in LPS animals and further increases in LPS ECMO animals.

Proteins related with acute lung injury and ARDS were detected in EBPs. These proteins included CXCL10, VEGF-A, MCP-1, MMP-1 and FAS ligand and were found to be significantly higher within both the LPS animals and LPS ECMO animals, a finding that further supports the conclusion that PFR can be used as a measurement of increasing lung injury over time.

Studying lung recovery with PFR is prohibitive in this animal model due to the intensive care facilities and the staff who would be needed to monitor lung recovery over days and weeks. To explore the utility of PFR for an extended time, we studied four patients in the ICU with ECMO treatment over a period of 3 weeks. All four patients had a similar PFR level at the start of the ECMO treatment. In the two patients who recovered lung function, there was a decrease in PFR over time. This occurred simultaneously with an increased V_t , increased lung compliance, and improved air content on chest X-ray. In the two patients whose lung function deteriorated during ECMO treatment, there was a significant increase in PFR over time. Additionally, their chest X-rays were reflective of a worsening condition.

As reported previously (55, 56), higher V_t generates a larger number of particles, and it might be expected that PFR would decrease accordingly if the V_t was the main factor determining PFR, as those patients whose condition deteriorated had lower V_t . Instead, we observed that patients had higher PFRs as their lung condition aggravated. These results demonstrate that PFR mirrors the clinical state of lung function. Trends in PFR could thus be used by clinicians to predict the progression of lung injury, even when the patient is treated with ECMO.

Paper III

Animal models have been used extensively over the years to mimic clinical scenarios of ALI and ARDS in humans with the intended goal of further understanding the underlying pathogenetic mechanisms. The use of such models allows for the evaluation of new diagnostic tools and treatments, the development of which is particularly needed given the high mortality rates for ARDS (65-67, 76). Given the heterogenous underlying causes of ARDS, the development of one sole animal model that includes all causes is challenging and perhaps impossible to develop. Different agents and methods have been utilized to induce lung injury with the most commonly used being bacterial toxins or injection of live bacteria, aspiration of gastric contents or acid equivalents, and repeated lavage in combination with harmful ventilatory strategies (65-67). These different ARDS models all have distinct advantages and disadvantages.

Bacterial toxins or live bacteria given as intravenous or endotracheal installation or as a 'dual hit' of both are considered a good representation of the clinical scenario. These models, however, are extremely challenging due to the accompanying sepsis-like conditions, massive cytokine release and hemodynamic instability that requires skilled anaesthesiologists to care for the animals. This injury model is particularly hard to stabilize given its susceptibility to right ventricular heart failure and septic shock (136, 137).

Aspiration models, with endotracheal installation of gastric contents or gastric acid equivalent, resembles a common clinical scenario seen in the ICU and do not normally require any advanced inotropic circulatory support but will require ventilatory optimization, especially during the endotracheal installation itself and the first 60 min thereafter. These aspiration models develop ALI and ARDS within 4-6 hours but there have even been reports of clear signs of ALI as little as 2 hours' post-installation (138, 139).

The repeated lavage models have been successful in combination with harmful ventilation. While the repeated lavage flushes out the surfactant of the alveoli, harmful ventilation with high Vt and low PEEP is often needed to induce sustained lung injury (140, 141). The repeated lavage methods have been the most useful to explore ventilatory strategies while the model might be less clinically relevant to ARDS, as a result of the lack of induced inflammatory response, and low representability among ICU patients (65).

In conditions without lung injury, the integrity of the lung microvascular endothelium, the endothelial cell adhesion molecules and cell junctions are sustained. The degree to which these remain intact may be reflected in decreased values of PFR. Inversely, under conditions facilitating ALI, the breach in integrity of these structures may result in an increased PFR. The motivation for our work was to investigate the potential of PFR to serve as a diagnostic measure of ALI

irrespective of the underlying cause. We therefore explored the diagnostic value of PFR in three different porcine animal models with ALI using an LPS-induced model, a gastric aspiration model and a repeated lavage model. These models correlate to clinical scenarios of infection, aspiration, and drowning, respectively, which may lead to the development of ARDS. ALI was further confirmed in all three models with histological assessment, with changes in the parenchyma and airways manifested by immune cell infiltration, septal thickening, and airway constriction. A significant increase in PFR could be seen in both the LPS and in the gastric porcine model while the lavage model gave a non-significant, non-sustained increase in PFR.

The $\text{PaO}_2/\text{FiO}_2$ ratio is used to assess the diffusion and oxygenation capacity of the lungs as well as establishing the degree of lung injury according to the Berlin definition of ARDS (34). In Paper III the increase in PFR was correlated to the $\text{PaO}_2/\text{FiO}_2$ ratio in the LPS and gastric animals while no such relation could be seen in the lavage model. Given the hypothesis that the increase in PFR and subsequent lung injury is correlated with depleted integrity of epithelium and endothelium and its cell adhesion molecules and cell junctions, the flushing of the RTL in the lavage model may explain the lack of correlation between PFR and $\text{PaO}_2/\text{FiO}_2$ ratio. This is supported by the initial increase in PFR, which is not sustained, reflecting the washing of the RTL and thus the absence of significant particles to be released within the exhaled breath. In addition, in the lavage model, the increased tendency of alveolar collapse and atelectasis based on clinical findings could also explain the lack of a sustained increase in PFR. The finding of atelectasis is reflected in the increased inspiratory pressure and decreased compliance resulting in decreased ventilated lung volume and increased PaCO_2 . The LPS model resulted in an enormous increase in PFR while the gastric model had a more moderate development. The LPS animals showed general sepsis-like changes in both hemodynamic measures and blood gas parameters, with a drop in blood pressure and base excess concomitant with an increase in cardiac output, heart rate and lactate which were not seen to the same extent in the gastric or the lavage animals.

To monitor the inflammatory response after the induction of lung injury and record the relationship between changes in plasma markers and changes in PFR, cytokine concentrations were measured in plasma and BALF before induction of lung injury and repeatedly during the experimental course. In both plasma and BALF, cytokines known to be implicated strongly in the pathology of ALI and ARDS were detected in the three porcine models of this study. The finding of these inflammatory changes, and in particular the increases in TNF- α , IL-1 β , and IL-8, all of which followed a timeline reflecting the increases seen in PFR, particularly in the LPS animals, underlined the potential of PFR to be used as a measure of lung injury. The sustained increase in PFR in the LPS and gastric groups contrasting to the short-lived moderate changes in the lavage group paralleled the changes seen in the

cytokine levels of these three groups, strengthening the belief that PFR should continue to be studied as a correlate of lung injury.

To further investigate the potential role of EBPs in diagnosing ALI, the protein composition of collected particles was analyzed. Eight proteins with a potential as biomarkers were found in all three models. Among these are proteins related to the innate immunity response, CD59, DEFA-1, EFEMP1 and LCN2 have been reported in other studies to be elevated in BALF and plasma following lung injury (142-146). CD59, also known as protectin, is a complement-regulated protein which binds complement factors C8 and C9 to inhibit their cytolytic activity and block the assembly of the membrane attack complex (147). It is also known to activate T-lymphocytes, with a role in immunoreaction regulation (148). DEFA-1 is known to be increased in both epithelial cells and diffusely throughout the mucosa, parenchyma, and vessels and has been identified as a contributor to the development of lung injury (149) in an acid-aspiration model. Furthermore, increased copies of DEFA-1 were shown to correlate to more severe sepsis due to dysfunction of the endothelial barrier and endothelial pyroptosis (150).

Analysis of the EBPs also revealed an increase in specific regulatory proteins (DPP4, IGFBP-3, TIMP1 and GAS6), which correlate to the onset of ALI (149, 151-154). Several studies have implicated DPP4 in pulmonary diseases, including ischemia-reperfusion injury, and specifically within LPS-induced lung injury models (155). In a model of ARDS, DPP4 linked to the release of key mediating cytokines TNF- α , IL-6, and IL-8, which were then reversed using DPP4-inhibitor sitagliptin (153). Another protein identified by this present study was the tissue inhibitor metalloproteinase 1 (TIMP1), which has been associated with worse outcomes in ARDS (156). The matrix metalloproteinases (MMPs) and their tissue inhibitors (TIMPs) are known to modulate the extracellular matrix and TIMP1 has been elevated in other models of LPS-induced ARDS (142). IGFBP-3 has been linked to ARDS through the finding of higher levels in BALF compared to healthy controls (146). The discovery of these proteins, known to be linked to ALI and ARDS, on the collected membranes shows that EBP measurements can be conducted in a non-invasive manner. From the demonstrated sensitivity of the tool to detect these proteins, the use of EBP presents an opportunity for rapid and early detection of known injury correlates but, as implicated in Paper II, this statement requires further study before EBP monitoring can be established as a valuable diagnostic method in the clinic.

Paper IV

This current study explores the implementation of a cytokine filter in the regeneration of ARDS-damaged lungs, rendering the organs suitable for transplantation. The results suggest that the use of a cytokine filter: 1) recovers pulmonary function and inflammation during EVLP, 2) restores pulmonary function and reduces inflammation in the 48-hours' follow-up post-transplantation, and 3) was correlated with decreased incidence of PGD in recipients. The value of this technique lies in the interest in restoring injured lungs and increasing the donor pool. Previous results by Hozain et al. have shown that cross-circulation may help rejuvenate injured human lungs (157); however, the implementation of xenogeneic or allogenic cross-circulation may prove challenging in ethical and practical application. In contrast, the use of EVLP is an already established method and can alone improve the condition of injured lungs by reconditioning. Together with a cytokine filter, EVLP is capable of rejuvenating healthy lungs from extended cold ischemic storage (111, 158). This method, however, has not examined the results of using cytokine filtration on lungs damaged by ARDS which are then transplanted and examined for PGD.

To address this issue, donor lungs with LPS-induced ARDS were transplanted and treated with cytokine filters. This form of inducing ARDS is well known in large animal models given the clinical translational potential of the disease and previously described by us (127, 159). Using an LPS-induced ARDS model represents an opportunity to explore the expansion of the donor pool considering the large number of organs that are rejected due to ALI. When studying EVLP and cytokine filtration, the focus on extended cold ischemic storage has resulted in the conclusion that lung tissue may be perfused for longer times, but these studies have not considered a condition in which the lung is damaged to begin with. The similarity of LPS-induced ARDS to a clinical scenario of ARDS combined with the current context of an added cytokine filter would address the issue of ameliorating donor tissue damaged prior to storage. All donor animals developed mild to moderate ARDS with significantly lower gas exchange capacities before lung harvest, as measured by the $\text{PaO}_2/\text{FiO}_2$ ratio. This adheres to the Berlin definition of the syndrome (34).

Further evidence of ARDS onset was supplemented by the blinded scoring conducted, in which graded samples based on proteinaceous debris, thickening of the alveolar walls, hemorrhage and atelectasis showed significant histological damage in LPS-treated lungs as compared to controls. The administration of LPS was also followed by a dramatic increase in early response cytokines, specifically IL-6, IL-8, IL-1b and TNF-a in all donors, a finding that is similar to previous results in Papers I-III. After completion of cytokine filtration for 4 hours during EVLP, harvested lungs were examined for recovery of function. While the $\text{PaO}_2/\text{FiO}_2$ ratios of non-treated lungs did not reach acceptable levels for transplantation, treated ones

had improved gas exchange capacity and most reached a PaO₂/FiO₂ ratio above 300 mmHg which is considered clinically acceptable for transplantation (160).

Furthermore, lungs in the treated group had significantly reduced BALF levels of IL-1b relative to non-treated lungs, a finding that is of particular interest given its previous identification as a prognostic indicator of non-recovery during EVLP (99). Other cytokines, together with immune cells, were also generally decreased throughout EVLP in the treated lungs relative to the non-treated ones. This indicates a state of reduced inflammation and restoration of lung function in the treated lungs after cytokine filtration further supported by the histological examination and reduced need for perfusate. The techniques of extracorporeal blood purification to reduce tissue damage has been used in several surgical conditions associated with increased inflammatory cytokines (101, 161, 162). Commercial products include cytokine filters that remove substances through polymer beads, which target middle- and low-molecular weight molecules, thus reducing levels of cytokines. They have been employed *in vivo* during human orthotopic heart transplantation and in human kidney transplantation settings (101, 161, 163). In patients with severe sepsis and acute lung injury, the device was reported to reduce the levels of IL-6, IL-8, IL-1b and TNF-a (162, 164-166).

Cytokine filtration was utilized in this study for its potential to rescue ARDS donor lungs for LTx (110, 111). The transplanted lungs were followed for 48 hours and were found to have a reduced need for inotropic support along with greater hemodynamic stability which mirrors the finding of reduced noradrenaline doses in septic patients with cytokine filtration (167). In this model, recipients were also found to have reduced cytokine levels and there were significant decreases in neutrophils and total white blood cells counts in the treated group. Decreasing levels of cytokines is particularly important in ARDS given that clinical studies have shown increased IL-6 and TNF-a in plasma and BALF samples in non-survivors, as well as a correlation of IL-6 with a longer time spent on mechanical ventilation (130, 133, 134). Histologically, the treated lung tissue in this study showed a reduction in accumulated immune cells. This reinforces the finding that cytokine filtration contributes to a decreased inflammatory state.

As double LTx is almost impossible in pigs due to anatomical challenges on the right bronchus, a single left LTx was conducted in this model. To evaluate the transplanted lung function, a right-sided pneumonectomy on the native lung was performed at the end of follow up, making the animal dependent on breathing only with the transplanted lung. Interestingly, there was no difference in the gas exchange capacity during the first day post-transplantation between the groups. However, during the second day and especially after the right pneumonectomy, a significant difference in gas exchange could be seen between the groups, wherein the treated lungs fared better.

Post-transplantation, two recipients showed signs of septicemia. One recipient in the treated group recovered with no subsequent signs of organ failure. Another recipient in the non-treated group could not be saved despite advanced intensive care and the animal died 9 hours later. Cytokine filtration may have potentially mitigated the risk of developing fatal septicemia in the treated recipient. Interestingly, one graft in the treated group developed dramatic pulmonary edema after 2 hours of EVLP. Up to 1.2 L of fluid were drained from the trachea during EVLP and measures were taken during transplantation to fit the enlarged graft into the chest. On the third day post-transplantation, virtually all edema had been resorbed and the graft showed excellent gas exchange capacity and no signs of PGD, suggesting that cytokine filtration was of particular importance during hemoperfusion post-transplantation. The wet-dry ratio assay was employed in order to determine the degree of pulmonary edema in the biopsies and provides evidence that the addition of a cytokine filter reduces accumulation of fluid in the tissue. Comparing the end of EVLP to the end of LTx showed a decrease in ratio in favor of LTx.

These incidences of edema and septicemia illustrate how the addition of a cytokine filter may support restoration of non-acceptable donor lungs in the critical days immediately following transplantation given the mortality associated with PGD. In this study, five of six treated recipients had no PGD at all. This contrasts with the five of six recipients who developed PGD grade 3 in the non-treated group. Immune cell populations were significantly lower in the treated animals. This could result in a curbed immunological response which could facilitate the acceptance of a new organ during the initial post-transplantation period. The diminished immunological response afforded by a cytokine filter could be responsible for the reduced incidence of PGD (168).

Paper V

Conventional monitoring of mechanical ventilation in the ICU is incapable of detecting subtle changes or mechanical stressors in the lung which may precede the onset of VILI. New techniques, and ideally those that are non-invasive, should strive to detect early changes in the lung with the goal of reducing mechanical stress to the lungs. Such strategies could make the ventilatory treatment more personalized and potentially reduce VILI. Considering that a contributing factor to VILI may be repeated opening and closing of the distal airways during mechanical ventilation (169), a method of monitoring the distal airways would be useful in the clinic.

PFR, measured by the PExA device, reflects EBPs transmitted by small airways (54, 61) and, as a result, low PFR is hypothesized to correlate with reduced opening and closure of the small airways and, thereby, more gentle ventilation. Our hypothesis regarding high PFR during PSV ventilation is based on the breathing pattern in PSV

that is similar to that of spontaneously breathing patients without a ventilator. As seen in a previous study, PFR in spontaneously breathing patients is significantly higher than the PFR that occurs in patients on mechanical ventilation (59), and changes in ventilation mode correlated to changes in PFR. A clinical study on LTx patients revealed no difference in PFR using VCV and PCV (57). This same observation was reproduced in Paper V.

According to clinical guidelines, PRVC is believed to be a gentle ventilation mode when a specific volume is desired, as it also maintains the lowest possible pressure to achieve this volume. A previous study compared PRVC to VCV and found significantly lower PIP when ventilating with PRVC (170). In the present study, a significantly lower PFR was noted when using PRVC relative to both PCV and VCV. Additionally, PSV as a mode resulted in a higher PFR compared to all other modes. As a result of such high PFR, the mechanics of breathing must be considered. While the patient is sedated with no spontaneous breathing, neither the diaphragm or the accessory respiratory muscles contribute to the work of breathing. Postoperatively, as sedation wears off and the patient recovers from anesthesia, the patient increasingly takes over more of the respiratory work and the ventilation mode is switched to PSV. During the shift from controlled mechanical breathing to more conscious control by the patient, with support from the ventilator, there is a significant increase in PFR. This increase is most likely the result of activation of respiratory muscles, as active breathing with negative pressures seems to open previously closed alveoli. This finding is similar to the result of higher PFR observed in spontaneously breathing patients relative to ventilated patients, as published previously (57).

As demonstrated in Papers I-IV, an increase in PFR precedes other clinical signs of ARDS in animal models and, in addition, LTx patients have shown higher PFR as a clinical indicator of PGD (57), suggests that PFR may be an early indicator of lung injury. None of the patients in the present study presented signs of increased PFR during the time of the study, and there were no other clinical signs of deteriorating condition, and so neither PCV, VCV or PRVC used during sedation appeared to be harmful to the lungs in patients with normal lung function. We noted that there is inter-individual variation in PFR values, which could also be incorporated into the assessment of each individual patient.

The recruitment maneuver applied in this study has been published in both a preclinical porcine study of abdominal surgery and in a clinical study of lung transplant patients. These publications showed a significantly higher PFR after the recruitment maneuver when using VCV (55, 57). This offered the rationale for using the same recruitment maneuver in Paper V, but we were not able to detect any differences in PFR after the recruitment maneuver, between the different ventilation modes, in our cohort. This result should be considered in the light of patients without lung pathology. In a study conducted by Broberg et al. (57), patients who had undergone LTx and recipients experience pulmonary inflammatory reactions

postoperatively and tissue trauma in the lungs from the surgery itself which might explain the different response to the recruitment maneuver regarding PFR. Considering the preclinical study on PFR following recruitment maneuver in a porcine model (55), anatomical differences and time spent on mechanical ventilation are potential explanations as to why the results of that study differ. In Paper V, before leaving the OR, all patients underwent a recruitment maneuver when taken off cardiopulmonary bypass, according to local clinical practice. This might be one explanation as to why we did not observe a change in PFR after the recruitment maneuver in the ICU.

PFR could be used as a clinical tool to monitor pulmonary status in the ICU since changes in PFR could be secondary to changes in ventilatory settings, or the result of patient transitioning from mechanical breathing to spontaneous breathing, or even the onset of lung pathology which would be readily apparent to the clinician.

Ethical aspects

The studies were performed according to the principles of the Helsinki declaration of human rights and approved by the regional ethical review board in Lund Sweden. Paper II: Dnr 2017/519, 2020-01864. Paper V: Dnr 2018/129. All participating patients in Paper V signed a written informed consent.

The experimental animal studies were approved by the Ethics committee for animal research, Lund University, Sweden, Dnr 8401/2017. All animals received care according to the European Convention for the Protection of Vertebrate Animals used for experimental and other Scientific Purposes, as well as to the USA Principles of Laboratory Animal Care of the National Society for Medical Research, and the Guide for the Care and Use of Laboratory Animals.

Conclusions

Paper I

To mimic a clinical situation in adult humans, we used LPS, both endotracheally and intravascularly, to successfully create our own large animal model of LPS-induced ARDS with histological confirmation of diffuse alveolar damage. To our knowledge, the PExA device has never been used to monitor PFR in an intubated lung injury model before. During a time frame of only 6 hours, all animals receiving LPS developed moderate-to-severe ARDS with a significant increase in PFR compared to animals receiving sham treatment whose PFR was unchanged from baseline levels. Before any ARDS state was achieved and before changes in blood gas parameters (e.g. hypoxemia), ventilatory settings (e.g. increased inspiratory pressure) and changes in cytokine response could be detected, a significant increase in PFR was detected. The results indicate that monitoring of PFR in real time may be a new and complementary approach in the clinic for the early detection of ARDS.

Paper II

The results from this study show that deterioration and recovery of lung function were reflected in PFR with a significant increase in PFR during deterioration in our *in vivo* animal model over time and when ECMO was initiated. Clinically there was a decrease in PFR observed during recovery of two patients whose lung function improved enough for them to be weaned off ECMO. The results imply that PFR can be used both for early detection of ARDS but also for monitoring the status of lung injury over time with changes in PFR. With the help of PFR, the physicians may obtain rapid and complementary clinical support in order to be able to assess lung function, which may reduce the need for invasive diagnostics and help optimize or personalize therapies.

Paper III

Acute lung injury induced by an infection-like condition and by aspiration could be detected using PFR in two clinically relevant models of ARDS. The results imply that PFR can be an early measure of ARDS and demonstrate the potential clinical use of such a non-invasive procedure to provide clinicians with an early diagnostic tool of progression of lung damage. These results encourage the further investigation of the implementation of PFR as a diagnostic tool in the ICU. This is

particularly important given the known value of early detection, which allows for early optimization of therapies.

Paper IV

This study has been shown to (1) reduce inflammation and restore pulmonary function during EVLP, (2) rejuvenate function and decrease inflammation following transplantation, and (3) reduce the incidence of PGD in transplanted recipients. The work outlined here represents the utilization of the filter in the novel context of lung transplantation using severely damaged donor lungs. Cytokine filtration may be an intervention that could lead to the acceptance of more lungs for transplantation. It may also increase the tolerability of such lungs in a recipient, an important outcome given that PGD remains the leading cause of early mortality and a contributor to chronic graft dysfunction.

Paper V

In this study, different ventilator settings resulted in different distributions of exhaled particles binned by size. This could serve as the basis for studying PFR in terms of distinctive distribution patterns as an indicator of lung and ventilatory condition. The results encourage the investigation of PRVC relative to VCV and PCV as the lower PFR might indicate that PRVC is a gentler method of ventilation, where the goal is to avoid mechanical stress to the lungs. We further concluded that a higher PFR was measured when ventilating in the PSV mode compared to PRVC, which may reflect the added contribution of the work of breathing initiated by the patient themselves. The results of this study, with PFR as a promising clinical tool for assessing ventilatory modes in patient care, support the continued investigation of PFR in terms of both rate and particle distribution.

Future perspectives

Detection and sampling of exhaled particles provide a novel opportunity to identify, quantify and monitor physiological and pathological processes in the small airways of the lungs. The next step to make the technique more accessible would be to incorporate an optional device into the ventilator to be able to measure PFR as soon as the patient is intubated, whether that be in the ICU or in the OR. This option would dramatically increase the number of samples available for research without the need for retrieval of equipment in a stressful situation and would also avoid unnecessary disconnection of the tubes.

In the future, it would also be interesting to study animal models of lung injury during recovery and see how spontaneous recovery, or different therapeutic interventions, might alter the PFR over time, both when the animals are sedated and also when awake. Further studies could also focus on longitudinal intra-individual observations of change in PFR over prolonged surgical procedures or lengthy ICU stays where a patient may be on mechanical ventilation for an extensive period of weeks, during which particle composition might change over time. We would also like to consider including a broader spectrum of patients with other types of pathology besides ALI and ARDS. This could be achieved by extending the study to other centers through national and international collaboration. This would allow the study of a less homogeneous population as well as conducting analyses of PFR over a greater period. Analyzing PFR in patients in the ICU on a larger scale would probably increase our knowledge of different causes of ARDS and make us more focused regarding ventilation modes and to optimize ventilatory parameters as we receive instant feedback from PFR measurement.

To enable this possibility, the clinic would require smaller and more portable devices, or devices that can be incorporated into the existing machines, as mentioned before. To our knowledge, there have not yet been any multicenter RCTs of EBP involving intubated patients. A prerequisite to do this is to focus on standardization of methods regarding sampling technique, ventilation modes and sampling analysis of EBP. Further research is needed to fully understand the mechanism of particle release from the airways and the clinical relevance of particles as exhaled biomarkers.

Acknowledgments

I would like to express my sincere gratitude and appreciations to everyone who has helped, supported, and encouraged me on this journey to complete this thesis. It has been hard work and much sacrifice but also very stimulating and I have enjoyed every moment working with you all.

A special thanks to my main supervisor and co-worker Professor **Sandra Lindstedt** who has guided me on the way to achieve a PhD. You truly are an inspirational person and a role model when it comes to science and research. Sometimes there has been doubt about the possibility of certain projects but your never-ending enthusiasm and problem-solving approach, together with your attitude that anything is possible, has instilled me with confidence. I hope we will continue to share interesting projects and laughs in the future.

Another person I would like to thank is my co-supervisor **Snejana Hyllén**, friend and colleague, for your hard work during laboratory weeks and input and support in the writing process. When it comes to cardiothoracic anesthesia, you are the best of teachers.

Darcy Wagner, my co-supervisor and associate Professor in Lung Bioengineering and Regeneration. Thank you for your work and input into my articles. Your help has been much appreciated.

Malin Malmsjö, my co-supervisor and Professor of Ophtalmology. Thank you for contributing with your knowledge and experience.

Two of my fellow PhD students and friends whose contributions have been extra valuable for my thesis are **Anna Niroomand** and **Gabriel Hirdman**, without you this thesis would not exist.

I am also especially grateful to **Ellen Broberg**, my co-worker and friend, whose PhD has been the foundation on which my work is based.

A special thanks to my co-authors Franziska Olm, Leif Pierre, Oskar Hallgren, Dag Edström, Haider Ghaidan, Filip Hallgren, Iran A. N. Silva, Deniz A. Bölükbas, Edgars Grins and Per Ederoth.

And last, but not least, many thanks to my wonderful family, **Anna**, **Adam** and **Julia** for your patience and understanding when times have been hectic and for reminding me of what matters most in life.

References

1. Angus GE, Thurlbeck WM. Number of alveoli in the human lung. *J Appl Physiol*. 1972;32(4):483-5.
2. Weibel ER. A retrospective of lung morphometry: from 1963 to present. *Am J Physiol Lung Cell Mol Physiol*. 2013;305(6):L405-8.
3. Weibel ER, Gomez DM. Architecture of the human lung. Use of quantitative methods establishes fundamental relations between size and number of lung structures. *Science*. 1962;137(3530):577-85.
4. Tortora GJ GS. Principles of anatomy and physiology 9th edition. Chichester, England: Wiley; 2000.
5. Ochs M, Nyengaard JR, Jung A, Knudsen L, Voigt M, Wahlers T, et al. The number of alveoli in the human lung. *Am J Respir Crit Care Med*. 2004;169(1):120-4.
6. Breeze RG, Wheeldon EB. The cells of the pulmonary airways. *Am Rev Respir Dis*. 1977;116(4):705-77.
7. Halliday HL. The fascinating story of surfactant. *J Paediatr Child Health*. 2017;53(4):327-32.
8. Hills BA. Surface-active phospholipid: a Pandora's box of clinical applications. Part I. The lung and air spaces. *Intern Med J*. 2002;32(4):170-8.
9. Fanali G, di Masi A, Trezza V, Marino M, Fasano M, Ascenzi P. Human serum albumin: from bench to bedside. *Mol Aspects Med*. 2012;33(3):209-90.
10. Greiff L, Andersson M, Erjefalt JS, Persson CG, Wollmer P. Airway microvascular extravasation and luminal entry of plasma. *Clinical physiology and functional imaging*. 2003;23(6):301-6.
11. Kelly FJ, Cotgrove M, Mudway IS. Respiratory tract lining fluid antioxidants: the first line of defence against gaseous pollutants. *Cent Eur J Public Health*. 1996;4 Suppl:11-4.
12. Ibsen B. The anaesthetist's viewpoint on the treatment of respiratory complications in poliomyelitis during the epidemic in Copenhagen, 1952. *Proc R Soc Med*. 1954;47(1):72-4.
13. Lassen HC. A preliminary report on the 1952 epidemic of poliomyelitis in Copenhagen with special reference to the treatment of acute respiratory insufficiency. *Lancet*. 1953;1(6749):37-41.
14. Ball L, Dameri M, Pelosi P. Modes of mechanical ventilation for the operating room. *Best Pract Res Clin Anaesthesiol*. 2015;29(3):285-99.
15. Hedenstierna G, Edmark L. Effects of anesthesia on the respiratory system. *Best Pract Res Clin Anaesthesiol*. 2015;29(3):273-84.

16. Tobin MJ. Mechanical ventilation. *N Engl J Med.* 1994;330(15):1056-61.
17. Tobin MJ. Advances in mechanical ventilation. *N Engl J Med.* 2001;344(26):1986-96.
18. Serpa Neto A, Hemmes SN, Barbas CS, Beiderlinden M, Biehl M, Binnekade JM, et al. Protective versus Conventional Ventilation for Surgery: A Systematic Review and Individual Patient Data Meta-analysis. *Anesthesiology.* 2015;123(1):66-78.
19. Serpa Neto A, Schultz MJ, Gama de Abreu M. Intraoperative ventilation strategies to prevent postoperative pulmonary complications: Systematic review, meta-analysis, and trial sequential analysis. *Best Pract Res Clin Anaesthesiol.* 2015;29(3):331-40.
20. Bates JHT, Smith BJ. Ventilator-induced lung injury and lung mechanics. *Ann Transl Med.* 2018;6(19):378.
21. Ricard JD, Dreyfuss D, Saumon G. Ventilator-induced lung injury. *Eur Respir J Suppl.* 2003;42:2s-9s.
22. Silva PL, Negrini D, Rocco PR. Mechanisms of ventilator-induced lung injury in healthy lungs. *Best Pract Res Clin Anaesthesiol.* 2015;29(3):301-13.
23. Guldner A, Kiss T, Serpa Neto A, Hemmes SN, Canet J, Spieth PM, et al. Intraoperative protective mechanical ventilation for prevention of postoperative pulmonary complications: a comprehensive review of the role of tidal volume, positive end-expiratory pressure, and lung recruitment maneuvers. *Anesthesiology.* 2015;123(3):692-713.
24. Chacko B, Peter JV, Tharyan P, John G, Jeyaseelan L. Pressure-controlled versus volume-controlled ventilation for acute respiratory failure due to acute lung injury (ALI) or acute respiratory distress syndrome (ARDS). *Cochrane Database Syst Rev.* 2015;1:CD008807.
25. Jiang J, Li B, Kang N, Wu A, Yue Y. Pressure-Controlled Versus Volume-Controlled Ventilation for Surgical Patients: A Systematic Review and Meta-analysis. *J Cardiothorac Vasc Anesth.* 2016;30(2):501-14.
26. Chatterjee K. The Swan-Ganz catheters: past, present, and future. A viewpoint. *Circulation.* 2009;119(1):147-52.
27. Demiselle J, Mercat A, Asfar P. Is there still a place for the Swan-Ganz catheter? Yes. *Intensive Care Med.* 2018;44(6):954-6.
28. Lee M, Curley GF, Mustard M, Mazer CD. The Swan-Ganz Catheter Remains a Critically Important Component of Monitoring in Cardiovascular Critical Care. *Can J Cardiol.* 2017;33(1):142-7.
29. Ranka S, Mastoris I, Kapur NK, Tedford RJ, Rali A, Acharya P, et al. Right Heart Catheterization in Cardiogenic Shock Is Associated With Improved Outcomes: Insights From the Nationwide Readmissions Database. *J Am Heart Assoc.* 2021:e019843.
30. Ashbaugh DG, Bigelow DB, Petty TL, Levine BE. Acute respiratory distress in adults. *Lancet.* 1967;2(7511):319-23.
31. Matthay MA, Zemans RL. The acute respiratory distress syndrome: pathogenesis and treatment. *Annu Rev Pathol.* 2011;6:147-63.

32. Ware LB, Matthay MA. The acute respiratory distress syndrome. *N Engl J Med.* 2000;342(18):1334-49.
33. Bernard GR, Artigas A, Brigham KL, Carlet J, Falke K, Hudson L, et al. The American-European Consensus Conference on ARDS. Definitions, mechanisms, relevant outcomes, and clinical trial coordination. *Am J Respir Crit Care Med.* 1994;149(3 Pt 1):818-24.
34. Ranieri VM, Rubenfeld GD, Thompson BT, Ferguson ND, Caldwell E, Fan E, et al. Acute respiratory distress syndrome: the Berlin Definition. *JAMA.* 2012;307(23):2526-33.
35. Bachofen M, Weibel ER. Alterations of the gas exchange apparatus in adult respiratory insufficiency associated with septicemia. *Am Rev Respir Dis.* 1977;116(4):589-615.
36. Acute Respiratory Distress Syndrome N, Brower RG, Matthay MA, Morris A, Schoenfeld D, Thompson BT, et al. Ventilation with lower tidal volumes as compared with traditional tidal volumes for acute lung injury and the acute respiratory distress syndrome. *N Engl J Med.* 2000;342(18):1301-8.
37. Parsons PE, Eisner MD, Thompson BT, Matthay MA, Ancukiewicz M, Bernard GR, et al. Lower tidal volume ventilation and plasma cytokine markers of inflammation in patients with acute lung injury. *Crit Care Med.* 2005;33(1):1-6; discussion 230-2.
38. Ranieri VM, Suter PM, Tortorella C, De Tullio R, Dayer JM, Brienza A, et al. Effect of mechanical ventilation on inflammatory mediators in patients with acute respiratory distress syndrome: a randomized controlled trial. *JAMA.* 1999;282(1):54-61.
39. Meade MO, Cook DJ, Guyatt GH, Slutsky AS, Arabi YM, Cooper DJ, et al. Ventilation strategy using low tidal volumes, recruitment maneuvers, and high positive end-expiratory pressure for acute lung injury and acute respiratory distress syndrome: a randomized controlled trial. *JAMA.* 2008;299(6):637-45.
40. Needham DM, Colantuoni E, Mendez-Tellez PA, Dinglas VD, Sevransky JE, Dennison Himmelfarb CR, et al. Lung protective mechanical ventilation and two year survival in patients with acute lung injury: prospective cohort study. *BMJ.* 2012;344:e2124.
41. Guerin C, Reignier J, Richard JC, Beuret P, Gacouin A, Boulain T, et al. Prone positioning in severe acute respiratory distress syndrome. *N Engl J Med.* 2013;368(23):2159-68.
42. Sud S, Friedrich JO, Adhikari NK, Taccone P, Mancebo J, Polli F, et al. Effect of prone positioning during mechanical ventilation on mortality among patients with acute respiratory distress syndrome: a systematic review and meta-analysis. *CMAJ.* 2014;186(10):E381-90.
43. Peek GJ, Mugford M, Tiruvoipati R, Wilson A, Allen E, Thalanany MM, et al. Efficacy and economic assessment of conventional ventilatory support versus extracorporeal membrane oxygenation for severe adult respiratory failure (CESAR): a multicentre randomised controlled trial. *Lancet.* 2009;374(9698):1351-63.
44. Gattinoni L, Vasques F, Quintel M. Use of ECMO in ARDS: does the EOLIA trial really help? *Crit Care.* 2018;22(1):171.

45. Zapol WM, Snider MT, Hill JD, Fallat RJ, Bartlett RH, Edmunds LH, et al. Extracorporeal membrane oxygenation in severe acute respiratory failure. A randomized prospective study. *JAMA*. 1979;242(20):2193-6.
46. Horvath I, Hunt J, Barnes PJ, Alving K, Antczak A, Baraldi E, et al. Exhaled breath condensate: methodological recommendations and unresolved questions. *The European respiratory journal*. 2005;26(3):523-48.
47. Chen SF, Danao MG. Decomposition and solubility of H₂O₂: implications in exhaled breath condensate. *J Breath Res*. 2013;7(4):046001.
48. Reinhold P, Jaeger J, Schroeder C. Evaluation of methodological and biological influences on the collection and composition of exhaled breath condensate. *Biomarkers*. 2006;11(2):118-42.
49. Reinhold P, Knobloch H. Exhaled breath condensate: lessons learned from veterinary medicine. *J Breath Res*. 2010;4(1):017001.
50. Davis MD, Montpetit A, Hunt J. Exhaled breath condensate: an overview. *Immunol Allergy Clin North Am*. 2012;32(3):363-75.
51. Montuschi P. Analysis of exhaled breath condensate in respiratory medicine: methodological aspects and potential clinical applications. *Ther Adv Respir Dis*. 2007;1(1):5-23.
52. Larsson P, Larstad M, Bake B, Hammar O, Bredberg A, Almstrand AC, et al. Exhaled particles as markers of small airway inflammation in subjects with asthma. *Clinical physiology and functional imaging*. 2017;37(5):489-97.
53. Larstad M, Almstrand AC, Larsson P, Bake B, Larsson S, Ljungstrom E, et al. Surfactant Protein A in Exhaled Endogenous Particles Is Decreased in Chronic Obstructive Pulmonary Disease (COPD) Patients: A Pilot Study. *PLoS One*. 2015;10(12):e0144463.
54. Almstrand AC, Bake B, Ljungstrom E, Larsson P, Bredberg A, Mirgorodskaya E, et al. Effect of airway opening on production of exhaled particles. *Journal of applied physiology*. 2010;108(3):584-8.
55. Broberg E, Pierre L, Fakhro M, Algotsson L, Malmsjo M, Hyllen S, et al. Different particle flow patterns from the airways after recruitment manoeuvres using volume-controlled or pressure-controlled ventilation. *Intensive care medicine experimental*. 2019;7(1):16.
56. Broberg E, Wlosinska M, Algotsson L, Olin AC, Wagner D, Pierre L, et al. A new way of monitoring mechanical ventilation by measurement of particle flow from the airways using Pexa method in vivo and during ex vivo lung perfusion in DCD lung transplantation. *Intensive care medicine experimental*. 2018;6(1):18.
57. Broberg E, Hyllen S, Algotsson L, Wagner DE, Lindstedt S. Particle Flow Profiles From the Airways Measured by PEXA Differ in Lung Transplant Recipients Who Develop Primary Graft Dysfunction. *Exp Clin Transplant*. 2019.
58. Ericson PA, Mirgorodskaya E, Hammar OS, Viklund EA, Almstrand AR, Larsson PJ, et al. Low Levels of Exhaled Surfactant Protein A Associated With BOS After Lung Transplantation. *Transplantation direct*. 2016;2(9):e103.
59. Broberg E, Andreasson J, Fakhro M, Olin AC, Wagner D, Hyllen S, et al. Mechanically ventilated patients exhibit decreased particle flow in exhaled breath as

compared to normal breathing patients. *ERJ Open Research*. Accepted 17 October 2019.

60. Almstrand AC, Ljungstrom E, Lausmaa J, Bake B, Sjoval P, Olin AC. Airway monitoring by collection and mass spectrometric analysis of exhaled particles. *Anal Chem*. 2009;81(2):662-8.
61. Bake B, Larsson P, Ljungkvist G, Ljungstrom E, Olin AC. Exhaled particles and small airways. *Respir Res*. 2019;20(1):8.
62. Behndig AF, Mirgorodskaya E, Blomberg A, Olin AC. Surfactant Protein A in particles in exhaled air (PExA), bronchial lavage and bronchial wash - a methodological comparison. *Respir Res*. 2019;20(1):214.
63. Rubenfeld GD, Caldwell E, Peabody E, Weaver J, Martin DP, Neff M, et al. Incidence and outcomes of acute lung injury. *N Engl J Med*. 2005;353(16):1685-93.
64. Brun-Buisson C, Minelli C, Bertolini G, Brazzi L, Pimentel J, Lewandowski K, et al. Epidemiology and outcome of acute lung injury in European intensive care units. Results from the ALIVE study. *Intensive Care Med*. 2004;30(1):51-61.
65. Ballard-Croft C, Wang D, Sumpter LR, Zhou X, Zwischenberger JB. Large-animal models of acute respiratory distress syndrome. *Ann Thorac Surg*. 2012;93(4):1331-9.
66. Matute-Bello G, Frevert CW, Martin TR. Animal models of acute lung injury. *Am J Physiol Lung Cell Mol Physiol*. 2008;295(3):L379-99.
67. Wang HM, Bodenstern M, Markstaller K. Overview of the pathology of three widely used animal models of acute lung injury. *Eur Surg Res*. 2008;40(4):305-16.
68. Zhang G, Meredith TC, Kahne D. On the essentiality of lipopolysaccharide to Gram-negative bacteria. *Curr Opin Microbiol*. 2013;16(6):779-85.
69. Hollenstein U, Homoncik M, Stohlawetz PJ, Marsik C, Sieder A, Eichler HG, et al. Endotoxin down-modulates granulocyte colony-stimulating factor receptor (CD114) on human neutrophils. *J Infect Dis*. 2000;182(1):343-6.
70. O'Grady NP, Preas HL, Pugin J, Fiuza C, Tropea M, Reda D, et al. Local inflammatory responses following bronchial endotoxin instillation in humans. *Am J Respir Crit Care Med*. 2001;163(7):1591-8.
71. Pugin J, Widmer MC, Kossodo S, Liang CM, Preas HL, Suffredini AF. Human neutrophils secrete gelatinase B in vitro and in vivo in response to endotoxin and proinflammatory mediators. *American journal of respiratory cell and molecular biology*. 1999;20(3):458-64.
72. Trembl B, Neu N, Kleinsasser A, Gritsch C, Finsterwalder T, Geiger R, et al. Recombinant angiotensin-converting enzyme 2 improves pulmonary blood flow and oxygenation in lipopolysaccharide-induced lung injury in piglets. *Crit Care Med*. 2010;38(2):596-601.
73. Wang HL, Akinci IO, Baker CM, Urich D, Bellmeyer A, Jain M, et al. The intrinsic apoptotic pathway is required for lipopolysaccharide-induced lung endothelial cell death. *J Immunol*. 2007;179(3):1834-41.
74. Kawasaki M, Kuwano K, Hagimoto N, Matsuba T, Kunitake R, Tanaka T, et al. Protection from lethal apoptosis in lipopolysaccharide-induced acute lung injury in mice by a caspase inhibitor. *Am J Pathol*. 2000;157(2):597-603.

75. Abraham E. Neutrophils and acute lung injury. *Crit Care Med.* 2003;31(4 Suppl):S195-9.
76. Lachmann B, Robertson B, Vogel J. In vivo lung lavage as an experimental model of the respiratory distress syndrome. *Acta Anaesthesiol Scand.* 1980;24(3):231-6.
77. Kloot TE, Blanch L, Melynn Youngblood A, Weinert C, Adams AB, Marini JJ, et al. Recruitment maneuvers in three experimental models of acute lung injury. Effect on lung volume and gas exchange. *Am J Respir Crit Care Med.* 2000;161(5):1485-94.
78. Bice T, Li G, Malinchoc M, Lee AS, Gajic O. Incidence and risk factors of recurrent acute lung injury. *Crit Care Med.* 2011;39(5):1069-73.
79. Wind J, Versteegt J, Twisk J, van der Werf TS, Bindels AJ, Spijkstra JJ, et al. Epidemiology of acute lung injury and acute respiratory distress syndrome in The Netherlands: a survey. *Respiratory medicine.* 2007;101(10):2091-8.
80. Kotloff RM, Thabut G. Lung transplantation. *Am J Respir Crit Care Med.* 2011;184(2):159-71.
81. Hornby K, Ross H, Keshavjee S, Rao V, Shemie SD. Non-utilization of hearts and lungs after consent for donation: a Canadian multicentre study. *Can J Anaesth.* 2006;53(8):831-7.
82. Mohan S, Chiles MC, Patzer RE, Pastan SO, Husain SA, Carpenter DJ, et al. Factors leading to the discard of deceased donor kidneys in the United States. *Kidney Int.* 2018;94(1):187-98.
83. Blomquist S, Aberg T, Solem JO, Steen S. Lung mechanics, gas exchange and central circulation during treatment of intra-abdominal hemorrhage with pneumatic anti-shock garment and intra-aortic balloon occlusion. An experimental study in pigs. *Eur Surg Res.* 1994;26(4):240-7.
84. Novitzky D, Wicomb WN, Rose AG, Cooper DK, Reichart B. Pathophysiology of pulmonary edema following experimental brain death in the chacma baboon. *Ann Thorac Surg.* 1987;43(3):288-94.
85. Lindstedt S, Dellgren G, Iversen M, Riise GC, Bjortuft O, Hammainen P, et al. Pulmonary retransplantation in the Nordic countries. *Ann Thorac Surg.* 2015;99(5):1781-7.
86. Cypel M, Keshavjee S. Strategies for safe donor expansion: donor management, donations after cardiac death, ex-vivo lung perfusion. *Curr Opin Organ Transplant.* 2013;18(5):513-7.
87. Manara AR, Murphy PG, O'Callaghan G. Donation after circulatory death. *Br J Anaesth.* 2012;108 Suppl 1:i108-21.
88. de Antonio DG, Marcos R, Laporta R, Mora G, Garcia-Gallo C, Gamez P, et al. Results of clinical lung transplant from uncontrolled non-heart-beating donors. *J Heart Lung Transplant.* 2007;26(5):529-34.
89. Steen S, Sjoberg T, Pierre L, Liao Q, Eriksson L, Algotsson L. Transplantation of lungs from a non-heart-beating donor. *Lancet.* 2001;357(9259):825-9.
90. Mohamed MS. Ex Vivo Lung Perfusion and Transplant: State of the Art and View to the Future. *Exp Clin Transplant.* 2015;13(6):493-9.

91. Linacre V, Cypel M, Machuca T, Nakajima D, Hashimoto K, Zamel R, et al. Importance of left atrial pressure during ex vivo lung perfusion. *J Heart Lung Transplant*. 2016;35(6):808-14.
92. Loor G, Howard BT, Spratt JR, Mattison LM, Panoskaltzis-Mortari A, Brown RZ, et al. Prolonged EVLP Using OCS Lung: Cellular and Acellular Perfusates. *Transplantation*. 2017;101(10):2303-11.
93. Beller JP, Byler MR, Money DT, Chancellor WZ, Zhang A, Zhao Y, et al. Reduced-flow ex vivo lung perfusion to rehabilitate lungs donated after circulatory death. *J Heart Lung Transplant*. 2020;39(1):74-82.
94. Ingemansson R, Eyjolfsson A, Mared L, Pierre L, Algotsson L, Ekmehag B, et al. Clinical transplantation of initially rejected donor lungs after reconditioning ex vivo. *Ann Thorac Surg*. 2009;87(1):255-60.
95. Van Raemdonck D, Neyrinck A, Cypel M, Keshavjee S. Ex-vivo lung perfusion. *Transpl Int*. 2015;28(6):643-56.
96. Wallinder A, Ricksten SE, Silverborn M, Hansson C, Riise GC, Liden H, et al. Early results in transplantation of initially rejected donor lungs after ex vivo lung perfusion: a case-control study. *Eur J Cardiothorac Surg*. 2014;45(1):40-4; discussion 4-5.
97. Kakishita T, Oto T, Hori S, Miyoshi K, Otani S, Yamamoto S, et al. Suppression of inflammatory cytokines during ex vivo lung perfusion with an adsorbent membrane. *Ann Thorac Surg*. 2010;89(6):1773-9.
98. Sadaria MR, Smith PD, Fullerton DA, Justison GA, Lee JH, Puskas F, et al. Cytokine expression profile in human lungs undergoing normothermic ex-vivo lung perfusion. *Ann Thorac Surg*. 2011;92(2):478-84.
99. Major T, Ball AL, Stone JP, Edge RJ, Lopez-Castejon G, Sjoberg T, et al. Pro-IL-1beta Is an Early Prognostic Indicator of Severe Donor Lung Injury During Ex Vivo Lung Perfusion. *Transplantation*. 2021;105(4):768-74.
100. Hosgood SA, Hoff M, Nicholson ML. Treatment of transplant kidneys during machine perfusion. *Transpl Int*. 2021;34(2):224-32.
101. Nemeth E, Kovacs E, Racz K, Soltész A, Szigeti S, Kiss N, et al. Impact of intraoperative cytokine adsorption on outcome of patients undergoing orthotopic heart transplantation-an observational study. *Clin Transplant*. 2018;32(4):e13211.
102. Fakhro M, Ingemansson R, Skog I, Algotsson L, Hansson L, Koul B, et al. 25-year follow-up after lung transplantation at Lund University Hospital in Sweden: superior results obtained for patients with cystic fibrosis. *Interact Cardiovasc Thorac Surg*. 2016;23(1):65-73.
103. Chambers DC, Yusen RD, Cherikh WS, Goldfarb SB, Kucheryavaya AY, Khusch K, et al. The Registry of the International Society for Heart and Lung Transplantation: Thirty-fourth Adult Lung And Heart-Lung Transplantation Report-2017; Focus Theme: Allograft ischemic time. *J Heart Lung Transplant*. 2017;36(10):1047-59.
104. Christie JD, Carby M, Bag R, Corris P, Hertz M, Weill D, et al. Report of the ISHLT Working Group on Primary Lung Graft Dysfunction part II: definition. A consensus statement of the International Society for Heart and Lung Transplantation. *J Heart Lung Transplant*. 2005;24(10):1454-9.

105. Diamond JM, Lee JC, Kawut SM, Shah RJ, Localio AR, Bellamy SL, et al. Clinical risk factors for primary graft dysfunction after lung transplantation. *Am J Respir Crit Care Med.* 2013;187(5):527-34.
106. Porteous MK, Diamond JM, Christie JD. Primary graft dysfunction: lessons learned about the first 72 h after lung transplantation. *Curr Opin Organ Transplant.* 2015;20(5):506-14.
107. Snell GI, Yusen RD, Weill D, Strueber M, Garrity E, Reed A, et al. Report of the ISHLT Working Group on Primary Lung Graft Dysfunction, part I: Definition and grading-A 2016 Consensus Group statement of the International Society for Heart and Lung Transplantation. *J Heart Lung Transplant.* 2017;36(10):1097-103.
108. Christie JD, Sager JS, Kimmel SE, Ahya VN, Gaughan C, Blumenthal NP, et al. Impact of primary graft failure on outcomes following lung transplantation. *Chest.* 2005;127(1):161-5.
109. Thakuria L, Reed A, Simon AR, Marczin N. Mechanical Ventilation After Lung Transplantation. *Chest.* 2017;151(2):516-7.
110. Iskender I, Arni S, Maeyashiki T, Citak N, Sauer M, Rodriguez JM, et al. Perfusate adsorption during ex vivo lung perfusion improves early post-transplant lung function. *J Thorac Cardiovasc Surg.* 2021;161(2):e109-e21.
111. Iskender I, Cosgun T, Arni S, Trinkwitz M, Fehlings S, Yamada Y, et al. Cytokine filtration modulates pulmonary metabolism and edema formation during ex vivo lung perfusion. *J Heart Lung Transplant.* 2017.
112. Matute-Bello G, Downey G, Moore BB, Groshong SD, Matthay MA, Slutsky AS, et al. An official American Thoracic Society workshop report: features and measurements of experimental acute lung injury in animals. *American journal of respiratory cell and molecular biology.* 2011;44(5):725-38.
113. Matthay MA, Zimmerman GA. Acute lung injury and the acute respiratory distress syndrome: four decades of inquiry into pathogenesis and rational management. *American journal of respiratory cell and molecular biology.* 2005;33(4):319-27.
114. Bhatia M, Moochhala S. Role of inflammatory mediators in the pathophysiology of acute respiratory distress syndrome. *The Journal of pathology.* 2004;202(2):145-56.
115. Gonzales JN, Lucas R, Verin AD. The Acute Respiratory Distress Syndrome: Mechanisms and Perspective Therapeutic Approaches. *Austin journal of vascular medicine.* 2015;2(1).
116. Wyns H, Plessers E, De Backer P, Meyer E, Croubels S. In vivo porcine lipopolysaccharide inflammation models to study immunomodulation of drugs. *Veterinary immunology and immunopathology.* 2015;166(3-4):58-69.
117. Liu CH, Kuo SW, Ko WJ, Tsai PR, Wu SW, Lai CH, et al. Early measurement of IL-10 predicts the outcomes of patients with acute respiratory distress syndrome receiving extracorporeal membrane oxygenation. *Scientific reports.* 2017;7(1):1021.
118. Falk L, Hultman J, Broman LM. Extracorporeal Membrane Oxygenation for Septic Shock. *Crit Care Med.* 2019;47(8):1097-105.
119. Finney SJ. Extracorporeal support for patients with acute respiratory distress syndrome. *Eur Respir Rev.* 2014;23(133):379-89.

120. Morris AH, Wallace CJ, Menlove RL, Clemmer TP, Orme JF, Jr., Weaver LK, et al. Randomized clinical trial of pressure-controlled inverse ratio ventilation and extracorporeal CO₂ removal for adult respiratory distress syndrome. *Am J Respir Crit Care Med.* 1994;149(2 Pt 1):295-305.
121. Lee HE, Yi ES, Rabatin JT, Bohman JK, Roden AC. Histopathologic Findings in Lungs of Patients Treated With Extracorporeal Membrane Oxygenation. *Chest.* 2018;153(4):825-33.
122. Millar JE, Fanning JP, McDonald CI, McAuley DF, Fraser JF. The inflammatory response to extracorporeal membrane oxygenation (ECMO): a review of the pathophysiology. *Crit Care.* 2016;20(1):387.
123. Robba C, Ortu A, Bilotta F, Lombardo A, Sekhon MS, Gallo F, et al. Extracorporeal membrane oxygenation for adult respiratory distress syndrome in trauma patients: A case series and systematic literature review. *J Trauma Acute Care Surg.* 2017;82(1):165-73.
124. Myers LC, Lee C, Thompson BT, Cudemus G, Raz Y, Roy N. Outcomes of Adult Patients With Septic Shock Undergoing Extracorporeal Membrane Oxygenation Therapy. *Ann Thorac Surg.* 2020;110(3):871-7.
125. Rhodes A, Evans LE, Alhazzani W, Levy MM, Antonelli M, Ferrer R, et al. Surviving Sepsis Campaign: International Guidelines for Management of Sepsis and Septic Shock: 2016. *Intensive Care Med.* 2017;43(3):304-77.
126. Shekar K, Badulak J, Peek G, Boeken U, Dalton HJ, Arora L, et al. Extracorporeal Life Support Organization Coronavirus Disease 2019 Interim Guidelines: A Consensus Document from an International Group of Interdisciplinary Extracorporeal Membrane Oxygenation Providers. *ASAIO J.* 2020;66(7):707-21.
127. Stenlo M, Hyllen S, Silva IAN, Bolukbas DA, Pierre LT, Hallgren O, et al. Increased particle flow rate from airways precedes clinical signs of ARDS in a porcine model of LPS-induced acute lung injury. *Am J Physiol Lung Cell Mol Physiol.* 2020.
128. Shi J, Chen Q, Yu W, Shen J, Gong J, He C, et al. Continuous renal replacement therapy reduces the systemic and pulmonary inflammation induced by venovenous extracorporeal membrane oxygenation in a porcine model. *Artif Organs.* 2014;38(3):215-23.
129. Risnes I, Wagner K, Ueland T, Mollnes T, Aukrust P, Svennevig J. Interleukin-6 may predict survival in extracorporeal membrane oxygenation treatment. *Perfusion.* 2008;23(3):173-8.
130. Butt Y, Kurdowska A, Allen TC. Acute Lung Injury: A Clinical and Molecular Review. *Arch Pathol Lab Med.* 2016;140(4):345-50.
131. Takeuchi O, Akira S. Pattern recognition receptors and inflammation. *Cell.* 2010;140(6):805-20.
132. Bauer TT, Monton C, Torres A, Cabello H, Fillela X, Maldonado A, et al. Comparison of systemic cytokine levels in patients with acute respiratory distress syndrome, severe pneumonia, and controls. *Thorax.* 2000;55(1):46-52.
133. Agrawal A, Zhuo H, Brady S, Levitt J, Steingrub J, Siegel MD, et al. Pathogenetic and predictive value of biomarkers in patients with ALI and lower severity of illness:

- results from two clinical trials. *Am J Physiol Lung Cell Mol Physiol*. 2012;303(8):L634-9.
134. Meduri GU, Kohler G, Headley S, Tolley E, Stentz F, Postlethwaite A. Inflammatory cytokines in the BAL of patients with ARDS. Persistent elevation over time predicts poor outcome. *Chest*. 1995;108(5):1303-14.
 135. Yang CY, Chen CS, Yiang GT, Cheng YL, Yong SB, Wu MY, et al. New Insights into the Immune Molecular Regulation of the Pathogenesis of Acute Respiratory Distress Syndrome. *Int J Mol Sci*. 2018;19(2).
 136. Kuida H, Hinshaw LB, Gilbert RP, Visscher MB. Effect of gram-negative endotoxin on pulmonary circulation. *Am J Physiol*. 1958;192(2):335-44.
 137. Taveira da Silva AM, Kaulbach HC, Chuidian FS, Lambert DR, Suffredini AF, Danner RL. Brief report: shock and multiple-organ dysfunction after self-administration of Salmonella endotoxin. *N Engl J Med*. 1993;328(20):1457-60.
 138. Meers CM, Tsagkaropoulos S, Wauters S, Verbeken E, Vanaudenaerde B, Scheers H, et al. A model of ex vivo perfusion of porcine donor lungs injured by gastric aspiration: a step towards pretransplant reconditioning. *J Surg Res*. 2011;170(1):e159-67.
 139. Raghavendran K, Nemzek J, Napolitano LM, Knight PR. Aspiration-induced lung injury. *Crit Care Med*. 2011;39(4):818-26.
 140. Dreyfuss D, Soler P, Basset G, Saumon G. High inflation pressure pulmonary edema. Respective effects of high airway pressure, high tidal volume, and positive end-expiratory pressure. *Am Rev Respir Dis*. 1988;137(5):1159-64.
 141. Rotta AT, Gunnarsson B, Fuhrman BP, Hernan LJ, Steinhorn DM. Comparison of lung protective ventilation strategies in a rabbit model of acute lung injury. *Crit Care Med*. 2001;29(11):2176-84.
 142. Chen G, Ge D, Zhu B, Shi H, Ma Q. Upregulation of matrix metalloproteinase 9 (MMP9)/tissue inhibitor of metalloproteinase 1 (TIMP1) and MMP2/TIMP2 ratios may be involved in lipopolysaccharide-induced acute lung injury. *J Int Med Res*. 2020;48(4):300060520919592.
 143. Diehl JL, Coolen N, Faisy C, Osman D, Prat G, Sebbane M, et al. Growth-arrest-specific 6 (GAS6) protein in ARDS patients: determination of plasma levels and influence of PEEP setting. *Respiratory care*. 2013;58(11):1886-91.
 144. Kang L, Li X, Liu J, Li Y, Li S, Zhao C. Recombinant human insulin-like growth factor binding protein 3 attenuates lipopolysaccharide-induced acute lung injury in mice. *Int J Clin Exp Pathol*. 2020;13(7):1924-31.
 145. Ricou B, Nicod L, Lacraz S, Welgus HG, Suter PM, Dayer JM. Matrix metalloproteinases and TIMP in acute respiratory distress syndrome. *Am J Respir Crit Care Med*. 1996;154(2 Pt 1):346-52.
 146. Schnapp LM, Donohoe S, Chen J, Sunde DA, Kelly PM, Ruzinski J, et al. Mining the acute respiratory distress syndrome proteome: identification of the insulin-like growth factor (IGF)/IGF-binding protein-3 pathway in acute lung injury. *The American Journal of Pathology*. 2006;169(1):86-95.

147. Fonsatti E, Altomonte M, Coral S, De Nardo C, Lamaj E, Sigalotti L, et al. Emerging role of protectin (CD59) in humoral immunotherapy of solid malignancies. *Clin Ter.* 2000;151(3):187-93.
148. Treon SP, Shima Y, Grossbard ML, Preffer FI, Belch AR, Pilarski LM, et al. Treatment of multiple myeloma by antibody mediated immunotherapy and induction of myeloma selective antigens. *Ann Oncol.* 2000;11 Suppl 1:107-11.
149. Bdeir K, Higazi AA, Kulikovskaya I, Christofidou-Solomidou M, Vinogradov SA, Allen TC, et al. Neutrophil alpha-defensins cause lung injury by disrupting the capillary-epithelial barrier. *Am J Respir Crit Care Med.* 2010;181(9):935-46.
150. Chen Q, Yang Y, Hou J, Shu Q, Yin Y, Fu W, et al. Increased gene copy number of DEFA1/DEFA3 worsens sepsis by inducing endothelial pyroptosis. *Proc Natl Acad Sci U S A.* 2019;116(8):3161-70.
151. Chang JC. Acute Respiratory Distress Syndrome as an Organ Phenotype of Vascular Microthrombotic Disease: Based on Hemostatic Theory and Endothelial Molecular Pathogenesis. *Clin Appl Thromb Hemost.* 2019;25:1076029619887437.
152. Kangelaris KN, Prakash A, Liu KD, Aouizerat B, Woodruff PG, Erle DJ, et al. Increased expression of neutrophil-related genes in patients with early sepsis-induced ARDS. *Am J Physiol Lung Cell Mol Physiol.* 2015;308(11):L1102-13.
153. Kawasaki T, Chen W, Htwe YM, Tatsumi K, Dudek SM. DPP4 inhibition by sitagliptin attenuates LPS-induced lung injury in mice. *Am J Physiol Lung Cell Mol Physiol.* 2018;315(5):L834-L45.
154. Morrell ED, Radella F, 2nd, Manicone AM, Mikacenic C, Stapleton RD, Gharib SA, et al. Peripheral and Alveolar Cell Transcriptional Programs Are Distinct in Acute Respiratory Distress Syndrome. *Am J Respir Crit Care Med.* 2018;197(4):528-32.
155. Vliegen G, Raju TK, Adriaensen D, Lambeir AM, De Meester I. The expression of proline-specific enzymes in the human lung. *Ann Transl Med.* 2017;5(6):130.
156. Hastbacka J, Linko R, Tervahartiala T, Varpula T, Hovilehto S, Parviainen I, et al. Serum MMP-8 and TIMP-1 in critically ill patients with acute respiratory failure: TIMP-1 is associated with increased 90-day mortality. *Anesth Analg.* 2014;118(4):790-8.
157. Hozain AE, O'Neill JD, Pinezich MR, Tipograf Y, Donocoff R, Cunningham KM, et al. Xenogeneic cross-circulation for extracorporeal recovery of injured human lungs. *Nat Med.* 2020;26(7):1102-13.
158. Mehaffey JH, Charles EJ, Sharma AK, Salmon M, Money D, Schubert S, et al. Ex Vivo Lung Perfusion Rehabilitates Sepsis-Induced Lung Injury. *Ann Thorac Surg.* 2017;103(6):1723-9.
159. Stenlo M, Silva IAN, Hyllen S, Bolukbas DA, Niroomand A, Grins E, et al. Monitoring lung injury with particle flow rate in LPS- and COVID-19-induced ARDS. *Physiol Rep.* 2021;9(13):e14802.
160. Orens JB, Boehler A, de Perrot M, Estenne M, Glanville AR, Keshavjee S, et al. A review of lung transplant donor acceptability criteria. *J Heart Lung Transplant.* 2003;22(11):1183-200.

161. Ferdinand JR, Hosgood SA, Moore T, Ferro A, Ward CJ, Castro-Dopico T, et al. Cytokine adsorption during human kidney perfusion reduces delayed graft function-associated inflammatory gene signature. *Am J Transplant.* 2021;21(6):2188-99.
162. Rieder M, Wengenmayer T, Staudacher D, Duerschmied D, Supady A. Cytokine adsorption in patients with severe COVID-19 pneumonia requiring extracorporeal membrane oxygenation. *Crit Care.* 2020;24(1):435.
163. Gruda MC, Ruggeberg KG, O'Sullivan P, Guliashvili T, Scheirer AR, Golobish TD, et al. Broad adsorption of sepsis-related PAMP and DAMP molecules, mycotoxins, and cytokines from whole blood using CytoSorb(R) sorbent porous polymer beads. *PLoS One.* 2018;13(1):e0191676.
164. Popescu M, Dima S, David C, Tudor A, Simionescu M, Tomescu D. Standard renal replacement therapy combined with hemoadsorption in the treatment of critically ill septic patients. *Ther Apher Dial.* 2021;25(5):663-70.
165. Schadler D, Pausch C, Heise D, Meier-Hellmann A, Brederlau J, Weiler N, et al. The effect of a novel extracorporeal cytokine hemoadsorption device on IL-6 elimination in septic patients: A randomized controlled trial. *PLoS One.* 2017;12(10):e0187015.
166. Schitteck GA, Zoidl P, Eichinger M, Orlob S, Simonis H, Rief M, et al. Adsorption therapy in critically ill with septic shock and acute kidney injury: a retrospective and prospective cohort study. *Ann Intensive Care.* 2020;10(1):154.
167. Friesecke S, Stecher SS, Gross S, Felix SB, Nierhaus A. Extracorporeal cytokine elimination as rescue therapy in refractory septic shock: a prospective single-center study. *J Artif Organs.* 2017;20(3):252-9.
168. Gelman AE, Fisher AJ, Huang HJ, Baz MA, Shaver CM, Egan TM, et al. Report of the ISHLT Working Group on Primary Lung Graft Dysfunction Part III: Mechanisms: A 2016 Consensus Group Statement of the International Society for Heart and Lung Transplantation. *J Heart Lung Transplant.* 2017;36(10):1114-20.
169. Beitler JR, Malhotra A, Thompson BT. Ventilator-induced Lung Injury. *Clin Chest Med.* 2016;37(4):633-46.
170. Guldager H, Nielsen SL, Carl P, Soerensen MB. A comparison of volume control and pressure-regulated volume control ventilation in acute respiratory failure. *Crit Care.* 1997;1(2):75-7.

Novel diagnostics and treatment of acute lung injury and transplantation

Martin Stenlo graduated with an MD from the University of Southern Denmark in June 2008 and carried out his internship at Ängelholm Hospital, Sweden. He started his residency in anesthesia and intensive care at Helsingborg County Hospital, Sweden in 2011 and finished his training in 2016 and became qualified in anesthesia and intensive care by the Swedish National Board of Health and Welfare. In September 2016 he began his present employment as a Consultant at the Department of Cardiothoracic Anesthesia and Intensive Care at Skåne University Hospital in Lund, Sweden. In 2018 he commenced his PhD studies and, a year later, he earned the award of the European Diploma in Anesthesiology and Intensive Care.



**FACULTY OF
MEDICINE**

Anesthesia and Intensive Care
Department of Clinical Sciences Lund

Lund University, Faculty of Medicine
Doctoral Dissertation Series 2021:112
ISBN 978-91-8021-119-2
ISSN 1652-8220

